# ALTERATIONS IN FAST AND SLOW-TWITCH MUSCLES OF GENETICALLY DYSTROPHIC MICE WITH SPECIAL REFERENCE TO PARVALBUMIN

By

MARJORIE ISABELLE JOHNSON

B.Sc., The University of Waterloo, 1978.

A THESIS SUBMITTED IN PARTIAL FULFILLMENT OF

THE REQUIREMENTS FOR THE DEGREE OF

DOCTOR OF PHILOSOPHY

in

THE FACULTY OF GRADUATE STUDIES
(Department of Anatomy)

We accept this thesis as conforming
to the required standard

THE UNIVERSITY OF BRITISH COLUMBIA
September 1987

In presenting this thesis in partial fulfilment of the requirements for an advanced degree at the University of British Columbia, I agree that the Library shall make it freely available for reference and study. I further agree that permission for extensive copying of this thesis for scholarly purposes may be granted by the head of my department or by his or her representatives. It is understood that copying or publication of this thesis for financial gain shall not be allowed without my written permission.

Department of Anatomy

The University of British Columbia
1956 Main Mall
Vancouver, Canada
V6T 1Y3

Date September 10, 1987

# ABSTRACT

Muscular dystrophy is a genetic disease which affects the morphology, physiology and biochemical nature of the muscle fiber. This study was designed to examine the progressive effects of muscular dystrophy on the differentiation process of skeletal muscle. Chapter 1 examines the neonatal development of muscle spindles and their intrafusal fibers in the soleus and extensor digitorum longus (EDL) of genetically dystrophic mice according to histochemical, quantitative, and ultrastructural parameters. Despite alterations in the surrounding extrafusal fibers, muscle spindles and their intrafusal fibers appeared enzymatically and histologically unaffected in incipient stages of murine dystrophy.

In the second chapter the distribution and concentration of parvalbumin (PV), a calcium-binding protein, in 32 and 2-week-old dystrophic mice was mapped by immunohistochemical and biochemical procedures. The number of parvalbumin-immunoreactive fibers was significantly reduced in the adult dystrophic EDL but slightly increased in the adult dystrophic soleus. No differences between strains were observed in the 2-week samples. These findings were supported by routine myosin ATPase histochemistry. Parvalbumin was isolated on SDS-PAGE gels and the concentration of PV was estimated by a RIA. These results confirmed the immunohistochemical data in that PV content was dramatically reduced in the adult dystrophic EDL and significantly increased in the dystrophic soleus. No changes were detected in the samples of the 2-week-old muscles. The similarity in the distribution and content of PV between the fast and slow dystrophic muscles at 32 weeks of age suggests an alteration in the distribution and phenotypic expression of fiber types in muscular dystrophy and supports the hypothesis that dystrophy alters the normal differentiation process of skeletal muscle.

TABLE OF CONTENTS

LIST OF TABLES

LIST OF FIGURES

ACKNOWLEDGEMENT

A study such as this is never the work of one person, and I truly have many people to whom I owe my gratitude. First and foremost I wish to extend my appreciation to my advisor Dr. William Ovalle who was determined that I receive the best possible all-round education while at UBC. I thank him for his patience, liberal guidance, persistence, and devoted interest in my education. I am also deeply indebted to Dr. Ken Baimbridge who took me under his wing, allowed me to work in his laboratory, and tried to make me a scientist. To the other members of my committee, Dr. Wayne Vogl, Dr. Joanne Emerman, and to Dr. Dow, thank you for always being there to help with my problems no matter how trivial. To the late Dr. Jasch I offer this work as a tribute to her devotion to the truths of science. I hope she would have approved of this extension of her work.

I owe a great deal to the technical staff who have assisted me throughout my studies. I am very appreciative of Jean McLeod for her work with the animals, performing the amputations and ovarian transplants, and for introducing me to several valuble techniques. I would also like to thank Hella Prochazska, Sue Finley and Bruce Anderson for their endless patience and instruction. A special thanks goes to Bernie Cox for the reproduction of my original prints.

Finally, I wish to thank my colleagues and peers, both in and outside of the department who have made these years of study a truly enjoyable experience. And last, but above all not the least, I thank my best friend and biggest fan, Paul Johnson.

# DEDICATION

To Auntie Bee,

who sparked my interest in the world of science

and in the unknown.

# GENERAL INTRODUCTION

Muscular dystrophy is a term used to describe a group of genetic disorders which are characterized by progressive and severe degeneration of skeletal muscle fibers. The disease affects the morphology, physiology and biochemical nature of the muscle fiber. Although numerous abnormalities have been reported in both muscle and non-muscle tissue the primary product of the mutant gene has not been identified. The recent isolation of a candidate for the cDNA's for a portion of the Duchenne muscular dystrophy gene appears to support the theory that the gene in this particular disorder is involved in the production of a muscle protein (Monaco et al., 1986).

## Animal Models

A number of animal models have been utilized in muscular dystrophy research, and these include the hamster, chicken and mouse. In this thesis, the murine model for hereditary muscular dystrophy will only be considered. Even though no animal model completely resembles the human form of muscular dystrophy, they have added an invaluable wealth of experimental data to our knowledge of the disease and to the response of muscle in an abnormal environment.

The two most frequently studied mouse models for progressive muscular dystrophy are the 129/ReJdy/dy (Michelson et al., 1955) and the C57BL/6Jdy$^{2J}$/dy$^{2J}$ (Meier and Southard, 1970) strains. Muscular dystrophy in these two strains of mouse is carried by an autosomal recessive gene (Harris and Slater, 1980). Mice that are homogeneous at the dystrophic allele are characterized at an early age of 2-3 weeks by splaying and clenching of the hindlimbs, inability to grasp with their hind feet, and a decreased ability to regain their balance. As the disease progresses, the hindlimbs undergo severe atrophy and become abnormally extended and dysfunctional. No clinical signs are evident in the forelimbs. In mice homozygous for the dy$^{2J}$ allele the disease is expressed in a milder form than that noted in mice of the dy allele.

Mice of the $dy^{2J}$ strain are characterized by a slower, progressive degeneration of muscle tissue. The disease does not appear to affect the myogenic process since myotubes are morphologically normal and only a few myofibers are altered at birth (Platzer and Powell, 1975).

Recently Bulfield et al. (1984) described an X-linked recessive mutant in the mouse (mdx). Although a genetic homology to the human locus may exist, and high serum enzyme levels similar to Duchenne dystrophy have been reported, this mutant has subsequently been characterized as a potential model for muscle regeneration. The mdx mouse shows signs of muscle fiber degeneration and altered physiological responses up to 3-4 weeks of age. There is a decreased twitch tension, muscle weight and a prolonged half-relaxation time compared to the control animal. However, the mdx adult mouse shows no signs of sustained muscle weakness, no changes in fiber type differentiation and measures of the physiological parameters have returned to normal. Therefore, due to its high regenerative capacity the mdx mutant has not served as a useful model for muscular dystrophy.

Histological Features

Several histological abnormalities occur in the postnatal and pre-clinical stages of the murine disease, indicating that its phenotypic expression occurs early in muscle development (Platzer and Powell, 1975; Mendell et al., 1979; Summers and Parsons, 1981b). The characteristic feature of dystrophic mouse muscle is the heterogeneity in appearance of extrafusal fibers. At early or later stages of the disease, muscle fibers of variable size and those that are necrotic, regenerating or splitting are commonly observed in a given fascicle next to those with a normal appearance (Cullen and Mastaglia, 1980). Fragmentation of muscle fibers is common in the initial stages, as are signs of abortive regeneration (Summers and Parsons, 1981b). During the later phases of the disorder there is a significant proliferation of endomysial connective tissue which may impair muscle fiber recovery (Mendell et al., 1979).

A characteristic histological feature of murine dystrophy is the presence of regenerative activity at some distance from the area of fiber necrosis (Banker et al., 1979; Summers and Parsons, 1981b). This feature has been attributed to an abnormal response of myosatellite cells to the events of fiber necrosis (Summers and Parsons, 1981a). Myosatellite cells fuse to form new myotubes. These investigators reported that dystrophic mouse muscle has an adequate number of satellite cells and, therefore, it is the subsequent development of the myotubes which is abnormal and not their initial formation. The myosatellite cell population is higher in dystrophic muscle than in normal muscle and decreases with age (Ontell et al., 1984). This factor was suggested to be responsible for the inability of the regenerative response of dystrophic muscle to keep pace with the muscle deterioration.

One of the first ultrastructural alterations in dystrophic mouse muscle is dilatation of the SR, including its network of longitudinal tubules and terminal cisternae (Platzer and Powell, 1975). Subsequently, mitochondria may appear swollen and filled with matrix granules, and myofibrils become fragmented and atrophied. Retraction clots form and the sarcolemma becomes slightly fragmented, eventually leading to coagulation necrosis and phagocytic infiltration. Ultrastructural studies of motor end-plates in dystrophic mice (Banker et al., 1979) have indicated the presence of both neural and muscular abnormalities associated with the disease in this animal model. Although no definite myotrophic influences on nerve have been observed in the $dy^{2J}$ strain, abnormal neurotrophic influences because of the degeneration of the motor neurons have been documented (Saito et al., 1983). Presynaptic and postsynaptic alterations, such as simplification and atrophy of the junctional folds and retraction of the nerve terminals from the postsynaptic membrane, have been described. As well, significant reductions in the number of myelinated axons have been reported in both allelic strains (Montgomery and Swenarchuk, 1978). In the $dy^{2J}$ mutant failure of the Schwann cell to ensheath the naked axons of spinal roots occurs early in postnatal development (Bray et al., 1978). This group concluded that the

Schwann cell deficit was a developmental abnormality associated with a neonatal impairment of Schwann cell multiplication. In addition, discontinuities in the basal laminas of Schwann cells is a common abnormality observed in the $dy^{2J}$ adult dystrophic mouse (Madrid et al., 1975).

Fiber Types

Extrafusal muscle fibers are classified into two major types, type 2 (fast) and type 1 (slow), according to myosin ATPase or glycolytic enzyme stains (Brooke and Kaiser, 1970; Peter et al., 1972). Type 1 muscle fibers have low myosin ATPase activity (pH 9.4), but are acid stable according to conventional histochemical staining procedures (Brooke and Kaiser, 1970). These fibers are usually associated with slow contraction times, a poorly developed glycolytic enzyme system, a high mitochondrial content, and a high potential for oxidative enzyme activities. Consequently, type 1 fibers are also termed slow-oxidative (SO) fibers (Peter et al., 1972). Conversely, type 2 extrafusal fibers have high myosin ATPase activity, fast contraction times, and a well developed glycolytic enzyme system. On the other hand, these fibers are characterized by a low mitochondrial content and poor oxidative enzyme activity. Type 2 fibers may be divided into several subgroups (types 2A, 2B, and 2C) on the basis of differential susceptibility to treatment with preincubation buffers at varying pH values (Brooke and Kaiser, 1970). Type 2A fibers are more acid-labile than fibers of type 2B, whereas type 2C fibers are stable at acid and alkaline preincubation. Generally, type 2A fibers are also termed fast-oxidative-glycolytic (FOG) while type 2B fibers are designated fast-glycolytic (FG) according to their oxidative and glycolytic enzyme systems (Peter et al., 1972). The two nomenclatures are often used interchangeably; however, this correlation does not always apply to type 2A and 2B fibers of all species (Green et al., 1982). It is, therefore, more appropriate to utilize combined terminology in referring to extrafusal fibers such as type 2A/FOG or type 2A/FG.

Fiber type susceptibility has been reported to differ between the two dy strains of dystrophic mouse. In the dy/dy strain, the fast-twitch muscles are preferentially involved in the early phases of the disease (Butler and Cosmos, 1977), whereas muscles composed of predominantly slow-twitch oxidative fibers are thought to be more severely affected in the $dy^{2J}/dy^{2J}$ strain (Dribin and Simpson, 1977). A number of reports provide evidence that murine muscular dystrophy can affect the histochemical character of the extrafusal fiber types in skeletal muscle (Butler and Cosmos, 1977; Dribin and Simpson, 1977; Silverman and Atwood, 1980; Parry and Parslow, 1981; Ovalle et al., 1983; Wirtz et al., 1983). It has recently been suggested that these changes involve a conversion to an 'intermediate' type of fiber with immature histochemical properties (Wirtz et al., 1983), or due to a retardation in their normal postnatal development (Ovalle et al., 1983). Studies of dystrophic mouse muscle during early stages of the disease (Parry and Parslow, 1981; Wirtz et al., 1983) point to a dramatic decrease in extrafusal fibers of the type 2/FG variety in fast-twitch muscles. During postnatal development of the slow-twitch soleus in dystrophic mice, an increase in type 2/FOG extrafusal fibers and a concomitant decrease in the type 1/SO fibers have also been reported (Ovalle et al., 1983). Both the percentage of FOG fibers and abnormal (or atypical) fibers which are histochemically similar to type 2C fibers, significantly increase with advancement of the disease. This cytochemical trend in extrafusal fiber types in murine dystrophy is also supported by physiological (Bressler et al., 1983) and biochemical (Jasch et al., 1982) data and is further complemented by investigations that point to the appearance of a fetal form of myosin in adult dystrophic human muscle (Fitzsimons and Hoh, 1981) and adult chicken dystrophic muscle (Bandman, 1985). Conversion of extrafusal fiber types to those resembling a type 2C fiber may indicate an alteration in the maturational process of skeletal muscle in murine dystrophy (Ovalle et al., 1983; Wirtz et al., 1983).

Less is known about the effects of dystrophy on the histochemical development of intrafusal fibers in the muscle spindle. These specialized and partially encapsulated

sensory stretch receptors appear relatively resistant to the disease (Swash, 1982). Morphologically abnormal intrafusal fibers have been noted in human Duchenne dystrophy (Swash and Fox, 1976). Light microscope studies of muscle spindles in murine dystrophy are limited and have not detected any abnormalities either in intrafusal fiber morphology (Meier, 1969) or histochemistry (Yellin, 1974b). A recent report (Ovalle and Dow, 1986) has shown some alterations in spindle morphology in terminal stages of murine muscular dystrophy. These studies dealt with either the morphology or histochemistry of the intrafusal fibers in a confined region of the spindle. In addition, the normal time course of intrafusal fiber type development in dystrophic muscle has not been considered. Since accurate identification of intrafusal fiber types by myosin ATPase staining methods requires that serial sections be cut throughout the length of an individual spindle (Soukup, 1976), further investigations of this type are necessary to determine the response, if any, of intrafusal fibers to dystrophy.

Physiological and Biochemical Changes

The results of studies of the mechanical properties of skeletal muscle in murine dystrophy are consistent with the histochemical findings. Generally, there is a decrease in both twitch and tetanic force, an increase contraction time and time-to-peak tension and a prolongation in the half-relaxation time of fast-twitch muscle (Parslow and Parry, 1981; Bressler et al., 1983; Parry and Desypris, 1983). For the dystrophic soleus, decreased twitch and tetanus tension has been observed in mice from 4 to 32 weeks of age (Bressler et al., 1983). However, the prolongation observed in the time-to-peak tension and half-relaxation time in the young dystrophic soleus was not significantly different from the normal values by 32 weeks of age. While the prolonged time-to-peak tension in the dystrophic fast-twitch muscle has been found to correlate with the presence of slow myosin, the prolonged twitch relaxation phase seen in these muscles has not (Parry and Desypris, 1983). These changes suggest a

deficit in both the activation of dystrophic muscle and in the relaxation phases of muscle contraction.

An altered excitation-contraction coupling in murine dystrophic muscle may be associated with a decreased rate of removal of calcium ions from the myoplasm during muscle contraction (Mrak, 1985). A deficiency in the calcium transport system may in turn be due to an abnormality in the handling of calcium ions by the sarcoplasmic reticulum or the calcium-binding proteins, to an altered signal propagation by the transverse tubules, to an abnormality in the muscle membrane surface, or to a lack of neurotrophic factor.

Biochemically, dystrophic mouse skeletal muscle is characterized by a decrease in the uptake and rate of $Ca^{2+}$ transport (Sreter et al., 1966; Mrak and Baskin, 1978; Wood et al., 1978), a decrease in maximum steady-state concentration of phosphoenzyme intermediate, and a decrease in $Ca^{2+}$-sensitive ATPase activity (Mrak and Baskin, 1978; Martonosi, 1982). In addition, densitometric analysis of dystrophic SR preparations indicate a decrease in calsequestrin in the $dy^{2J}$ mutant (Butcher and Tomkins, 1986).

Calcium functions as an intracellular messenger in many cellular processes from muscle contraction to hormone secretion (Carafoli and Penniston, 1985). Regulation of calcium is mediated by certain proteins that interact with the ion governing its transmission, reception and removal, thereby controlling its concentration in the intracellular milieu. The roles of calcium, and its affiliated binding proteins (calmodulin, myosin phosphorylated light-chain, parvalbumin, and troponin C) in muscle contraction have been investigated extensively (reviewed by Carafoli and Penniston, 1985). Binding of calcium to troponin C (Tn-C) causes the muscle to contract, and binding of calcium to calmodulin initiates an important enzyme reaction in a process that produces ATP. Parvalbumin, on the other hand, is thought to act as a calcium buffer and a soluble relaxing factor in fast-twitch muscle (Pechère et al., 1977; Haiech et al., 1979a). A disturbance of calcium homeostasis in skeletal muscle fibers of

dystrophic mice has been linked to an elevated sarcoplasmic $Ca^{2+}$ concentration, possibly due to permeability changes in the sarcolemma (Duncan, 1978). Even though the calcium uptake ability of the SR has decreased, calcium release from the SR may be unaffected in murine dystrophy (Volpe et al., 1984). This would indicate that the problem lies in the calcium regulation system during the relaxation phase and not the initiation of contraction. In light of the proposed functions of PV in fast-twitch muscle, an alteration in the functional capacity of this protein may be of significance in the regulation of $Ca^{2+}$ in the diseased muscle (Klug et al., 1985). Hence, PV has become a topic of interest in $Ca^{2+}$-regulated processes such as those occurring during muscle contraction and in myopathies (Celio and Heizmann, 1982; Stuhlfauth et al., 1984). In murine dystrophy, the PV content of some fast-twitch muscles is significantly reduced in the later stages of the disease (Jasch and Moase, 1985; Pette et al., 1985; Johnson and Ovalle, 1986). The extent to which this decreased concentration of PV affects the buffering capacity of intracellular $Ca^{2+}$ in dystrophic muscle is unclear.

The etiology of murine muscular dystrophy is unknown, but evidence pointing to an altered membrane structure or function has been accumulating. Extracellular tracers focally penetrate the sarcolemma of muscle fibers in dystrophic murine muscle (Banker et al., 1979; Mendell et al., 1979) indicating that membrane integrity is disrupted. Leakage of calcium into muscle fibers occurs during early cellular necrosis suggesting that focal defects in the plasma membrane do not represent the initial event in cellular degeneration (Mendell et al., 1979). Abnormal properties apply to the internal membrane systems of dystrophic muscle as well. In addition to the ultrastructural studies of the SR in mouse dystrophy (Platzer and Powell, 1975) freeze-fracture images have been published showing SR dilatation and fragmentation with no abnormalities of the transverse tubules (Mrak and Baskin, 1978).

A correlation of the morphological, biochemical and physiological data on dystrophic muscle is difficult because of a combination of factors that may contribute

to false impressions. Interpretation of the data is complicated and limited by changes in fiber type composition, species variations, and sampling problems due to the particular stage of the disease. Biochemical preparations of homogenized tissue are hindered by the presence of increased amounts of fibrous and fatty connective-tissue, protease activity, and the release of lysosomal enzymes during preparation. As well, the possibility that some of the observed biochemical alterations could be secondary reactions to an unexposed primary defect must be considered (Martonosi, 1982; Engel, 1986).

Statement of the Objectives

I have divided this project into two studies. Firstly, I wished to study the morphological, histochemical and quantitative changes in muscle spindles and their intrafusal fibers in fast and slow-twitch muscles during the neonatal stages of murine muscular dystrophy. This work has recently been published (Johnson and Ovalle, 1986). Secondly, I wished to test the hypothesis that differences in the profile of certain proteins isolated from dystrophic muscle reflect a loss or alteration of muscle type differentiation. This was attempted by determining if the physiological response of fast and slow-twitch muscle in the $dy^{2J}$ mouse, with respect to half-relaxation time, and the accompanying changes in extrafusal fiber type expression are associated with an alteration in the calcium-binding protein parvalbumin. An alteration in parvalbumin may also be responsible for a disturbance in the calcium homeostasis of dystrophic muscle. As well, I wished to determine whether parvalbumin as an immunochemical marker could be used to detect the expression of dystrophy in muscle fibers at an earlier stage than myosin ATPase histochemistry. A more extensive review of the muscle spindle and of parvalbumin is given in the introduction to the corresponding chapters.

# CHAPTER 1. Postnatal development of muscle spindles in genetically dystrophic mice

## INTRODUCTION

Mammalian muscle spindles are sensory stretch receptors that contain encapsulated intrafusal muscle fibers. These fibers can be differentiated into three types and have been designated $bag_1$, $bag_2$ and chain fibers according to their morphological (Banks et al., 1977), histochemical (Ovalle and Smith, 1972), and physiological (Kennedy et al., 1980; Boyd and Smith, 1984) features.

In contrast to their neighbouring extrafusal fibers, mammalian intrafusal fibers vary histochemically along their individual lengths (Yellin, 1974a; Banks et al., 1977; Kucera, 1977; Kucera and Dorovini-zis, 1979; Soukup et al., 1979;). Immunohistochemical studies indicate that the myosin composition of the intrafusal fibers differs between bag and chain fibers (Pierobon Bormioli et al., 1980; et Kronnie et al., 1981).

Unlike the extrafusal fibers, which are morphologically altered in human (Cullen and Mastaglia, 1980) and murine (Law et al., 1983) muscular dystrophy, spindles and their intrafusal fibers appear to be relatively resistant to the disease (Swash, 1982). Although abnormal intrafusal fibers have been reported in myotonia (Swash and Fox, 1975; Maynard, et al., 1977) and Duchenne dystrophy (Swash and Fox, 1976) in humans, studies of spindle morphology in murine dystrophy (Meier, 1969; Yellin, 1974b; James and Meek, 1979) have failed to show any pathological changes associated with the disease. These studies either dealt with either the morphology or histochemistry of the intrafusal fibers in a confined region of the spindle. In addition, the normal time course of intrafusal fiber type development in dystrophic muscle has not been considered.

Despite the extensive literature published on muscular dystrophy, information concerning the early development of the disease with respect to muscle spindles is

lacking. Thus, the present study was undertaken to elucidate whether intrafusal fiber type alterations could be detected in dystrophic animals during initial stages of the disease. This study, therefore, assesses the early postnatal development of muscle spindles in dystrophic mice and compares their distribution and morphology in selected fast and slow-twitch muscles of normal age-matched controls.

## MATERIALS AND METHODS

Normal C57BL/6J(+/+) and dystrophic C57BL/6J($dy^{2J}/dy^{2J}$) mice were housed in the mouse colony maintained in our department. The original breeding pairs of both the normal and dystrophic strain were obtained from Jackson Laboratories, Bar Harbour, ME. Male homozygous offspring were selected at postnatal ages of 1, 2, and 3 weeks. When possible, normal controls of similar ages were sampled at the same time as their dystrophic counterparts. A total of 28 muscles from 14 normal mice and 30 muscles from 15 dystrophic mice were examined.

### Histochemistry

Animals were killed by either cervical dislocation or decapitation. The right extensor digitorum longus (EDL) and soleus were exposed, superficial fascia removed and then quickly excised. Each muscle was placed on surgical gauze moistened by physiological saline and wet muscle weights were measured. Muscles were embedded in fresh mouse liver, taking care to note the location of the tendons for future orientation. The specimens were mounted on chucks using gum tragacanth and quickly frozen in isopentane cooled with liquid nitrogen. The chucks were allowed to equilibrate to -20°C in the cryostat for 1 hour prior to sectioning. Muscles were serially sectioned (10μm thick) from origin to insertion, and sections were collected on glass coverslips. At every 100μm, three consecutive transverse sections were mounted on separate coverslips for myosin ATPase histochemistry at acid (pH 4.2 and pH 4.6) and alkaline (pH 9.4) preincubations (Dubowitz and Brooke, 1973). This sequence was followed throughout the length of each muscle, and the distribution of muscle spindles was mapped over their full extent at acid and alkaline preincubations using the light microscope 40x objective. Intrafusal fibers were typed according to the $bag_1$, $bag_2$ and chain classification (Ovalle and Smith, 1972). The histochemical profile for each intrafusal fiber was then established throughout its length, except for the equatorial

zone, where little or no staining occurred. In addition, morphological criteria used to distinguish chain from bag fibers and $bag_1$ from $bag_2$ fibers included cross-sectional diameters and fiber lengths. In most cases, chain fibers were smaller than bag fibers; however, those that were similar in size to bag fibers exhibited the staining properties of smaller chain fibers.

Quantitation

Muscle spindles, or nonencapsulated intrafusal fibers, were located under the microscope at each 100μm interval and drawn on a replica sketch of the entire muscle cross section. The length of each spindle was approximated by counting the number of cross-sections in which the intrafusal fibers were seen. The number of spindles and intrafusal fibers per spindle and the location of each receptor relative to myotendon and nerve tissue were noted for diagrammatic longitudinal reconstructions of spindle distribution. The muscle spindle index (number of muscle spindles per gram muscle weight) was calculated for each muscle examined.

Electron Microscopy

Mice at postnatal ages 2 and 3 weeks were anesthetized intraperitoneally with aqueous sodium pentobarbital at a dosage of 1mg/gm body weight, and perfusion was fixed with 2.5% glutaraldehyde in 0.1 M Sorensen's phosphate buffer (pH 7.3) at room temperature. Animals 1 week old were decapitated, and hindlegs were removed and rapidly immersed in fixative. The right EDL and soleus were dissected from each animal and minced with a razor blade into 1 to 2 $mm^2$ segments. Muscle pieces were placed in fresh fixative for a further 2 hrs and then postfixed with 1% aqueous $OsO_4$, dehydrated in graded ethanol and propylene oxide, and embedded in an Araldite/Epon mixture. Thick sections (0.5-1.0μm) of random blocks from each group were cut with glass knives and stained with toluidine blue. Selected areas of the blocks were retrimmed, and ultrathin sections collected on copper grids, stained with uranyl

acetate and lead citrate and examined with a Phillips EM 200 transmission electron microscope.

## OBSERVATIONS

A total of 598 muscle spindles from the normal and dystrophic EDL and soleus muscles were examined in serial transverse sections, from proximal to distal ends of each muscle. Most spindles consisted of two bag fibers and usually two chain fibers. As in other species (see review by Boyd and Smith, 1984), the bag fibers extended outside of the spindle capsule and beyond the termination of the chain fibers.

### Histochemistry

Intrafusal fibers of the soleus stained similarly to those in the EDL for myosin ATPase (Figs. 1,2) and could be differentiated into three types in all muscle spindles. Under acid preincubation conditions, chain fibers were lightly stained, $bag_1$ fibers were usually moderately stained, and $bag_2$ fibers was darkly stained. This histochemical profile of intrafusal fibers could be seen by 1 week of age in both the soleus and EDL (Figs. 1,2), regardless of genotype. At 1 week of age, $bag_2$ fibers appeared darkly stained and chain fibers were lightly stained. The staining pattern of $bag_1$ fibers were variable. Within the same zone of a spindle, the $bag_1$ fiber was observed to be either lightly or moderately stained, or sometimes as intensely stained as the $bag_2$ fiber (Figs. 1,2). This staining profile was noted in muscle spindle polar regions of both normal and dystrophic muscles. No changes in intrafusal fiber typing were seen between 1, 2, and 3 weeks of age. However, by 2 weeks $bag_1$ fibers no longer stained as darkly as $bag_2$ fibers.

Serial sections treated after alkaline preincubation were compared to those after acid preincubation. Under alkaline conditions, chain fibers were darkly stained as were $bag_2$ fibers, only the $bag_1$ fiber was lightly stained. Therefore, $bag_2$ fibers were stable under both pH conditions, whereas the $bag_1$ showed only moderate stability after acid preincubation. The chain fibers underwent a complete reversal in staining from light at acid pH to dark at alkaline pH. Thus the staining pattern exhibited by

Figures 1,2

Transverse frozen sections of portions of a normal soleus (Fig. 1) and EDL (Fig. 2) muscles at 1 week of age, stained for myosin ATPase, pH 4.2. Intrafusal fibers of spindles in the soleus appear histochemically similar to those in the EDL. $Bag_2$ (asterisks) and $bag_1$ (arrowheads) fibers are more reactive than chain fibers (arrows). Neighbouring extrafusal fibers of types 1 (1) and 2 (2) show differences in staining from each other. Bar=20 μm; x1,200.

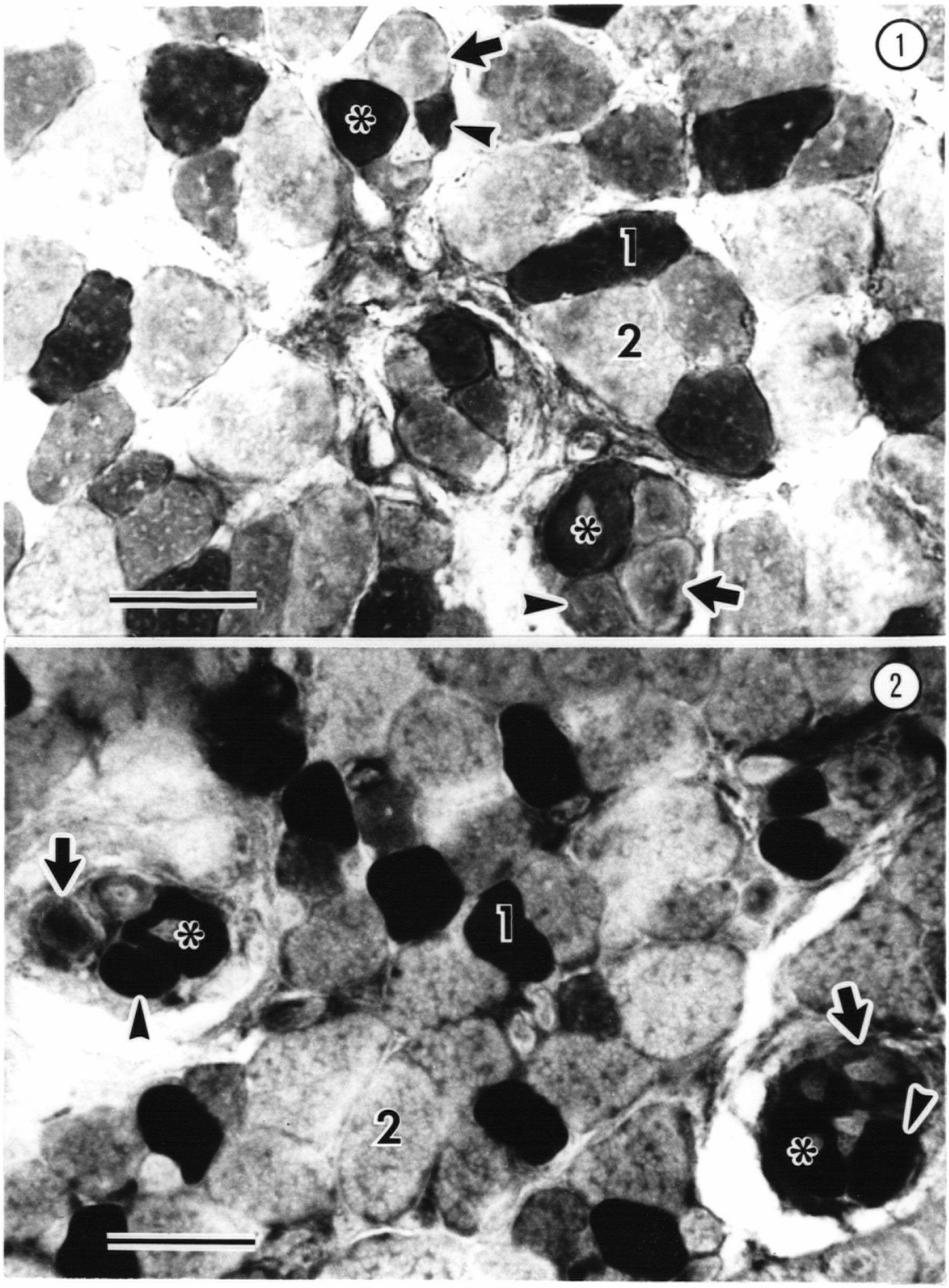
1
1
2
2
1
2

the chain fibers resembled the typical reversal observed in the surrounding extrafusal fibers of the type 2 variety (Figs. 3-6). In contrast, the bag fiber reactivity differed from that of the type 2 or type 1 extrafusal fibers (Figs. 5-6). Regardless of murine genotype, animal age, or muscle phenotype, this pattern remained consistent (Figs 7-10).

Myosin ATPase reactivity of the three intrafusal fiber types varied slightly along the length of an individual spindle. These variations are summarized schematically in Figure 11. The $bag_1$ fiber stained darkly in the extracapsular polar region after acid preincubation, and gradually lost this reactivity toward the equatorial zone. Under alkaline conditions this fiber stained lightly throughout its length. The $bag_2$ fiber showed a dual reactivity under both pH conditions, with no regional variations. The chain fibers were acid-labile and alkaline-stable, also with no regional variation. This overall staining pattern was typical of neonatal intrafusal fibers of both the soleus and EDL at each age group studied, and it did not differ between normal and dystrophic animals.

Morphology and Ultrastructure

The first obvious microscopic changes in the muscles examined were detected in the soleus of dystrophic animals at 3 weeks of age. The EDL, however, appeared unaffected by dystrophy in all neonatal ages studied. Interestingly, the alterations in the soleus occurred in areas of the muscles that were rich in muscle spindles (Fig. 12). Within these areas of dystrophic muscle, the endomysium surrounding the extrafusal fibers as well as muscle spindles was infiltrated with an increased population of connective tissue cells (Fig. 12). Some of the extrafusal fibers appeared to be undergoing pathological changes typical of dystrophic muscle. The variability in fiber size and the presence of extrafusal fibers with centrally located nuclei was greater in the dystrophic muscles than in their normal counterparts. Despite these changes in the surrounding muscle, spindles and their intrafusal fibers in dystrophic

Figures 3-6

Serial sections of part of a normal (Figs. 3,4) and dystrophic (Figs. 5,6) soleus at 3 weeks of age, stained for myosin ATPase after acid (left) and alkaline (right) preincubations. In both normal and dystrophic muscles, polar regions of spindles contain $bag_1$ fibers (arrowheads) that stain moderately at acid pH and lightly at alkaline pH. $Bag_2$ fibers (asterisks) react intensely under both conditions, whereas chain fibers (arrows) undergo a reversal from light in acid to dark in alkaline. A typical reversal in staining is also noted in extrafusal fibers of types 1 (1) and 2 (2). Bar=20 μm; x1,200.

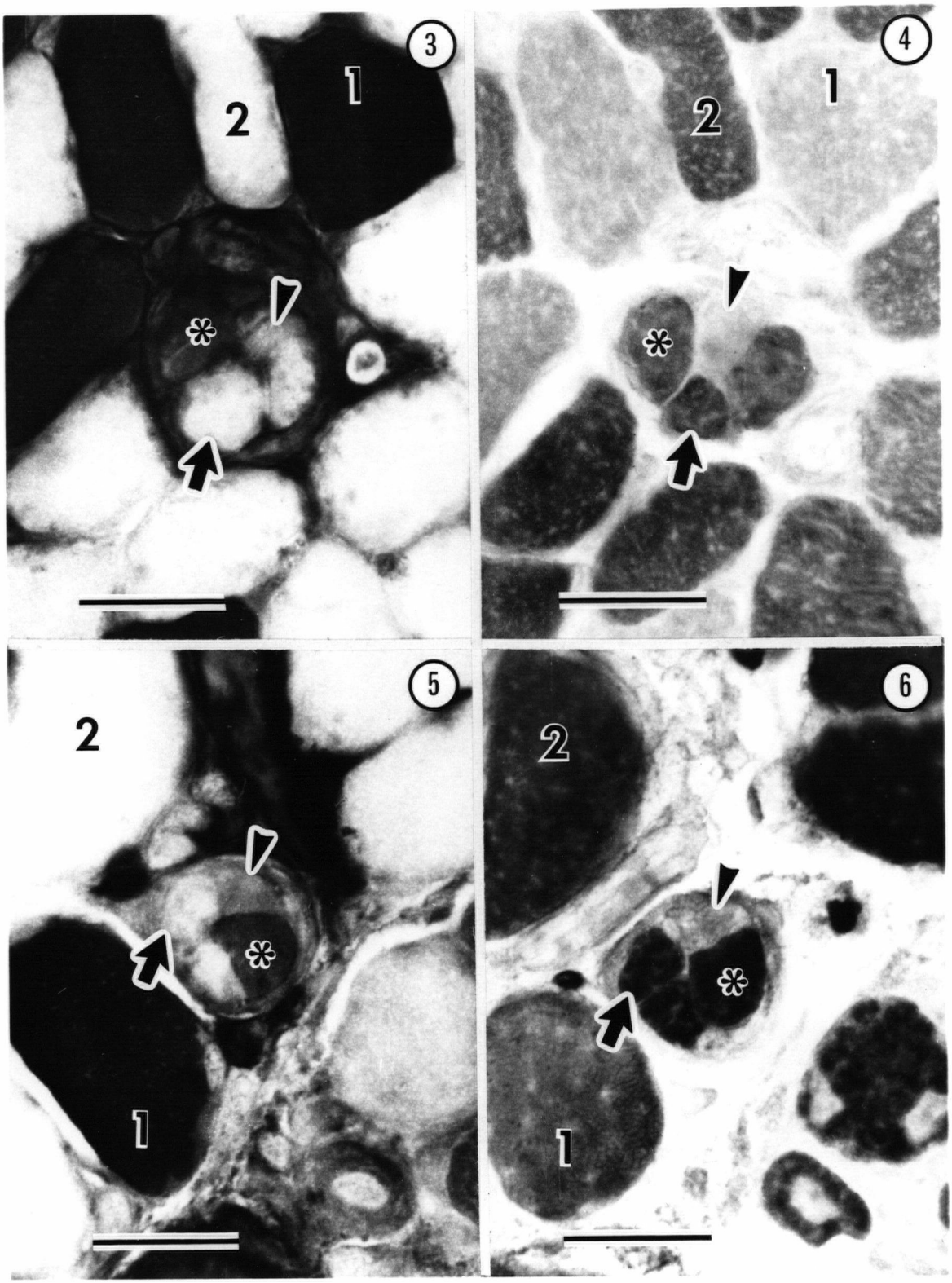
3
2
1
4
2
1
5
2
1
6
2
1

Figures 7-10

Alternate sections of part of a normal (Figs. 7,8) and a dystrophic (Figs. 9,10) EDL at 3 weeks of age, stained for myosin ATPase at pH 4.2 (left) and pH 9.4 (right). $Bag_2$ fibers (asterisks) are highly reactive at both preincubations, whereas $bag_1$ fibers (arrowheads) vary in intensity of staining. Chain fibers (arrows) stain similarly to extrafusal type 2 (2) fibers, being acid-labile and alkaline-stable. Bar=20 μm; x1,200.

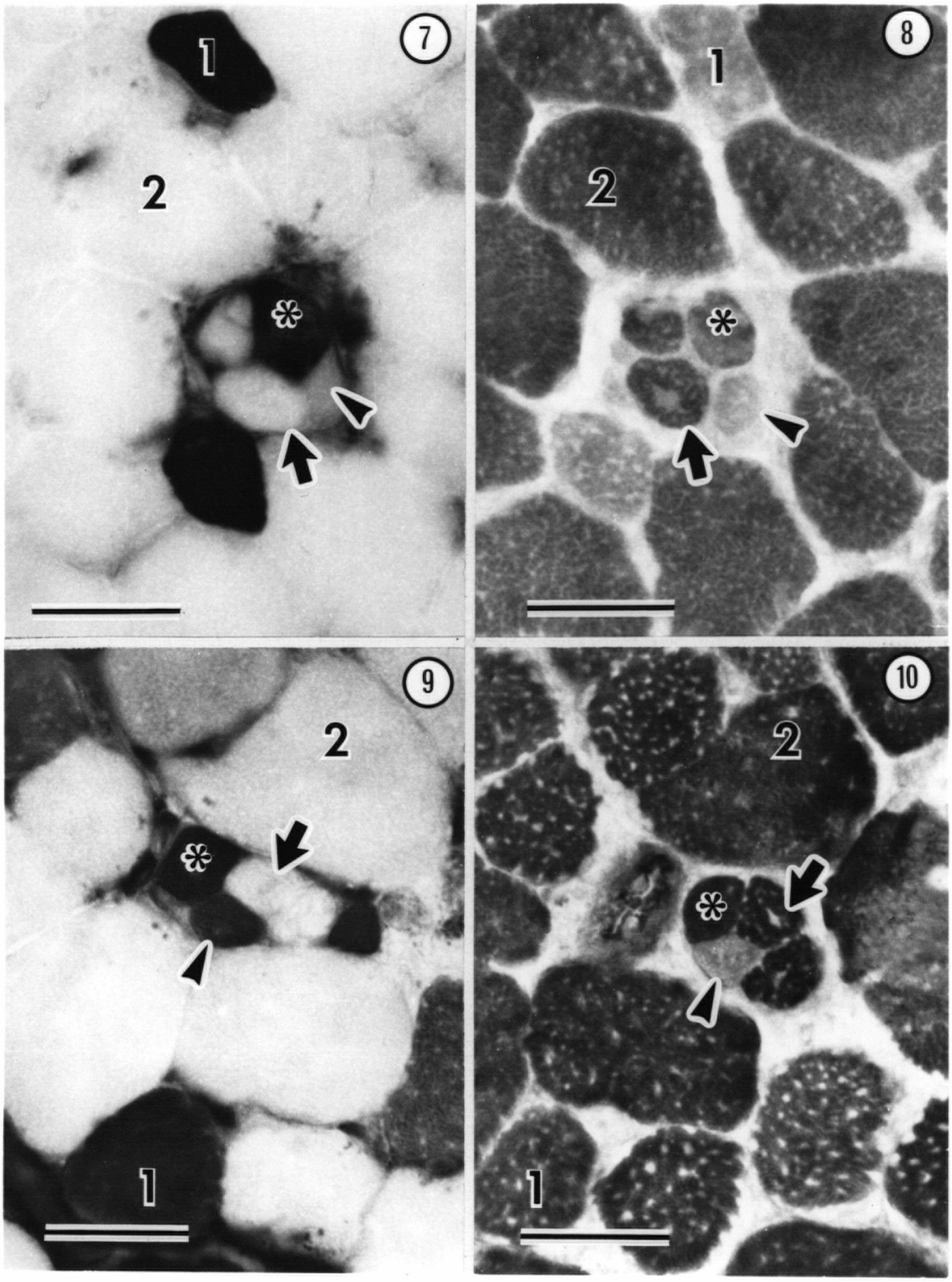
7
1
2
8
1
2
9
2
1
10
2
1

Figure 11

Schematic diagram illustrating the overall myosin ATPase staining properties of the $bag_1$ ($B_1$), $bag_2$ ($B_2$) and chain (C) intrafusal fibers in the neonatal mouse. Composite longitudinal reconstructions (above) were made from transverse serial sections (below). Spindles were traced from their extracapsular polar regions through to the equatorial zone. This is a symmetrical representation of one half of a spindle, comparing intrafusal fiber reactions after acid (left) and alkaline (right) preincubations.

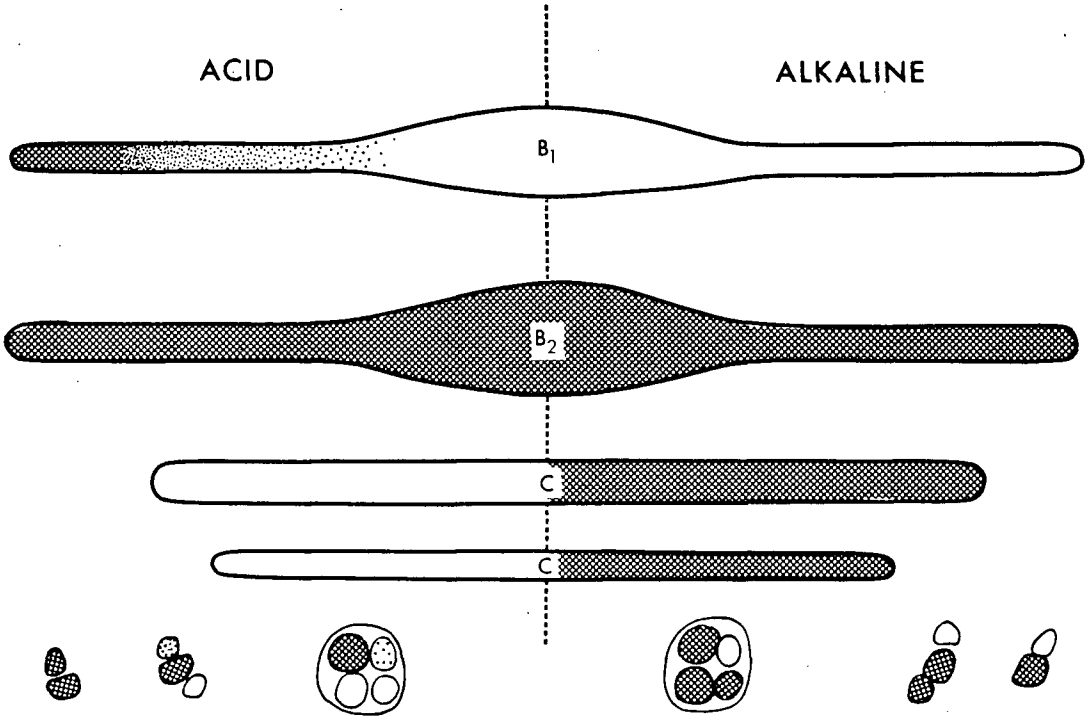
ACID
ALKALINE
B1
B2
C
C

animals were similar in appearance to those of normal controls (Fig. 12).

Ultrastructural examination was confined to the intracapsular regions of spindles, where bag and chain fibers were easily distinguished (Figs. 13,14). At least two spindles from each age group were examined under the electron microscope. In each case, the ultrastructural morphology of spindles in the dystrophic animals was similar to that in muscles of their normal counterparts. Figures 13 and 14 are electron micrographs of a muscle spindle from a 3-week dystrophic soleus and EDL, respectively, and represent the typical appearance of both normal and dystrophic spindles at this age. Within the central equatorial region, each spindle was enveloped by a multilayered capsule consisting of concentric lamellae of perineurial epithelial cells (Fig. 14). A single-layered inner capsule was surrounded by a clear periaxial space, from which it isolated the intrafusal fibers. Like the perineurial cells of the outer capsule, the thin inner capsular was also composed of flattened, contiguous cells. The inner capsule formed separate compartments around the intrafusal fibers and their sensory nerve endings (Fig. 14).

The myofilament content of both bag and chain fibers was reduced in the equatorial zone (Fig. 14). Myofilaments in the juxtaequatorial portions of the spindles formed discrete myofibrils, often separated by mitochondria of varying sizes (Fig. 13). Satellite cells were found beneath the external lamina associated with either bag or chain fibers (Fig. 13). Sensory terminals abundant with mitochondria were either situated in shallow cavities on the intrafusal fiber surface (Fig. 14) or partially encircled the muscle cell (Fig. 13).

Quantitation and Distribution

The total number of muscle spindles per muscle was tabulated for each age group (Table I). No dramatic differences were noted in mean spindle numbers between the slow and fast muscles of either the normal or dystrophic animals. For a more accurate assessment of spindle density in the two muscles, the muscle-spindle index

Figure 12

Light micrograph of a transverse plastic section of portion of a 3-week dystrophic soleus, stained with toluidine blue. The polar spindle in the center of the field (arrow) lies close to a neurovascular trunk and appears normal. A neighbouring area of muscle (asterisk) contains a plethora of degenerating and abnormal extrafusal fibers and connective tissue cell infiltration. Bar=20 µm; x1,100.

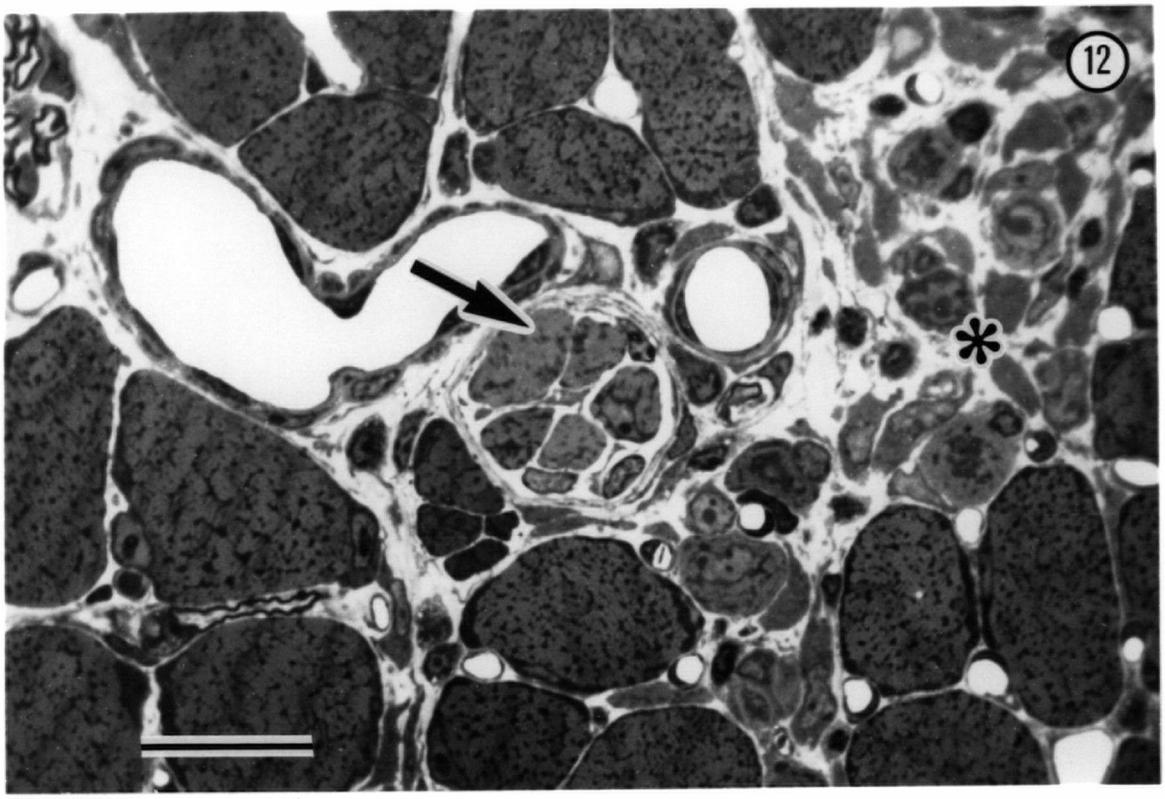
12

Figure 13

Electron micrograph of a portion of a juxtaequatorial spindle from a 3-week dystrophic soleus. Parts of a bag fiber, a chain fiber, and a satellite cell (Sat) are indicated. Outer (OC) and inner (IC) capsular components and a sensory nerve terminal (arrow) appear normal. The periaxial space (asterisk) is clear. Bar=1μm. x13,600.

Figure 14

Electron micrograph of part of an equatorial spindle from a 3-week dystrophic EDL. Inner capsule cells and their processes (IC) envelop two pairs of bag (B) and chain (C) fibers and their sensory terminals (arrow). A clear periaxial space (asterisk) is surrounded by an intact outer capsule (OC). Bar=10 μm; x4,000.

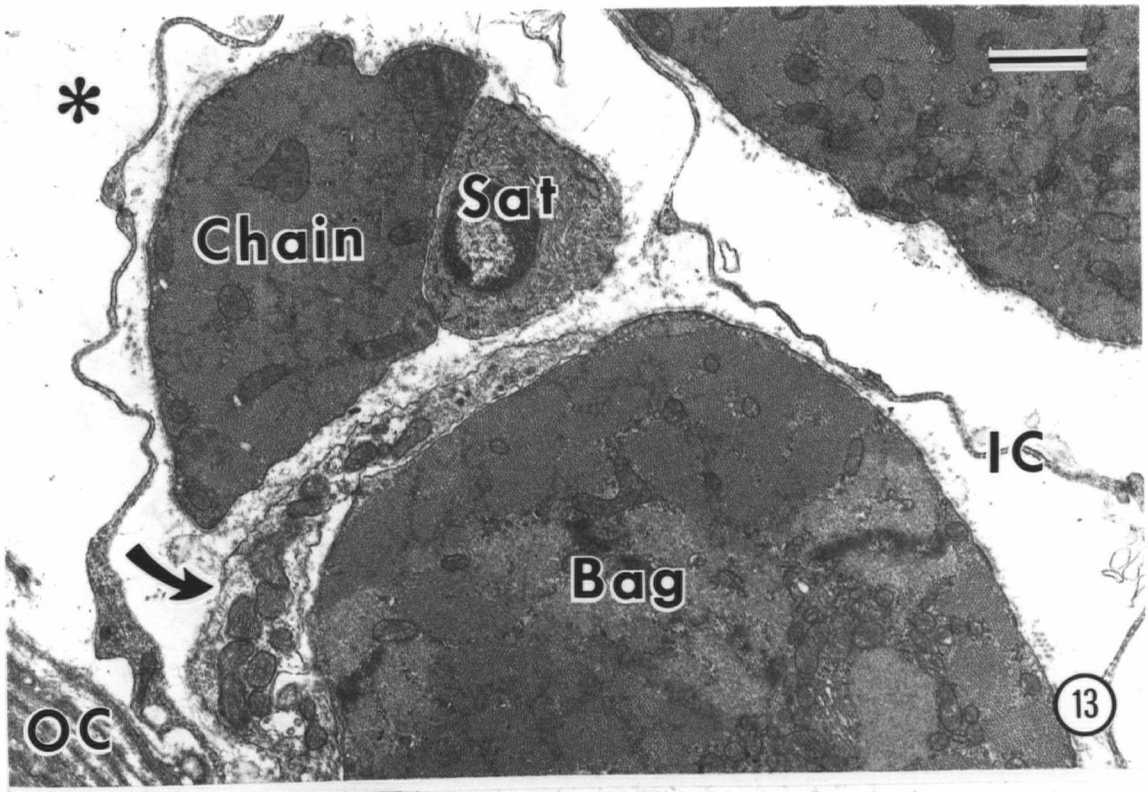
*
Chain
Sat
IC
Bag
OC
13

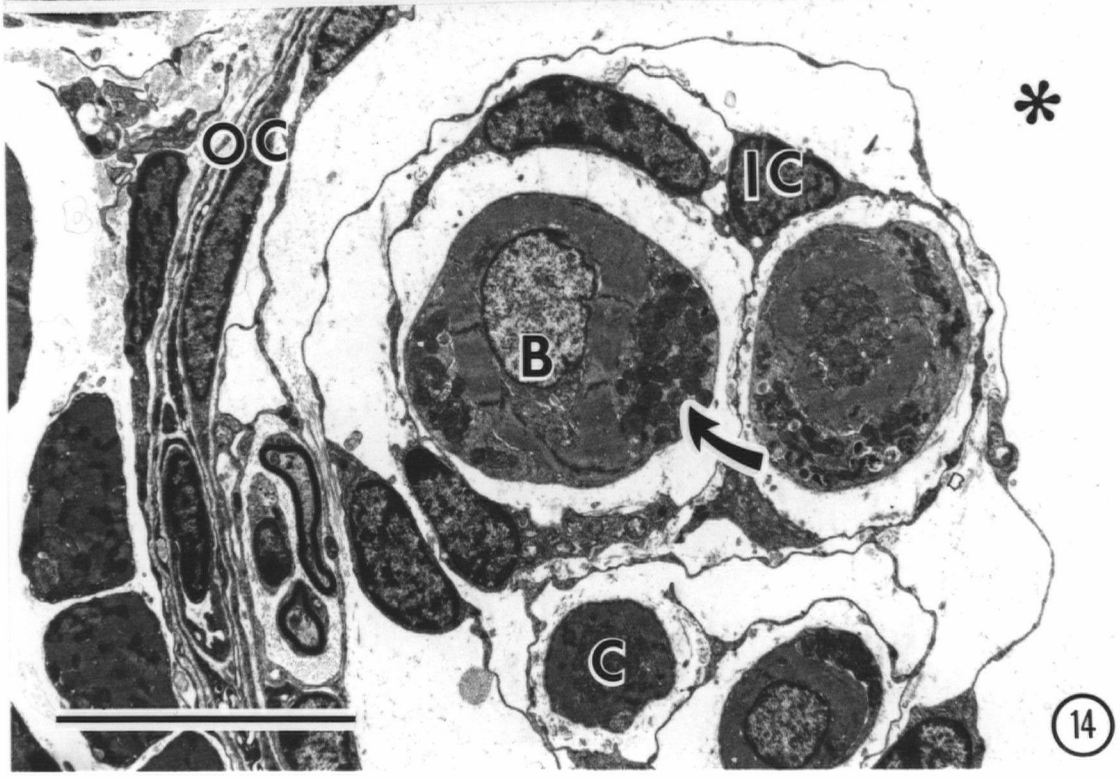
OC
IC
*
B
C
14

was also calculated for each age group. The muscle-spindle index is defined as the total number of spindles in a given muscle expressed per milligram of muscle weight. Whereas mean muscle weights increased steadily with age, reflecting growth of the animals, mean spindle numbers from 1 to 3 weeks remained constant for each muscle group. This would explain the gradual decrease in mean muscle-spindle index from 1 to 3 weeks for all groups (Table I). No obvious differences were apparent in this parameter either between normal and dystrophic animals or between the soleus and EDL for a given group.

The distribution of muscle spindles in the soleus was compared to that in the EDL for both normal and dystrophic mice. Longitudinal reconstructions were made from serial transverse sections extending from origin to insertion (Figs. 15 and 16). Prior to sectioning, the muscles were mounted in such a way that medial and lateral sides and positions of the tendon and the entry point of the neurovascular bundle could be determined. Muscle spindle lengths were estimated from the number of serial sections in which the spindle could be identified. Longitudinal reconstructions were made for an EDL and soleus muscle from each group studied in both normal and dystrophic animals. Figure 15 depicts the distribution of spindles in a normal soleus and EDL muscle. This typical pattern of localization was also observed in muscles of dystrophic animals regardless of age or muscle type (Figure 16). The range in absolute number of spindles in the soleus was 9-14 and that in the EDL 9-12. Typically, the spindles in both muscles were concentrated along the neurovascular pathway.

TABLE I. Comparison of mean spindle number and mean spindle index for normal (N) and dystrophic (DY) soleus and EDL muscles at 1, 2, and 3 weeks of age.

| | 1 WK | | 2 WK | | 3 WK | |
|---|---|---|---|---|---|---|
| | No. | Index | No. | Index | No. | Index |
| SOLEUS | | | | | | |
| N | 9.5 | 9.0 | 12.0* | 4.2 | 11.3 | 2.8 |
| DY | 10.4 | 8.2 | 10.0 | 3.3 | 10.4 | 2.9 |
| EDL | | | | | | |
| N | 10.5 | 8.0 | 11.2 | 3.8 | 11.3* | 2.5 |
| DY | 10.4 | 7.1 | 9.2 | 2.9 | 9.2 | 2.4 |

* $P < 0.05$ between N and DY groups, as determined by Student's t-test. Comparisons were also made between the soleus and EDL across all groups, but these did not prove significant at $p<0.05$.
n=5, with the exception of the 1-week normal groups and the 2-week normal EDL spindle index data, where n=4.

Figure 15

Longitudinal reconstructions (Fig. 15a) showing the distribution of muscle spindles in the soleus (SOL) and EDL muscles at 3 weeks of age. Each line in the diagram designates a spindle. Origin (O), insertion (I) and medial (M) and lateral (L) borders of each muscle are indicated. Figure 15b depicts the corresponding transverse reconstructions of the normal soleus and EDL showing the distribution of muscle spindles from origin to insertion. Each dot represents a muscle spindle. Dorsal (D) and ventral (V) surfaces are indicated as well as the medial (M) and lateral (L) borders. The interval between each transverse section is 1000 μm.

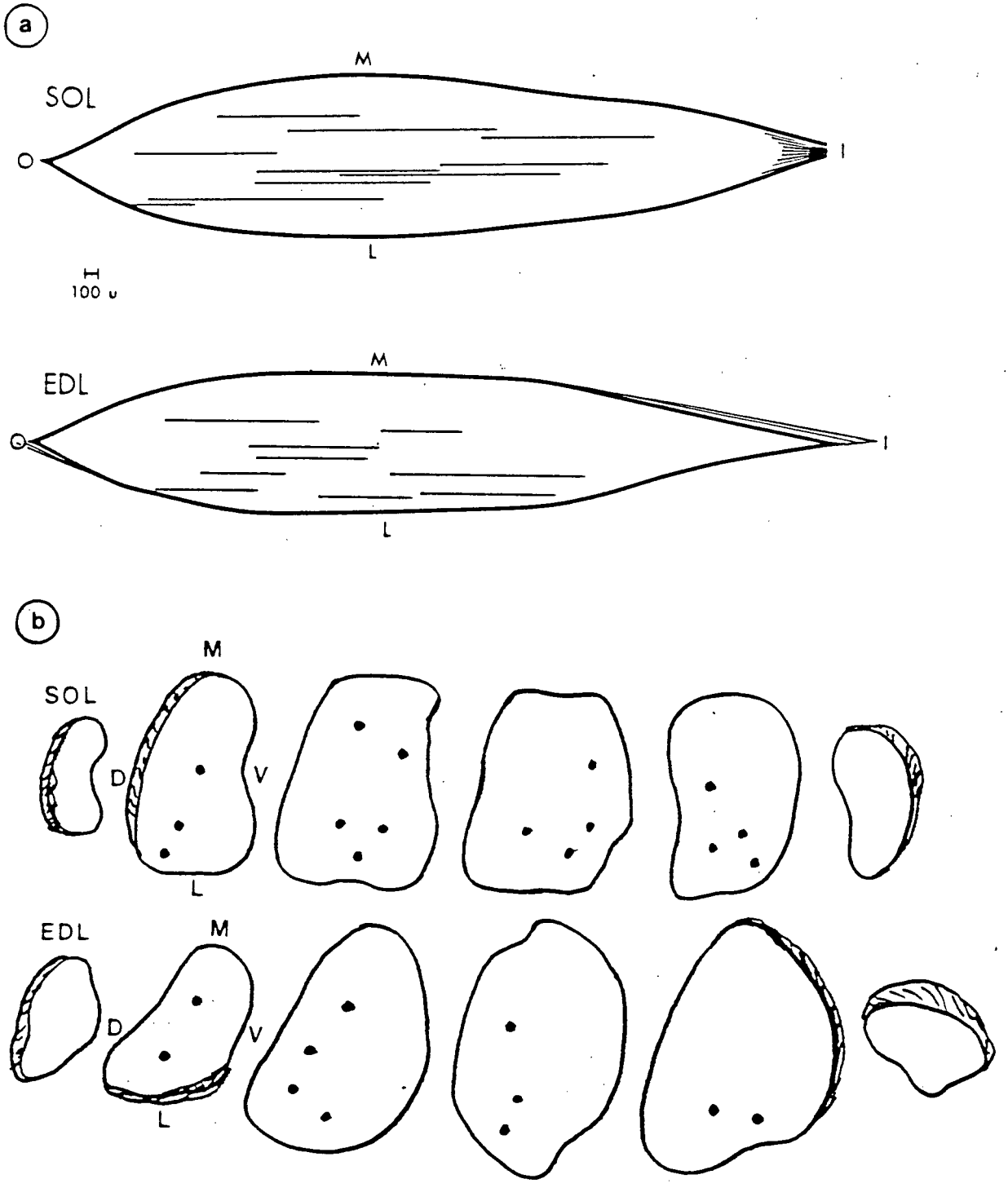
a
SOL
M
O
I
L
H
100 u
EDL
M
O
I
L
b
SOL
M
D
V
L
EDL
M
D
V
L

Figure 16

Longitudinal reconstructions (Fig. 16a) showing the distribution of muscle spindles in the dystrophic soleus (SOL) and EDL muscles at 3 weeks of age. As in Figure 15, each line represents a muscle spindle as they were observed from the origin (O) to insertion (I). Figure 16b shows the corresponding distribution in transverse reconstructions. Each dot indicates a muscle spindle and intervals between traced transverse sections are 1000 μm. Medial (M), lateral (L), dorsal (D) and ventral borders are indicated.

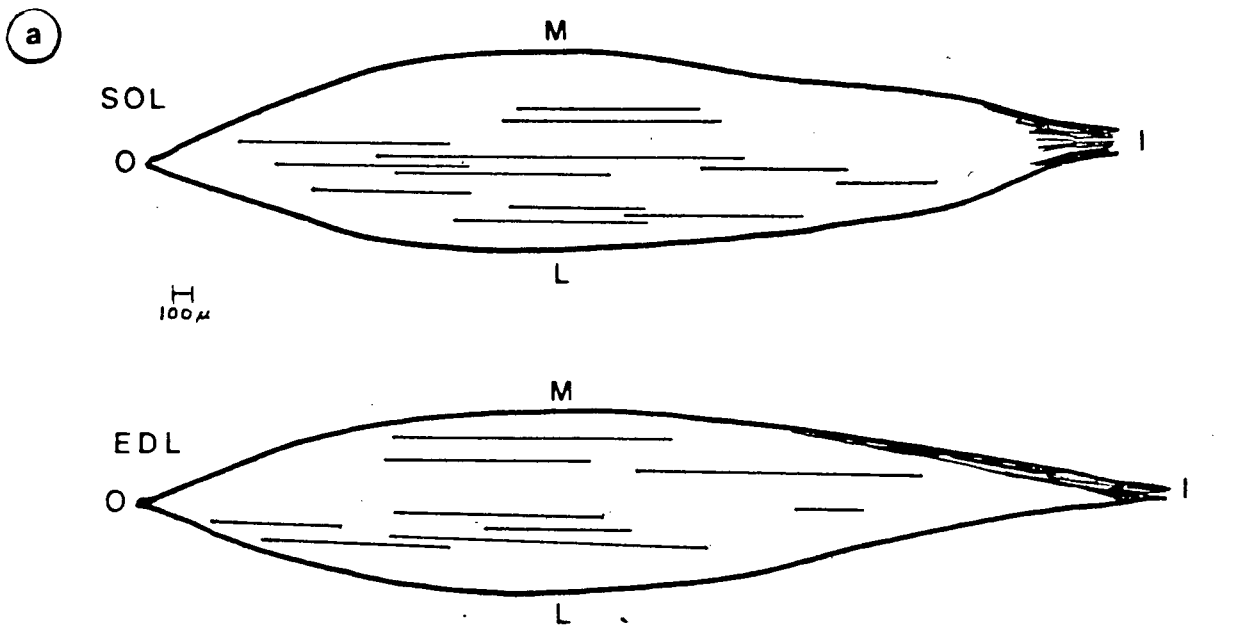
a
SOL
M
O
I
L
100μ
EDL
M
O
I
L

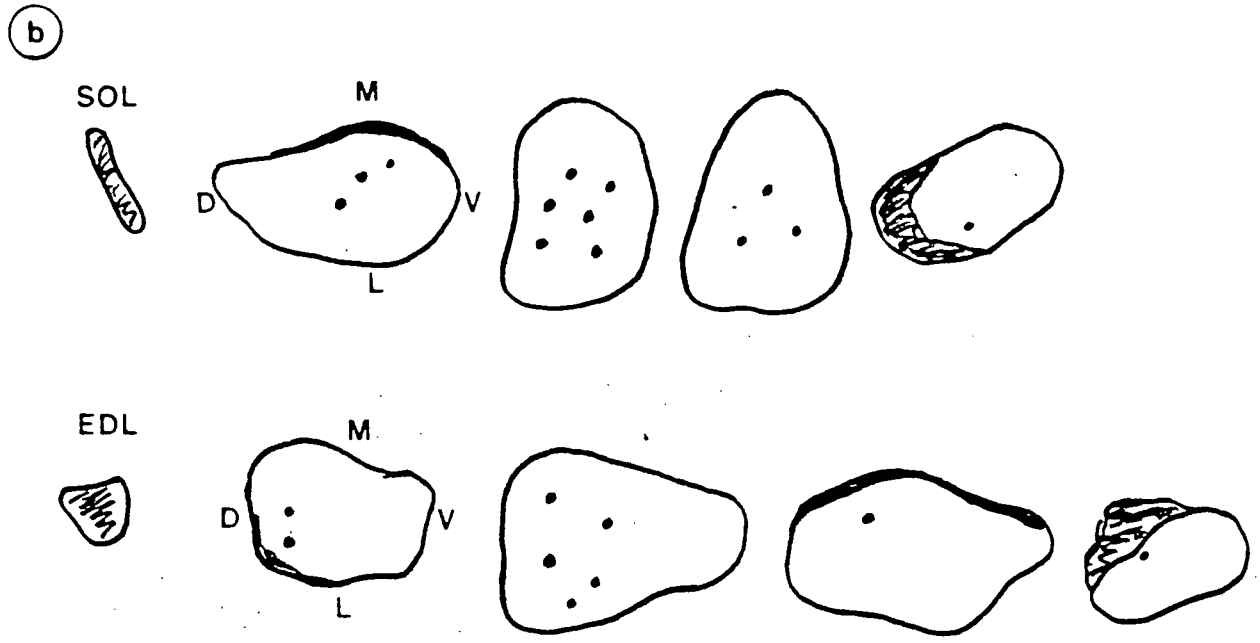
b
SOL
M
D
V
L
EDL
M
D
V
L

# DISCUSSION

The results of the present study complement previous observations that muscle spindles in dystrophic murine muscles are morphologically unaffected by the disease process (Meier, 1969; Yellin, 1974b; James and Meek, 1979). In addition, we have shown that neonatal spindles in the dystrophic slow-twitch soleus and fast-twitch EDL muscles resemble those from their age-matched normal controls.

Our results confirm those previously reported (Meier, 1969; Yellin, 1974b) but also indicate that, in contrast to the changes in extrafusal fibers, intrafusal fibers in dystrophic muscles differentiate normally into three types. In both normal and dystrophic animals, $bag_1$, $bag_2$ and chain fibers could be differentiated on the basis of ATPase reactivity after acid and alkaline preincubations. Regional variations in staining characteristics similar to those noted in other muscles and species, namely the rat (Soukup, 1976; Banks et al., 1977; Khan and Soukup, 1979), cat (Banks et al., 1977; Bakker and Richmond, 1981; Kucera, 1981), monkey (Ovalle and Smith, 1972), and human (Kucera and Dorovini-zis, 1979) were also observed in the mouse.

We have shown that, as in other species, $bag_1$ fibers in the mouse are acid-stable and have low alkali activity. $Bag_2$ fibers, in contrast, are acid-stable and display high alkali reactivity, whereas chain fibers are acid-labile with high alkali activity. These staining patterns were consistently observed in extracapsular polar regions of muscle spindles. In contrast to previous reports, however, slight regional differences were observed in the mouse when compared to other species. Whereas our results show that $bag_1$ fibers exhibit low alkali activity over the entire length of the spindle, Kucera (1977) has reported that the degree of alkali stability varies from capsular to polar regions. Banks and coworkers (1977) noted the $bag_1$ fibers in rabbit, rat and cat spindles are more reactive in extracapsular polar regions under alkaline conditions, a feature similar to the $bag_2$ fibers. On the other hand, under acid conditions, the regional variations noted by us in $bag_1$ fibers of the mouse are

similar to those reported in other species. Thus, as serial sections of a spindle are followed from the polar end toward the equator, the staining pattern gradually changes in a sequential fashion from dark to light.

It has been suggested that variations in myosin ATPase staining of the intrafusal fibers may be dependent on motor innervation (Yellin, 1969; Milburn, 1973). This hypothesis, however, has been disputed by Zelena and Soukup (1974) who showed that rat spindles selectively de-efferented at birth eventually differentiate and mature to obtain their normal histoenzymatic characteristics. As well, Kucera (1981) found no correlation between regional ATPase activity and the location, number, or type of motor endings determined by cholinesterase staining. He suggested that the histochemical response of intrafusal fibers may not be governed by the same factors that control extrafusal fiber typing. The integrity of the intrafusal fibers may instead be influenced by beta innervation in polar regions, or by sensory innervation in the confined environment of the capsule.

It is also possible that different regions of the intrafusal fibers in an individual spindle may contain different myosin isoforms. Immunohistochemical reports (Pierobon Bormioli, 1980; Celio, 1981; et Kronnie, 1981,1982) have recently presented evidence that there are three myosin types associated with intrafusal fibers. $Bag_2$ fibers react to anti-slow myosin, chain fibers to anti-fast myosin, and $bag_1$ fibers to both anti-slow and anti-slow tonic myosin. Future studies designed to evaluate serial sections of an entire spindle stained with various antimyosin antibodies may reveal regional variations in myosin isoforms as well.

It is noteworthy that muscular dystrophy in the mouse can dramatically affect extrafusal fiber typing as early as three weeks of age (Parry and Parslow, 1981; Wirtz et al., 1983) Perhaps the postnatal age range selected in this study was too early to detect alterations in intrafusal fiber type in response to the disease. Histochemical changes in rat extrafusal fibers in response to denervation or exercise are preceded by transitions in other proteins such as parvalbumin and the peptide pattern of

sarcoplasmic reticulum (Green et al., 1984; Müntener et al., 1985). While a similar phenomenon may occur in response to dystrophy in the mouse, it is also possible that myosin ATPase staining methods are not sensitive indicators of early abnormal fiber type. Immunohistochemical studies with antisera to various myosin light chains and heavy chains might reveal a more reliable marker for alterations in fiber type.

Muscle spindles may be spared manifestations of disease by some protective nature of the outer and inner capsules, which are known to regulate the internal environment of these receptors (Dow et al., 1980). Only recently have any studies been conducted to investigate the extent to which the capsule may influence the capacity of the spindle to maintain normal function in the face of an abnormal environment. It has been shown that spindle formation in regenerating mammalian muscle following muscle grafts depends on the survival of the capsule (Rogers and Carlson, 1981). Inadequate sensory innervation in the face of an intact and viable capsule, however, results in abnormal patterns of myosin ATPase activity in intrafusal fibers of regenerating muscle (Rogers, 1982). When muscle spindles are selectively deafferented, the periaxial fluid space is significantly decreased and only the intracapsular myosin ATPase staining pattern in bag fibers is altered (Kucera, 1980). This abnormality may reflect the loss of trophic interaction between afferent innervation and the muscle spindle capsule, thereby diminishing the regulatory function of the capsule.

Spindles in slow-twitch versus fast-twitch muscles

The muscle spindle population density is usually determined by the host muscle's function (Voss, 1937; Cooper, 1960; Barker, 1974). Generally, the spindle density is higher in muscles initiating fine movements, maintaining posture, or exhibiting slow contractile properties (Barker and Chin, 1960; Swett and Eldred, 1960; Yellin, 1969).

Our observations indicate that spindles in the slow-twitch soleus do not differ histochemically from those in the fast-twitch EDL with respect to myosin ATPase

activity. In addition, the number and distribution of spindles were not significantly different between these two muscles in neonatal animals. Our histochemical findings complement results reported by others for bag fibers in rat soleus and EDL muscles (Soukup, 1976, et Kronnie, 1981). Soukup (1976) however, employed the Guth and Samaha (1970) staining protocol and noted that chain fibers in the soleus reacted with variable intensities after acid preincubation, whereas the EDL consistently displayed the typical light staining pattern for myosin ATPase. This slight difference in the soleus and EDL chain fiber reactivities was not observed in the present study, nor has it been reported by others.

In the present study, the mean number of spindles in both the soleus and EDL in all age groups was approximately ten. This number is similar to counts made by others for the soleus (Yellin, 1974a) and EDL (Kozeka and Ontell, 1981) of the mouse. Slightly higher averages have been published for similar muscles in the rat (Yellin, 1969; Kucera, 1977). As a general rule, spindle density is greater in muscles that assist in postural maintenance, such as the soleus (Barker, 1974). Our results did not show a significant difference in spindle density in the soleus from that of the EDL in any of the neonatal groups studied. An explanation for this observation may be that spindle density is not a reliable measure when applied to developing muscle since, owing to growth, the weight of the muscle has not yet stabilized.

As expected, the distribution of muscle spindles followed the course of the neurovascular trunk in both types of muscle. This pattern was not altered by dystrophy or age of the animal. Owing to the heterogeneity of extrafusal fiber types in both the soleus and the EDL of the mouse, no segregation of spindles within a particular area of the muscle was noted. This observation is in agreement with previous reports of the distribution of spindles in selected hindlimb muscles of the rat (Yellin, 1969), and mouse (Kozeka and Ontell, 1981).

Morphogenesis

Muscle spindle development in the mouse begins at day 15 in utero (Kozeka and Ontell, 1981), about 3 days prior to that reported in the rat (Milburn, 1973). The definitive number of muscle spindles in the mouse is established 2 days after primitive sensory contacts are made between nerve fibers and developing myotubes. In addition, the number of intrafusal myotubes in adults has been shown to be present at birth (Kozeka and Ontell, 1981). Again, this is earlier than similar events reported for muscle spindles in the rat, where the full complement of intrafusal fibers is established by 4 days of age (Landon, 1972; Milburn, 1973). Furthermore, polar regions of these fibers are still in an immature state and do not obtain differentiation of their distinct adult fiber type until 12 days postnatally (Milburn, 1973). The findings of Kozeka and Ontell (1981) strongly support the hypothesis proposed by Landon (1972) and Milburn (1973) that successive generations of new intrafusal myotubes occur by fusion of primitive mononucleated cells. In addition, the newly formed myotubes appear to originate in close affiliation with the sensory region of the primary myotube (Kozeka and Ontell, 1981). This close relationship has a profound influence on differentiation of the intrafusal fiber type.

The results of the present study indicate that the adult histochemical profile of intrafusal fibers is present by 1 week of age in the mouse, regardless of genotype. In both the soleus and EDL, myosin ATPase staining at 1 week was the same as that noted at 2 and 3 weeks of age with one exception. At 1 week of age, the $bag_1$ fiber frequently stained as intensely as the $bag_2$ fiber under acid conditions (see Fig. 1) for a distance that extended into the capsular zone. This was not observed at 2 or 3 weeks. It is possible, therefore, that the histochemical differentiation of the $bag_1$ fiber lags behind that of the other intrafusal fibers. While it has been reported that mammalian bag fibers develop in close association with each other (Kozeka and Ontell, 1981; Barker and Milburn, 1984), it has also been shown that $bag_2$ fibers and chain fibers share a single compartment within a developing spindle (Butler, 1979, 1980).

Thus, if $bag_1$ fibers in the mouse were to develop as a separate group, one might expect the time course of their histochemical differentiation to vary from that of $bag_2$ and chain fibers.

The variability in differentiation into distinct intrafusal fiber types may be influenced by the gradual elongation of the spindle capsule from the equatorial sensory region to the exposed polar ends (Kozeka and Ontell, 1981). While it has been shown that sensory innervation is necessary for spindle differentiation (Zelena, 1957) and that fusimotor innervation is required for the development of myosin characteristics (et Kronnie, 1982), the degree of influence of the spindle capsule on differentiation of fiber type is unknown.

Functional and clinical considerations

In agreement with the initial findings of James and Meek (1979), none of the spindles in the $dy^{2J}$ dystrophic muscles appeared ultrastructurally abnormal at any age group examined in the present study. Morphologically, no signs of capsule thickening, enlargement of the periaxial space, or intrafusal fiber atrophy could be detected. These observations also confirm the earlier light microscopic studies of Meier (1969) and Yellin (1974b) in the dy strain of dystrophic mouse. Pathological changes such as intrafusal fiber splitting, collagenous thickening of the capsule, and abnormal innervation are common findings in human dystrophia myotonia (Swash and Fox, 1975; Maynard et al., 1977). While some alterations in spindle morphology have also been noted in terminal stages of muscular dystrophy in humans (Swash and Fox, 1976) and mice (Dow and Ovalle, 1985), their functional implications remain enigmatic.

In human Duchenne and congenital muscular dystrophy, the extent to which muscle spindles are affected is related to the stage of the disease process (Cazzato and Walton, 1968). In preclinical or early dystrophy, the proportion of affected spindles is diminished, and the degree of pathological change is less prominent than that seen in more advanced cases. It would appear therefore that muscle spindles

may be affected in the progressive course of the disease and that any changes that may occur within the spindle during more advanced stages of dystrophy are probably nonspecific long-term responses that are not directly related to the primary etiology of the disease itself.

The complex polyneuronal innervation of muscle spindles has been the subject of extensive reviews (Barker, 1974; Kennedy et al., 1980; Boyd and Smith, 1984). However, our knowledge of the exact pattern and functional significance of the dual sensory and fusimotor innervation is still incomplete. It is tempting to speculate that subtle changes in neuronal activity that are not reflected in structural characteristics in the spindle do occur in dystrophy, and that this functional alteration is reflected in the relatively early onset of abnormal tendon reflexes noted in human muscular dystrophy (Walton and Gardner-Medwin, 1981). If extrafusal fiber degeneration is partially the result of an abnormal neurotropic influence (Saito et al., 1983), it is noteworthy that a morphologically abnormal nerve, such as that observed in the $dy^{2J}$ allelic strain of mouse (Bray et al., 1977; Montgomery and Swenarchuk, 1978), does not appear to affect the development of muscle spindles or the differentiation of intrafusal fibers. It is possible that the polyneuronal innervation, unique to intrafusal fibers in mature muscle, provides a defense mechanism for the spindle during incipient stages of the disease.

Unfortunately the development of spindle abnormalities in muscular dystrophy is not fully understood. This may be due to the fact that not only have few spindles been studied in this neuromuscular disease but they have only received cursory inspection. With the aid of more sensitive biochemical and immunological markers we may better understand the role of the muscle spindle in normal muscle and its alteration in muscular dystrophy. One such immunological marker could be the calcium-binding protein parvalbumin. This protein is associated with fast-twitch muscle fibers and the degree of parvalbumin immunoreactivity in muscle fibers has been established as an alternative to myosin ATPase fiber typing (Celio and Heizmann,

1982). In a previous report from The Muscular Dystrophy Group at the University of British Columbia parvalbumin was noted to be significantly altered in both fast and slow-twitch muscles of adult dystrophic mice (Jasch and Moase, 1985). In addition, changes in the calcium-binding and sequestering system occur earlier than the transition of the isoforms of myosin in response to electro-stimulation (Sreter et al., 1973; Heilmann and Pette, 1979; Klug et al., 1983b; Green et al., 1984). Therefore, parvalbumin, as an immunochemical marker, may detect the expression of dystrophy in extrafusal and intrafusal fibers at an earlier stage than myosin ATPase histochemistry. The remainder of this thesis will deal with the localization of parvalbumin in intrafusal and extrafusal fibers and quantification of parvalbumin in normal and dystrophic mice.

# CHAPTER 2. Biochemical and Immunochemical localization of parvalbumin

## INTRODUCTION

### Historical Background of Parvalbumin

Deuticke (1934) described slow sedimenting fractions in frog muscle at low salt concentrations using ultracentrifugation. Henrotte (1955) subsequently observed similar low molecular weight, acidic proteins with an unusual ultraviolet absorption spectrum from carp muscle. Pechère (1968) referred to these proteins as parvalbumins, based on their small size and high water solubility. In lower vertebrates, as many as 6 isotypes of parvalbumin (PV) have been isolated from the same muscle (Focant and Pechère, 1965), whereas higher vertebrates contain a single isotype in a given muscle (Pechère et al., 1971; Haiech et al., 1979b). Carp muscle, which contains 4 main isotypes of PV, soon became the subject of the first three-dimensional crystallization descriptions (Nockolds et al., 1972) of all the related $Ca^{2+}$-binding proteins (Troponin-C, calmodulin, myosin light chains). Based on peptide maps (Pechère and Capony, 1969), it was concluded that these proteins constitute a family of homologous proteins. More importantly, Pechère and coworkers (1971) discovered that parvalbumins have a high affinity for calcium.

Originally it was thought that parvalbumins were confined to white muscle of fish, amphibia and certain reptiles (Focant and Pechère, 1965). Although it is barely detectable in fish red muscle, PV constitutes approximately 0.7% of the wet weight of carp white muscle (Gosselin-Rey, 1974). Significant amounts of PV have, however, been found in turtle (Lehky et al., 1974), chicken (Strehler et al., 1977; Heizmann and Strehler, 1979), rabbit (Lehky et al., 1974; Pechère, 1974), rat (Berchtold et al., 1982a), cat (Stichel et al., 1986), and human (Lehky et al., 1974; Berchtold et al., 1985). Parvalbumins have not been identified either in invertebrate tissues or in

smooth muscle, and it is present only in low amounts in cardiac muscle (Gosselin-Rey, 1974, Baron et al., 1975; Le Peuch et al., 1979; Gerday et al., 1979).

Evolution

The evolutionary history of parvalbumins divides these proteins into two main groups, designated $\alpha$ and $\beta$; both are derived from an ancestral gene duplication (Goodman et al., 1979). These two groups separate PV according to isoelectric points, $\alpha$-parvalbumin (pH greater than 5.0) being less acidic than $\beta$-parvalbumins. The $Ca^{2+}$-binding proteins are thought to have evolved from a four-domain precursor, binding 4 calcium ions (Goodman and Pechère, 1977). Parvalbumin arose by a deletion of domain I and the deprivation of the $Ca^{2+}$-binding properties of domain II. Calmodulin, troponin-C and the alkali myosin light chains are most similar to the ancestral protein (review by Gerday, 1982).

Biochemistry of Parvalbumin

Despite the polymorphism of parvalbumins (Pechère et al., 1971; Gosselin-Rey et al., 1978), it is remarkable how consistent these proteins are in their physicalchemical properties. Parvalbumin is a heat-stable and water-soluble acidic protein with an isoelectric point (pI) ranging from 3.9 in the carp to 6.6 in the lungfish, and a molecular weight (Mr) of 9 - 13 KD (Gerday et al., 1979). The size of this protein is also reflected in its high diffusion constant and low sedimentation rate (Pechère et al., 1973). The amino acid composition of PV (Table II) is characterized either by the absence or presence of only one tyrosine or tryptophan residue per molecule, and a high number of phenylalanine residues and acidic amino acids such as aspartic and glutamic acid (Pechère et al., 1973). Due to the high ratio of phenylalanine to tyrosine and tryptophan, PV shows a characteristic ultraviolet absorption spectrum in which the absorbtion bands of phenylalanine are visible.

TABLE II. Amino acid composition of parvalbumin in the rat and mouse.

| Amino Acid | Rat Brain | Rat Muscle | Mouse Muscle |
|---|---|---|---|
| Lysine | 15.5 | 16.0 | 16.0 |
| Histidine | 2.2 | 2.0 | * 1.9 |
| Arginine | 1.0 | 1.0 | 1.0 |
| Aspartic acid | 14.6 | 14.0 | 13.8 |
| Threonine | 5.2 | 5.0 | 4.2 |
| Serine | 10.6 | 11.0 | 8.1 |
| Glutamic acid | 9.5 | 8.0 | 12.4 |
| Proline | 0.0 | 0.0 | 0.9 |
| Glycine | 9.4 | 9.0 | 9.2 |
| Alanine | 11.4 | 11.0 | 11.4 |
| Valine | 5.2 | 5.0 | 6.0 |
| Methionine | 2.4 | 3.0 | 2.1 |
| Isoleucine | 6.0 | 6.0 | 5.9 |
| Leucine | 9.6 | 9.0 | 9.3 |
| Tyrosine | 0.0 | 0.0 | 0.0 |
| Phenylalanine | 8.5 | 8.0 | 9.1 |
| Tryptophan | 0.0 | 0.0 | 0.0 |
| Cysteine | 0.0 | 0.0 | 0.0 |

This table has been extracted from data presented by Heizmann, 1984.
* Indicates the amino acid histidine which was iodinated for use in the RIA described on page 70.

Calcium and Magnesium Binding

The basic polypeptide structural unit common to PV and the other $Ca^{2+}$-binding proteins such as troponin-C and calmodulin, is an α-helix -$Ca^{2+}$-binding loop-α-helix and a nonhelical N-terminus. Octahedral calcium-binding loops occur between helices C and D and between helices E and F. These sites also have a high affinity for magnesium. The AB domain is not $Ca^{2+}$-binding (Van Eldik et al., 1982; Wnuk et al., 1982). The structure formed by helices E and F and helices C and D are called the EF and CD hands, respectively. The primary sequence of PV differs from that of Tn-C and calmodulin. The latter have four domains which contain the basic structural α-helical unit. All four regions bind $Ca^{2+}$, and in the case of Tn-C, sites 3 and 4 have high affinity for $Ca^{2+}$ but also bind $Mg^{2+}$. All of the calcium sites on calmodulin resemble the EF hands of parvalbumin.

The calcium-binding properties of PV have been extensively investigated (Wnuk et al., 1982), and these studies have clarified our understanding of its physiological role in muscle. Under physiological conditions (1 mM $Mg^{2+}$) in the resting muscle, myoplasmic $Ca^{2+}$ concentrations are estimated to be $10^{-8}$ M and the majority (80-85%) of the binding sites of PV are occupied by $Mg^{2+}$ (Cox et al., 1979; Potter et al., 1977; Robertson et al., 1981). Magnesium binding induces a conformational change at the hydrophobic core and AB loop (Haiech et al., 1979a). A decrease in the affinity of PV for calcium in the presence of elevated magnesium concentrations is indicative of simple competition for the same binding sites. Therefore, in vivo, PV is always in a metal-bound state.

Association constants for the binding of $Ca^{2+}$ and $Mg^{2+}$ to PV differ slightly according to the method of determination, the type of PV investigated, and the conditions of measurement (Benzonana et al., 1972; Cox et al., 1979; Haiech et al., 1979b). The apparent constants for calcium range from $10^6$ to $10^9$ $M^{-1}$, whereas the range of values for magnesium is $10^4$ to $10^5$ $M^{-1}$. The two binding sites are considered independent and equivalent with respect to their metal binding properties

(Cox et al., 1979; Cave et al., 1979; Haiech et al., 1979a). Evidence suggests, however, that the properties of the two calcium sites are different (Smith and Woledge, 1985).

Functional Aspects

Although parvalbumins have been studied extensively, significance of their biological function(s) is limited. Due to the homology of PV with calmodulin, troponin-C (Tn-C) and myosin light chains it is reasonable to suggest that the function of parvalbumin may be related to $Ca^{2+}$-activated processes. However, despite the common evolutionary origin, PV cannot substitute for the other $Ca^{2+}$-binding proteins (Wnuk et al., 1982). Parvalbumin has no known enzymatic functions (Cohen, 1980; Walsh et al., 1980), it does not interact with troponin-I or tropomyosin, nor can it be phosphorylated (Blum et al., 1977).

In light of the observed muscle type specificity of PV, it has been suggested that this protein may have a more specialized function in muscle contraction and glycolysis (Focant and Pechère, 1965; Heizmann, 1984). However, many of these functions have now been attributed to calmodulin (Cohen, 1980). Calmodulin is a soluble protein found in many eukaryote cells. It is present in both fast and slow muscle (Eibschutz et al., 1984) where it mediates long-term metabolic changes such as the breakdown of glycogen to glucose. However, its role in skeletal muscle calcium-transport is less well defined.

The role of parvalbumins remained obscure until Pechère and coworkers (1977) suggested that they could be involved in the contraction-relaxation process of skeletal muscle. Briggs (1975) had earlier suggested that PV is the 'soluble relaxing factor' of muscle.

Calcium free PV can take up calcium from Tn-C (Pechère et al., 1977) and thereby completely inactivate the ATPase activity of the myofibrils (Gerday and Gillis, 1976), while fragmented SR will return PV to the calcium-free state (Gerday and

Gillis, 1976; Blum et al., 1977). Parvalbumin, therefore, probably works as the shuttle mechanism for $Ca^{2+}$ between the myofibril and the SR during muscle relaxation (Pechère, et al., 1977). A scheme illustrating the movement of $Ca^{2+}$ in fast skeletal muscle (Fig. 17) was developed by Pechère et al (1977) and later modified by Heizmann (1984). When the muscle cell is activated to release calcium from the SR, the liberated ion is not trapped by PV immediately but interacts with troponin-C. This sequence of events is possible due to the different binding kinetics of PV and Tn-C (Haiech et al., 1979a). Although the affinity of parvalbumin for $Ca^{2+}$ is similar to that of Tn-C, the rate of binding of Tn-C exceeds that of PV. As well, in the calcium-free state the binding sites on the PV molecule are occupied by magnesium ($Mg^{2+}$) which must first dissociate to allow $Ca^{2+}$-binding. The dissociation of $Mg^{2+}$ and subsequent uptake of $Ca^{2+}$ by parvalbumin is the rate limiting step, making possible the binding of $Ca^{2+}$ to Tn-C which triggers contraction (Haiech et al., 1979a). Calcium binding to PV is dependent on the $Mg^{2+}$ concentration and on temperature (Ogawa and Tanokura, 1986).

The actual distribution of calcium between the PV and Tn-C binding sites, as studied by computer simulation (Gillis, 1980; Gillis et al., 1982), is such that 97% of the cation binding sites of Tn-C are saturated at the time of a $Ca^{2+}$ pulse (Robertson et al., 1981). Conversely, the transfer of $Ca^{2+}$ to the binding sites of PV is achieved in approximately 200 ms. Initially following muscle relaxation, much of the calcium is still parvalbumin-bound and will be transported back to the SR during the recovery period (Gillis, 1980). Hence, it has been proposed that the biological significance of PV is to allow fast relaxation of muscle because of its relaxing effect due to the binding of calcium (Ashley and Griffiths, 1983; Gillis 1980; Gillis et al., 1985).

The preceding hypothesis has been questioned on a number of accounts. Firstly, the kinetics suggest that the slow off rate of both $Ca^{2+}$ and $Mg^{2+}$ prevents PV from being directly involved in the rapid decay of tension after a single twitch (Johnson et al., 1981; Robertson et al., 1981). Secondly, in the event of a tetanus, PV would

Figure 17

Schematic diagram illustrating the proposed function of parvalbumin (PV) in fast-twitch muscle. In the relaxed state the calcium-binding sites are bound by magnesium ($Mg_2$) and calcium ($Ca^{2+}$) is stored in the sarcoplasmic reticulum (SR). Upon arrival of an action potential, $Ca^{2+}$ is released from the SR and taken up by the first available binding sites which are on the troponin-C molecule of the myofibrils (mf). Because of the high affinity of PV for $Ca^{2+}$, magnesium is displaced from PV and $Ca^{2+}$ then binds to the free sites. PV is then thought to transport $Ca^{2+}$ back to the SR at which point Mg again binds to the free sites and the muscle relaxes (Adopted from Heizmann, 1984).

RELAXED STATE

CONTRACTION

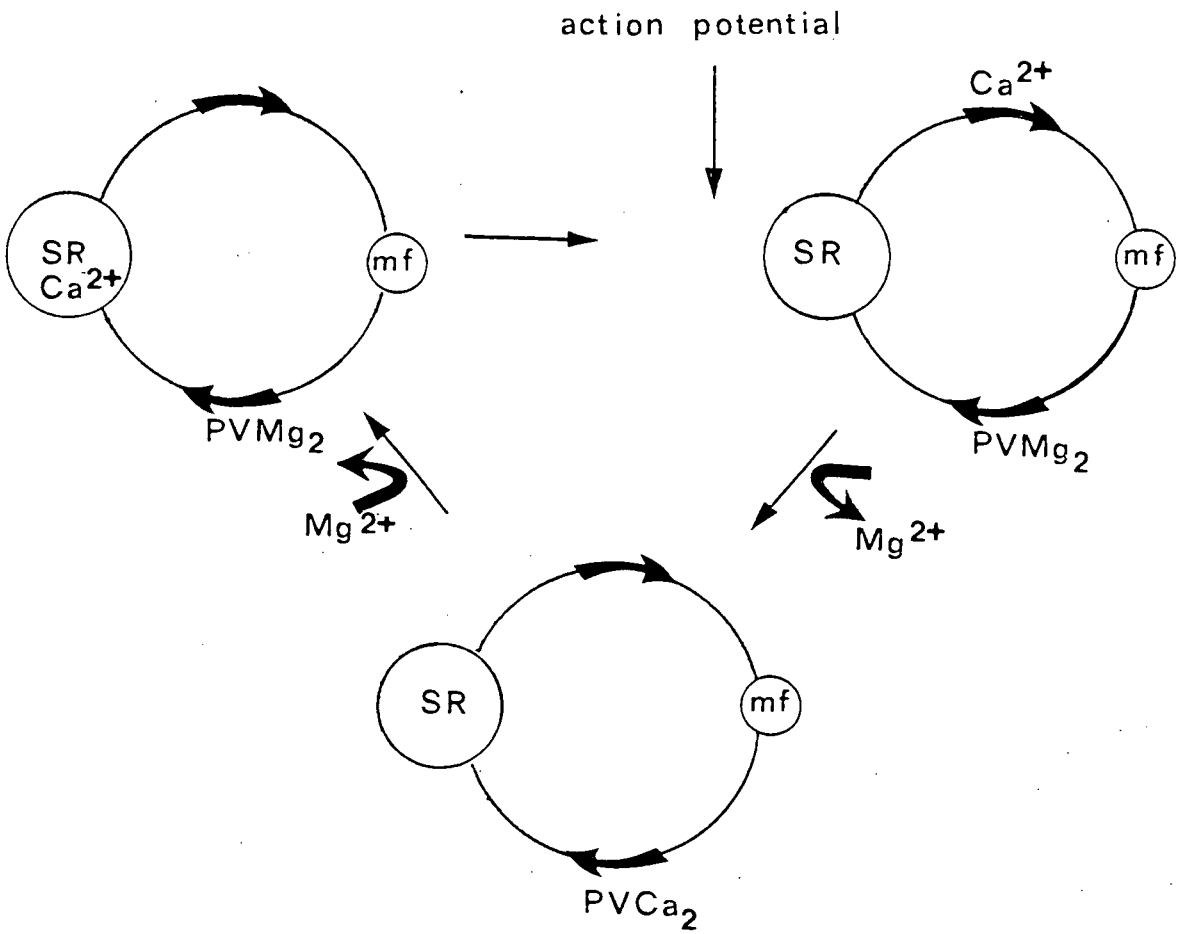


TRANSITIONAL STATE

quickly become saturated with calcium because of the slow dissociation rate and thereby diminish its relaxing effect (Gerday, 1982; Ogawa and Tanokura, 1986). These queries continue to demand a more precise explanation for the role of PV in muscle contraction/relaxation.

The metal-binding properties of calmodulin are similar to those of the calcium-specific sites of troponin-C (Potter et al., 1977). Calmodulin contains 4 $Ca^{2+}$-specific sites, none of which bind $Mg^{2+}$. The association constants and rate of binding for the calcium-sites of calmodulin are similar to those of troponin-C, however, the concentration of calmodulin in skeletal muscle is much lower than that of troponin (Robertson et al., 1981). Mathematical models expressing the time-course of $Ca^{2+}$-binding to calmodulin, troponin, parvalbumin and myosin in response to transient increases in free myoplasmic calcium concentrations (pCa), indicate that all $Ca^{2+}$-sites bind calcium in response to a single pCa transient (Robertson et al., 1981). However, only the $Ca^{2+}$-specific sites of troponin and calmodulin become adequately saturated fast enough to play a role in rapid calcium regulation of contraction. The calcium content of the $Ca^{2+}$-$Mg^{2+}$-sites of troponin, parvalbumin, and myosin increases only slightly. Moreover, exchange of calcium onto and off each class of sites, analogous to a contraction-relaxation cycle, only occurred with the $Ca^{2+}$-specific sites of troponin and calmodulin.

Present in the 2-0.05 mM range, PV exists in adequate quantities to bind all the calcium of the sarcoplasm (Ashley, 1983). At 20°C, an estimated 330 μmol of $Ca^{2+}$/liter is bound to PV at rest (Ogawa and Tanokura, 1986). This increases to 650-670 μmol $Ca^{2+}$/liter during a tetanus and is further accentuated when the temperature is lowered (Ogawa and Tanokura, 1986). Since the binding sites on PV appear to have a higher affinity for calcium but a slower association rate than for the regulatory sites on troponin (Haiech et al., 1979a), the amount of calcium required to activate fast-twitch muscle when PV is present is lower than would be predicted by the myofibrillar $Ca^{2+}$-binding capacity (Robertson et al., 1981). The calculated gain in

calcium by PV and dissociation by Tn-C following a stimulation, indicates that 2 out of 3 $Ca^{2+}$ ions that leave troponin are temporarily bound to PV before being sequestered by the SR (Baylor et al., 1983). In addition, the maximum rate at which the SR must function to remove calcium from the myofibrils is decreased by more than 50% (Baylor et al., 1983), further supporting the role of PV as a soluble relaxing-factor in fast-twitch muscle. A disturbance in the functional capacity of parvalbumin may, therefore, have serious implications for the regulation of intracellular calcium and muscle contraction.

Intracellular Distribution

Parvalbumins are not restricted to muscle tissue alone. Recently, their presence has been reported in nervous tissue (Gosselin-Rey, 1974: Celio and Heizmann, 1981; Berchtold et al 1985; Gerfen et al., 1985; Endo et al., 1986b), and in other tissues such as the skin, testis, spleen, kidney, bone, teeth, and the ovary (Berchtold et al., 1984). Such a diverse distribution indicates that PV may have multiple functions associated with various calcium-dependent processes.

The distribution of PV, primarily determined using immunological methods, is summarized in Table III on page 57. Studies have shown that PV has a restricted immunological response in that cross-reactivity is limited to closely related species. In addition, no cross-reactivity has been observed between different isotypes of PV, or with the other $Ca^{2+}$-binding proteins (Gerday, 1982). It is therefore important when mapping the distribution of this protein by immunological means, to use antisera specific to a particular species.

Early studies of PV concluded that its localization was restricted to white muscle of fish and amphibians (Focant and Pechère, 1965). A decade later, evidence was presented indicating that the distribution of PV included tissues of higher vertebrates as well (Lehky et al., 1974; Pechère, 1974). More recently it has become clear that parvalbumins are present to some degree in all vertebrates including man (review by

Wnuk et al., 1982).

Even though parvalbumins are essentially muscle proteins, their quantity and distribution differ according to muscle type. High PV contents are found in white muscle, (Gosselin-Rey and Gerday, 1977) while low levels are noted in red muscles with high myoglobin contents (Hamoir et al., 1980). With regard to fiber type, PV is abundant in type 2 fibers but virtually absent in type 1 extrafusal fibers when compared to standard myofibrillar ATPase staining (Celio and Heizmann, 1982). Within the type 2 categorization of fibers (types 2A, 2B, and 2C) there is a continuum of PV concentrations (Celio and Heizmann, 1982), closely following the aerobic and anaerobic metabolism in these cells. This histochemical finding is supported by electrophoretic analysis of typed single muscle fibers (Heizmann et al., 1982). Only those fibers judged as type 2B/FG produced a large PV spot at the characteristic molecular weight and isoelectric point on two-dimensional gels. No spot could be identified on the gels from type 1/SO fibers. Type 2A fibers with fast-oxidative-glycolytic properties vary in their PV content. However, there are a few exceptions to this categorization. Significant amounts of PV are present in red muscles (with predominantly slow-oxidative fibers) of the electric eel (Childers and Siegel, 1976) and carp (Gosselin-Rey et al., 1978). In the chicken, on the other hand, PV is absent from white breast muscle (Le Peuch et al., 1979). Therefore, the relationship between high PV and low myoglobin content (Gerday et al., 1979) does not hold for all species.

More convincing is the correlation of PV immunoreactivity with relaxation time and the development of the SR (Celio and Heizmann, 1982). Parvalbumin antisera react the strongest toward fibers with the fastest relaxation times and consequently the most well developed SR, such as that in type 2/FG fibers. A continuum of PV staining intensities results as these two properties change within the muscle.

In muscle spindles, PV has been localized in one of the nuclear chain intrafusal fibers but in none of the nuclear bag fibers (Celio and Heizmann, 1982). These workers suggested that the intrafusal chain fiber probably has faster relaxing

properties than do the bag fibers or the non-reactive chain fiber. A comprehensive study of the regional distribution of PV in intrafusal fibers does not exist at this time.

Of the non-muscle tissues examined, the cerebellum and neocortex of the brain contain significant quantities of PV (Table III). The PV found in many of these non-muscle tissues cross-reacts with muscle anti-PV serum (Heizmann, 1984). Rat brain PV, the only non-muscle PV that has been fully isolated and characterized (Berchtold et al., 1982b , is indistinguishable biochemically and immunologically from muscle PV.

Parvalbumin appears to be a soluble protein, freely dispersed throughout the cytosol. Indirect immunofluorescence applied to carp muscle (Benzonana et al., 1975, 1977) has shown a uniform distribution of PV in myofibrils with no specific localization to any particular intracellular organelle. In skinned muscle fibers, PV will diffuse completely out of the cells (Gillis et al., 1979). The data from these morphological and biochemical studies indicate that PV is not associated with any particular structure(s) within the cell even though its relationship with $Ca^{2+}$-regulation suggests that it might be.

Ultrastructural localization of PV in cells of the brain is inconclusive (Heizmann and Celio, 1986). Pre-embedding staining techniques used to study PV in zebra finch (Zuschratter et al., 1985) and rat (Heizmann and Celio, 1986), revealed labelling associated with microtubules, intracellular membranes and postsynaptic densities. Post-embedding techniques performed on rat cerebellum (Heizmann and Celio, 1986) concluded that PV was indeed homogeneously dispersed throughout the cytoplasm of the cell. Similar kinds of studies have not been published on muscle or other non-muscle tissue.

Quantitation of Parvalbumin

Parvalbumin has been identified in every mammalian species studied, and it has been localized in a wide variety of cells by immunohistochemical techniques

(Heizmann, 1984). Quantitatively, its content differs considerably between individual cells or between tissue types as well as within particular tissues. Estimations of the amount of PV contained within these various tissues has aided in the understanding of its biological significance. Table III summarizes the various tissues examined to date and their corresponding PV content. Reports of PV concentrations may vary somewhat due to the method of detection. Instead of the more conventional methods, high performance liquid chromatography (HPLC) is now commonly used for small quantities of tissue because of the high percent yield obtained with this technique. In addition, HPLC is a sensitive and efficient tool for peptide analysis (Berchtold et al., 1983). Immunochemical quantification of PV has also been successful by recently developed RIA procedures (Berchtold et al., 1985; Endo et al., 1985a, 1985b) and ELISA methods (Leberer and Pette, 1986a, 1986b).

The aim of this section of the thesis was to document the changes in the concentration and distribution of PV in intrafusal and extrafusal muscle fibers of the fast-twitch EDL and the slow-twitch soleus muscles of normal and genetically dystrophic mice by biochemical and immunochemical techniques. Because muscular dystrophy is a progressive disease and PV content appears to be developmentally regulated, this study was conducted on mice at 2 and 32 weeks of age. Animals at 2-weeks of age were chosen because clinical signs of dystrophy have not yet appeared and by 32-weeks of age the disease has reached an advanced state. An antiserum to mouse PV was raised in rabbits and used for immunological localization of PV at the light microscopic level. Since PV has been shown to be localized in specific fiber types, and since alterations in fiber types are a common feature of muscular dystrophy, a correlation between PV and fiber type was conducted using a modification of the conventional myosin ATPase staining procedure.

TABLE III. Summary of parvalbumin content in various species and tissue.

| Species/Tissue | Reference | PV Content |
|---|---|---|
| Mice | | |
| gastrocnemius | Heizmann et al., 1982 | 4.9 g/kg wet wt |
| soleus | (HPLC) | 0.01 |
| EDL | | 4.4 |
| Tibialis Anterior | | 4.8 |
| gastrocnemius | Klug et al., 1985 | 5.53 mg/g wet wt |
| Tibialis Anterior | (electrophoresis) | 4.86 |
| quadriceps | | 5.82 |
| Dystrophic Mice | | |
| gastrocnemius | Klug et al., 1985 | 3.24 mg/g wet wt |
| Tibialis Anterior | | 2.98 |
| quadriceps | | 3.44 |
| brain cultures | Pfyffer et al., 1984 | 5% total heat stable protein |
| Rat | | |
| gastrocnemius | Heizmann et al., 1982 | 3.3 g/kg wet wt |
| soleus | | 0.004 |
| EDL | | 2.4 |
| Tibialis Anterior | | 2.7 |
| brain (total) | Schneeberger et al., 1985 (HPLC & RIA) | 0.02 g/kg wet wt |
| cerebellum | Berchtold et al., 1984 | 15 mg/kg wet wt |
| cerebrum | (HPLC) | 2 |
| cerebellum | Endo et al 1986b | 3217 ng/mg TSP |
| cerebrum | (RIA) | 128 |
| retina | | 1710 |
| lung,liver,spleen | | 10 |
| prostate | Berchtold et al., 1984 | 24 mg/kg wet wt |
| bone | (HPLC) | 15 |
| testis | | 11 |
| skin | | 86 |
| Horse | | |
| deep gluteus | Heizmann et al., 1982 | 0.001 g/kg wet |
| Man | | |
| vastus, triceps | | 0.001 |
| Guinea Pig | | |
| soleus | | 0.007 |
| sartorius | | 0.25 |
| Rabbit | | |
| EDL | Leberer & Pette, 1986a | 544 µg/g wet |
| soleus | (ELISA) | 4.4 |
| vastus (superficialis) | | 1200 |

# MATERIAL AND METHODS

## General

Normal (+/+) and dystrophic ($dy^{2J}/dy^{2J}$) adult male and neonatal male or female mice of the C57BL/6J strain were obtained from our own mouse colonies. Original breeding pairs were purchased from the Jackson Laboratories, Bar Harbour, ME and maintained by the cross-intercross system (Flaherty, 1981). Sibling +/+ mice were used as controls and homozygous $dy^{2J}/dy^{2J}$ animals were used as dystrophics for all experiments. Some of the normal mice were backcrossed with $dy^{2J}/dy^{2J}$ dystrophic mice resulting in $+/dy^{2J}$ heterozygotes. Heterozygote pairs were intercrossed for the production of $dy^{2J}/dy^{2J}$ progeny. This system was successful for all adult mice used in the project. Some modifications to this breeding system were necessary for the neonatal age group.

Clinical signs of muscular dystrophy are not manifested in the young mice of this strain until 3-4 weeks (Atwood and Kwan, 1978) so that the use of heterozygote intercross offspring is unreliable for animals less than 3 weeks of age. Therefore, only homozygote matings were used for mice of 1 and 2 weeks of age. This dystrophic murine strain is not a prolific breeder. Males are often infertile and have difficulty mounting their mates, whereas females often have problems delivering their offspring (Younger and Silverman, 1984). Methods were undertaken to obtain $dy^{2J}/dy^{2J}$ dystrophic animals, and included ovarian transplantation (Jones and Krohn, 1960; Tanioka et al. 1973) and artificial insemination (Wolfe and Southard, 1962) techniques. In addition, hindlimb amputations were performed to identify mice of the appropriate genotype in the 2-week age group.

Two-week-old mice were obtained from a cross between heterozygote males ($+/dy^{2J}$) and normal female mice carrying ovaries transplanted from homozygote females ($dy^{2J}/dy^{2J}$). Animals were anesthetized with ether, and the right leg from each 2-week-old heterozygote ($+/dy^{2J}$) mouse was amputated proximal to the knee

joint. The EDL and soleus muscles were subsequently dissected out and processed according to the methods described for immunohistochemical and histochemical analysis. At the time of surgery, the free endings of the major blood vessels were tied, the skin was sutured and clamped, and mice were allowed to recover under a heat lamp before returning them to their mothers. At 3 weeks of age, the mice were checked for clinical signs of dystrophy. Animals were considered dystrophic according to the following tests: splaying and clenching of the left hind leg and foot, inability to immediately recover balance after being spun by the tail, and inability to grasp the rungs of the cage top with the left foot while climbing the rungs or while the cage top was suspended upside down. Out of a total of 34 amputations, 31 animals survived the surgery and 14 of these were judged to be dystrophic. From this group, 10 mice were used for the immunohistochemistry experiments.

A general outline for the methodology involved in the immunocytochemical and biochemical aspects of this thesis work is depicted in Figure 18. The sample size (n) for each experimental group was 5 mice, unless otherwise specified. Parvalbumin was characterized in both age groups on one-dimensional sodium dodecyl sulfate (SDS) slab gels from which the proteins were electrophoretically transferred to nitrocellulose paper and immunoblotted with the PV antisera. Parvalbumin content was assessed by a radioimmunoassay (RIA) developed in Dr. K. Baimbridges's laboratory in the Department of Physiology, The University of British Columbia. The immunohistochemical localization of PV was accomplished by the standard peroxidase-antiperoxidase methodology. Histochemical fiber typing for myofibrillar ATPase was conducted according to a modification of the Brooke and Kaiser (1970) method utilizing metachromatic toluidine blue (Doriguzzi et al., 1983).

Characterization of Parvalbumin

Parvalbumin was initially characterized in samples of EDL and soleus muscles of 32-week and 2-week-old mice by the two-dimensional gel electrophoresis method of

Figure 18

Schematic illustration outlining the general methodology followed in this portion of the study. A. Parvalbumin from the fast-twitch muscle of normal mice was isolated on isoelectric focusing (IEF) tube gels. The band was excised and emulsified in PBS and Freund's complete adjuvant, and this solution was injected into rabbits. The antisera (1 AB) collected was tested for parvalbumin specificity and then used for immunocytochemistry (ICC), radioimmunoassays (RIA) and immunoblots. B. The actual experiments involved removing the extensor digitorum longus (EDL) and soleus (SOL) from both normal and dystrophic adult and neonatal mice. The muscles were either homogenized separately, lyophilized and the soluble protein subjected to one (1-D) or two (2-D) dimensional electrophoresis, or, alternatively, the muscles were cut in half and immediately frozen. One half was processed for ICC and the other for myofibrillar ATPase histochemistry.

## METHODS

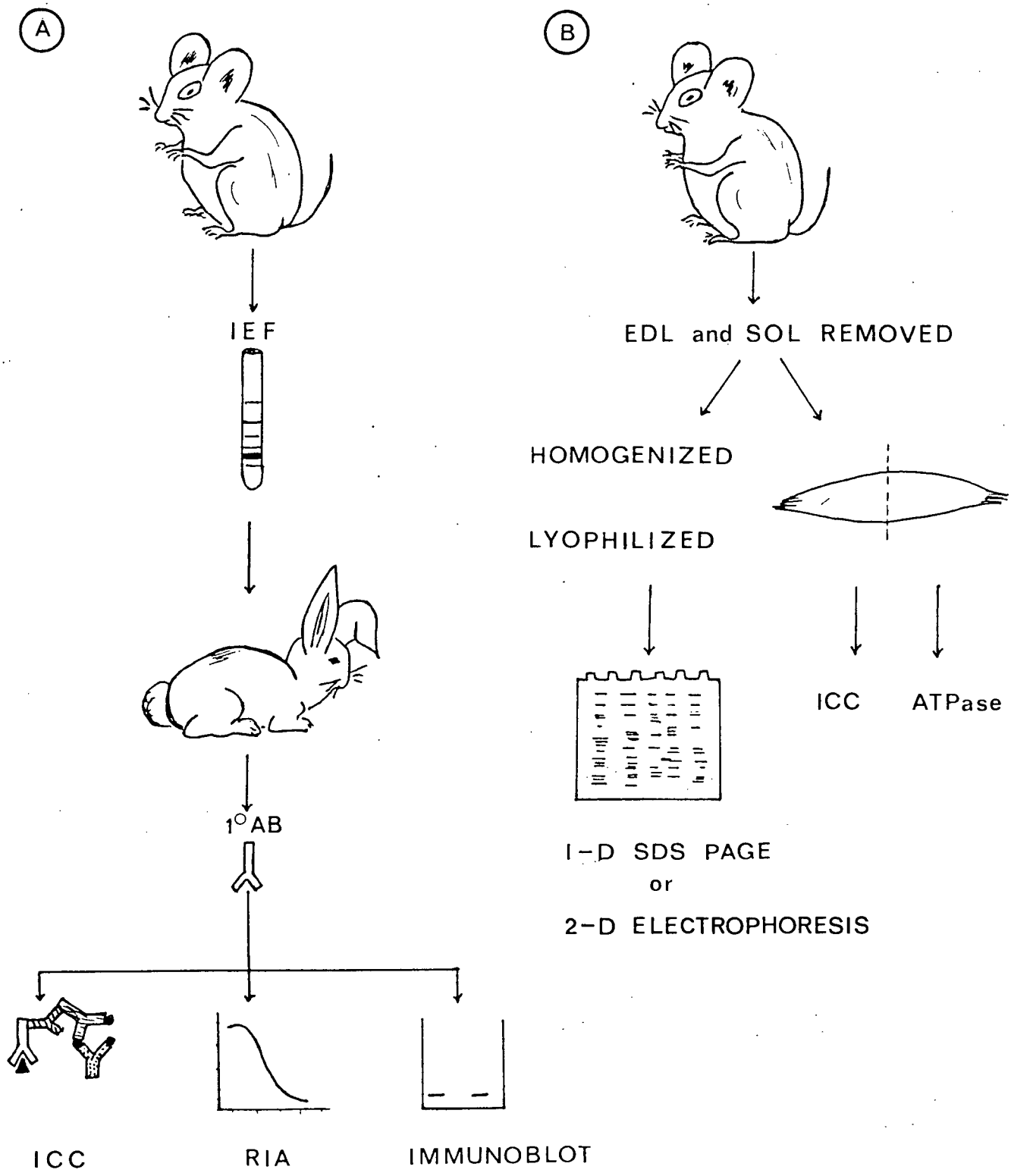
A
IEF
1°AB
ICC
RIA
IMMUNOBLOT
B
EDL and SOL REMOVED
HOMOGENIZED
LYOPHILIZED
ICC
ATPase
1-D SDS PAGE
or
2-D ELECTROPHORESIS

O'Farrell (1975). The protein band thought to be parvalbumin in the 32-week samples was identified in a series of comigration studies with authentic rat parvalbumin. This work was reported previously by Jasch et al., 1982 and Jasch and Moase (1985) and therefore, the two-dimensional electrophoresis data of the 32-week samples was not repeated in the present study.

i) Tissue Preparation. Normal and dystrophic mice were killed by cervical dislocation, and the EDL and soleus muscles were dissected out in toto from right and left hindlimbs. The muscles were weighed and homogenized separately with a glass-Teflon pestle homogenizer (TRI-R Instruments) for 5 min in 2 ml of 1 mM tris buffer at pH 7.4. An aliquot of homogenate containing 5 mg of muscle wet weight was placed in polypropylene tubes covered with Miracloth (Chicopee Mills), frozen in liquid nitrogen, and then lyophilized for 20 hr. These samples were run on 3 x 125 mm isoelectric focusing (IEF) tube gels that were subsequently used for two-dimensional electrophoresis. Aliquots of homogenate containing 11 mg of muscle wet weight were processed with the 5 mg aliquots, and subsequently run on 5 x 125 mm IEF tube gels. The concentration of the sample used for the IEF tube gels was based on the weight/volume ratio of 135 mg muscle wet weight/ml lysis buffer described previously (O'Farrell, 1975; Jasch et al., 1982).

ii) Two-Dimensional Electrophoresis. Lyophilized muscle samples from the 2-week-old mice were partially solubilized in the lysis buffer of O'Farrell (1975) using pH 5-7 ampholines (LKB). The sample was applied to the top of either 3 x 125 mm or 5 x 125 mm IEF tube gels. The first dimension was run according to the method of O'Farrell (1975), separating parvalbumin from the other muscle proteins by their isoelectric points. The samples were focused for 17 hr at 400 V and then for 1 hr at 800 V. The 3 x 125 mm gels were removed from the glass tubes by expulsion with air through a 30 ml syringe. These gels were stored at -70°C in 16x150 mm capped culture tubes containing 10 ml SDS sample buffer (10% glycerol, 5% mercaptoethanol, 2.3% SDS, 62.5 mM Tris) at pH 6.8 until running of the second dimension. The 5 x

125 mm gels were removed from the glass tubes in the same manner as with the 3 x 125 mm gels, but they were then placed into 7 mm diameter glass tubes and fixed for 2 hr at room temperature in a solution containing 150 ml methanol, 350 ml distilled water, 17.25 gm sulfosalicylic acid and 57.5 gm trichloracetic acid. The gels were then destained for 30 min in 25% ethanol and 8% acetic acid before being stained with Coomassie Brilliant Blue R250 (Eastman, 0.0287 gm/50 ml destain solution) for 30 min in a 60°C water bath. The gels were then rinsed with destain solution and stored in capped culture tubes for 3 days in the dark, with one to two solution changes. The tube gels were photographed on a fluorescent light box with Technical Pan 2415 Kodak film.

Comigration of authentic rat muscle parvalbumin with the EDL homogenate samples on IEF and two-dimensional gels was conducted in a previous study (Jasch and Moase, 1985). Comigration of pure rat muscle parvalbumin with the dystrophic soleus homogenate on 5 x 125 mm IEF gels was performed in one experiment in the present study, as described previously by Jasch and Moase (1985).

The second dimension was performed on 5-22.5% exponential acrylamide gradient SDS slab gels, 17 cm x 10 cm x 1 mm. The 3 x 125 mm IEF tube gel was adhered to the top of the SDS slab gel with 2% agarose, in SDS sample buffer, such that the acidic end of the tube gel could migrate down the right-hand side of the slab gel. A notch was made in the agarose for molecular weight markers (B-galactosidase, 13 kilodaltons (KD); phosphorylase-a, 10 KD; human serum albumin, 66 KD; pyruvate kinase, 57 KD; DNAse I, 43 KD; soybean trypsin inhibitor, 21.5 KD; lysozyme, 14.3 KD) next to the acidic end of the gel. All were purchased from Millipore whereas bovine serum albumin (66 KD) was obtained from Sigma. Electrophoresis was carried out as described by O'Farrell (1975) for 10-12 hr at an initial constant current of 25 mA. Once the dye front had migrated through the stacking gel, about 2 hr, the amperage was increased to 30 mA for the remainder of the run. The slab gels were soaked in a deampholizing solution of 50% ethanol, 7% acetic acid and 0.005% Coomassie Blue R250

for 36 hr. After the gels were rehydrated for 2 hr in 7% acetic acid and 0.005% Coomassie Blue R250, the protein and polypeptide spots were visualized by staining for 30 min in 50% trichloroacetic acid (TCA) and 0.1% Coomassie Blue R250. The gels were destained for several days in 7% acetic acid, vacuum sealed in plastic bags, and photographed on a light box with Technical Pan 2415 Kodak film.

Antisera production

Prior to the initial immunization injections, approximately 50 ml of preimmune serum was collected from rabbits and 100 µl aliquots were stored for use later as control antiserum. Antisera to mouse and rat skeletal muscle parvalbumin was raised in 2 adult rabbits based on the procedure described by Lazarides and Hubbard (1976). Rat parvalbumin purified by high performance liquid chromatography (HPLC) was purchased from CalBiochem-Behring. Mouse muscle parvalbumin was resolved from crude muscle homogenate samples obtained from the medial gastrocnemius of normal adult mice. Parvalbumin was resolved in 5 mm x 125 mm isoelectric focusing (IEF) gels, as described above, as a single prominent band at pI = 5.45. A number of these bands were carefully excised from the stained gels, and emulsified in 1 ml 0.15 M phosphate buffer at pH 7.4 and 1 ml Freund's complete adjuvant (DIFCO Laboratories). The emulsion was subsequently injected intramuscularily into the hindlimb of each rabbit, alternating right and left sides with each booster injection. Each injection contained approximately 150-200 µg parvalbumin. The amount of parvalbumin in each band was estimated by simultaneously running 50 µg quantities of the pure rat parvalbumin on IEF gels as a standard for spectrophotometric readings. Gels were scanned on a Gilford spectrophotometer (Leeds and Northrup) before the bands were removed, and the absorbance was compared to the rat parvalbumin standard.

Immunizations were in 2-week intervals. The first bleeding was performed 10 days after the eighth week. Approximately 1 ml of blood was collected into an equal volume of phosphate buffered saline (PBS), 5 mM ethyleneglycol-bis-β-aminoethyl ether

(EGTA) and 0.02% sodium azide (pH 7.3). The blood was centrifuged for 15 min at 2500 x g, and aliquots of the serum were stored at -70°C. Specificity of the antisera was tested by the procedures described below.

The rabbit in which the antisera to mouse parvalbumin was raised was bled a total of 3 times over a 52 -week period, whereas the rabbit in which the antisera to rat parvalbumin was raised was bled a total of 5 times over 78 weeks. Each bleeding resulted in approximately 30 ml of antiserum. The rabbits were bled by a small incision to the marginal vein of the right ear, and the blood was allowed to drip into a glass beaker containing PBS, EGTA and sodium azide. The blood was centrifuged for 30 min at 5000 x g and the serum was pooled. Separate aliquots of 20 ml, 1.5 ml and 100 µl were stored either at -70°C or at -20°C.

Characterization of the Antibody

The antibody to mouse skeletal muscle PV was characterized by the following methods. Triplicate enzyme-linked immunosorbent assays (ELISA) were conducted to determine the titre of the antiserum and its cross-reactivity with purified rat skeletal muscle PV. Monospecificity of the antiserum was evaluated by polyacrylamide gel electrophoresis (PAGE) and Western blotting, and radioimmunoassay (RIA).

i) Enzyme-Linked Immunosorbant Assay (ELISA). The standard ELISA test used in this study was based on that described previously (Engvall and Perlmann, 1971; Butler et al., 1978; Kelly et al., 1979). Falcon 3912 microtest assay plates (Fisher) were coated with pure rat parvalbumin (CalBiochem) at concentrations of 25, 50, 75 and 100 ng/well dissolved in carbonate buffer (pH 9.6), and incubated overnight at 4°C. The plates were washed three times with PBS-Tween, and the serum to be tested for anti-mouse parvalbumin was then added in doubling dilutions of 1:25 to 1:3200. Following an incubation for 90 min at room temperature with subsequent washing, the developing second antibody, sheep anti-rabbit immunoglobulin conjugated to alkaline phosphatase (SARIg) was applied at a 1:1000 dilution. After a final 90 min incubation and buffer

wash, p-nitrophenyl phosphate disodium (Sigma, 5 mg/5 ml 10% diethanolamine buffer), was added and the reaction was allowed to continue for 30 min. The reaction was measured for absorbance at 405nm on a Dynatech MR 580 microelisa reader. Each test was run in triplicate, and the preimmune rabbit serum was used as a control for each dilution. The results (Fig. 19) indicated that the titer of the antiserum against mouse parvalbumin was in the range of 1:200 - 1:1600. A working dilution of 1:400 was chosen for all immunohistochemistry experiments.

ii) Tissue Preparation for Immunochemical Studies. Preparation of tissue extracts that were used for one-dimensional gel electrophoresis, immunoblots, and radioimmunoassays was as follows. Individual muscles were weighed and minced with a razor blade. Two to four of the minced adult muscles were combined and homogenized in 20 times the volume of cold Tris buffer (62.5 mM Tris, 1 mM EDTA, and 0.02% sodium azide) at pH 6.7 with a Tekmar Tissumizer homogenizer. The normal 2-week muscles were combined to give an approximate final wet weight of 10 mg which was also homogenized in 20 times the volume of Tris buffer. Due to the scarcity of homozygous dystrophic neonates, the 2-week dystrophic muscles were combined to give an approximate final wet weight of 5 mg which was homogenized in 500 µl Tris buffer at 50% the concentration (31.25 mM Tris, 0.5 mM EDTA and 0.01% sodium azide). All homogenates were centrifuged at 39,000 x g for 45 min at 4°C, and the supernatant was divided into 100 µl aliquots. Muscle extracts used for gel electrophoresis and immunoblotting were divided into aliquots in 0.5 ml Eppendorf vials, and lyophilized for 12-18 hr. These freeze-dried samples were stored at -20°C until the SDS slab gels were run. The supernatant used for the RIA was stored in 10x12 cm siliconized glass tubes at -20°C until the assay was performed.

iii) Immunoblots. Electrophoretic blotting of proteins was performed according to the procedure of Towbin et al., (1979). The samples used in these experiments were aliquots of the muscles originally homogenized in twenty times the volume tris sample buffer as described previously. The 100µl freeze-dried tissue extracts from normal and

Figure 19

Binding response of the anti-mouse parvalbumin antiserum at various dilutions, to decreasing concentrations of the rat muscle parvalbumin (antigen concentration), as detected by an enzyme-linked immunosorbant assay (ELISA). Absorbance was measured at 405 nm. Antigen concentrations were measured in ng/100µl. The values given are the means of triplicate assays, normalized at each dilution to the background non-specific binding (absorbance of 0.065) determined by the preimmune control serum.

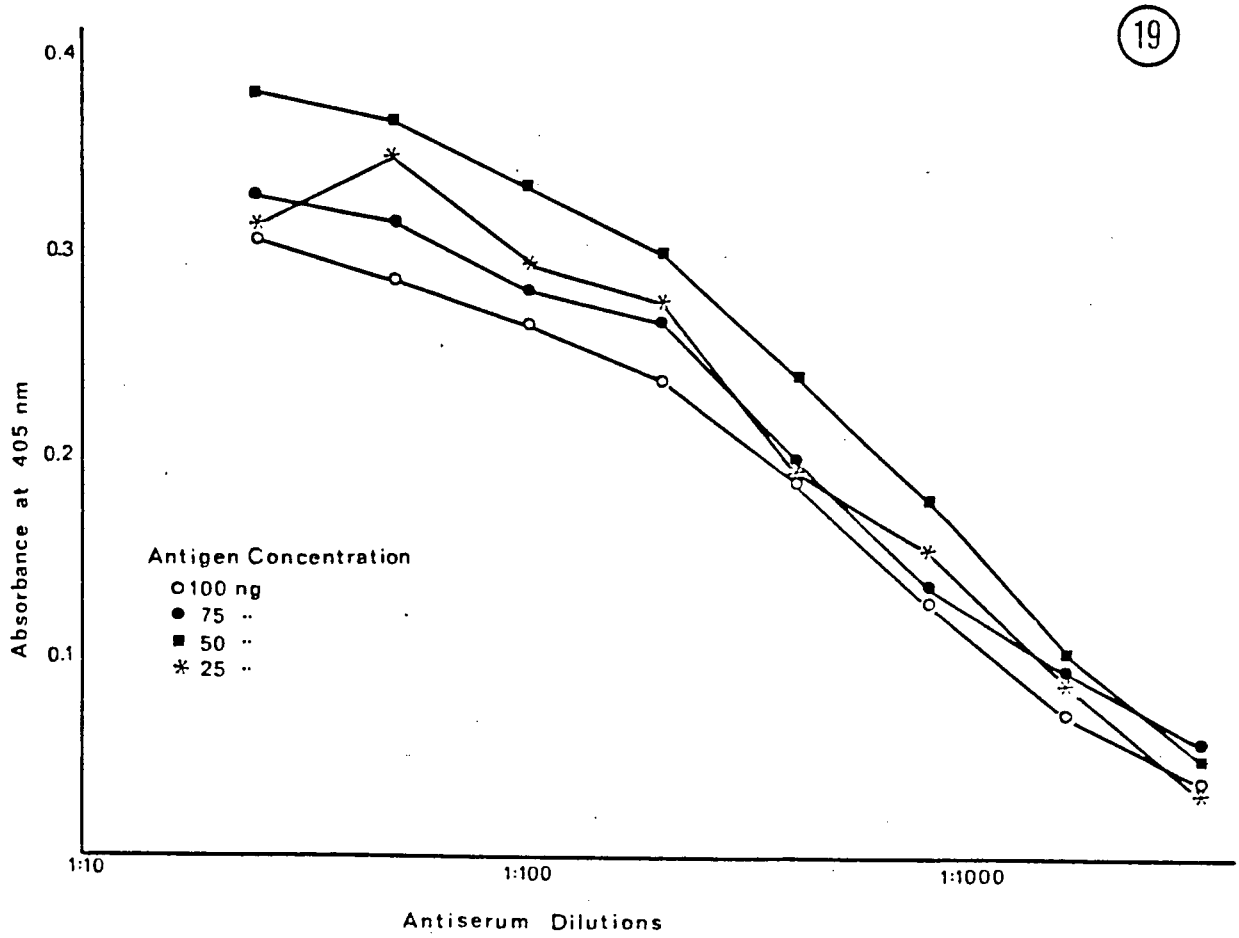
19
0.4
0.3
0.2
0.1
Absorbance at 405 nm
Antigen Concentration
o 100 ng
● 75 ··
■ 50 ··
* 25 ··
1:10
1:100
1:1000
Antiserum Dilutions

dystrophic mice at 32 and 2 weeks of age, were reconstituted with 50 µl of 10% glycerol, 2% SDS, and 0.1 M dithiothreitol (DTT). They were subsequently applied in duplicate halves to a 5-22.5% exponential gradient SDS slab gel, and run according to the second dimension of the two-dimensional technique described above. For a control, 25 µg of authentic rat muscle parvalbumin was run on the half of the gel to be blotted. At the end of the run the slab gel was divided in half, and one half was then stained and subsequently destained as described above. The corresponding half was notched in one of the lower corners and equilibrated in 500 ml of transfer buffer (25 mM Tris, 192 mM glycine, 20% v/v methanol) for 30 min at room temperature. The proteins were then electrophoretically transferred to a 0.45 µm pore nitrocellulose membrane on a Bio-Rad Trans-Blot Cell and power supply (Model 250/2.5). The transfer was run either cooled for 3 hr at high intensity (150 V) or cooled overnight at 40 V. After the nitrocellulose membrane was dried for 30 min at room temperature, it was washed for 1 hr in a blocking solution of 20 mM Tris, 500 mM NaCl, 3% fetal calf serum (FCS, CalBiochem-Behring), and 1% NGS pH 7.5, to saturate the free binding-sites. The gel was stained and destained as described above, and examined carefully for any remaining protein. The membrane was further washed in Tris-buffered saline containing 0.05% Tween-20 (TTBS, Bio-Rad) for 5 min and then incubated in anti-mouse parvalbumin antiserum (1:200) overnight at 4°C. Following two 5 min washes in TTBS, the membrane was incubated in goat anti-rabbit IgG-horseradish peroxidase conjugate (1:3000, Bio-Rad) at room temperature for 2 hr. The membrane was again washed twice in TTBS and then for a final 5 min in TBS. Colour development was achieved by soaking the blots in a 100 ml TBS solution containing 0.015% $H_2O_2$ and 60 mg 4-chloro-1-napthol (Sigma) which was first dissolved in 20 ml cold methanol. All incubations and washes were done with gentle agitation. The reaction was terminated after 20-30 min by repeated washing in distilled water, and the gels were photographed while wet with Technical Pan 2415 Kodak film. The blots were stored and protected from light, on filter paper covered with plastic wrap.

The spots from one of the 2-week normal EDL two-dimensional runs were cut out of the gel, and the proteins were eluted separately in 300 µl of 0.1% SDS at 4°C for 2-3 days. They were then minced and mashed, and centrifuged at 4,000 x g to separate the gel fragments. A 200 µl volume of 125 mM borate buffer (25 mM sodium borate, 75 mM NaCl, 1 mM EDTA, pH 8.4 ) was added to the supernatant and the PV concentration determined by RIA, as described below. Only the extracts from the spot believed to be parvalbumin resulted in complete displacement of $^{125}$I-PV binding to the antiserum used in the RIA. All the other spot extracts showed no displacement indicating an absence of parvalbumin.

iv) Radioimmunoassay. Cross-reactivity of the anti-mouse PV antiserum was tested on a RIA against two other calcium-binding proteins, bovine brain calmodulin and calcium-binding protein (CaBP). Calmodulin (16,723 daltons) was purchased from Calbiochem whereas CaBP was purified by Dr. Baimbridge, of the Department of Physiology, from bovine cerebellum. The principle for the RIA used in this study is outlined in Figure 20 and the general procedure for all the radioimmunoassays used in this study is as follows.

Rat skeletal muscle parvalbumin (CalBiochem) was iodinated according to the Chloramine-T technique of Greenwood and Hunter (1963). Since mouse or rat PV contains no tyrosine residues (Table II) the pH of the iodination buffer was increased from 7.4 to 8.6 in order to tag histidine. Briefly, 5 µg of rat parvalbumin was dissolved in 10 µl of 0.05 M disodium hydrogen phosphate buffer at pH 8.6, 10 µl of $^{125}$I (Amersham), and 10 µl of Chloramine-T (5 mg/ml buffer). This solution was kept on ice and the reaction was allowed to proceed for 2 min. Iodination was stopped by the addition of 10 µl of Na metabisulphite (24 mg/ml buffer) and quenched with 1 ml potassium iodine (10 mg/ml buffer). Unreacted iodine was separated from that bound to the protein on a Sephadex G-25 column, and eluted with 0.05 M sodium phosphate buffer (pH 7.4), 2 g/l BSA and 0.02% sodium azide at 4°C. The resulting $^{125}$I-parvalbumin had a specific radioactivity of 3 Ci/m mole.

Figure 20

Schematic diagram outlining the radioimmunoassay procedure used to quantitate the parvalbumin content in muscle samples. Unlabelled antigen (Ag), parvalbumin, in the muscle sample is mixed with a known dilution of antibody (Ab), so that the system is in antigen excess. Labelled parvalbumin ($^{125}I$) of a known concentration is added to the solution, and also becomes Ag-bound. The amount of labelled parvalbumin bound to the antibody is inversely proportional to non-labelled parvalbumin in the muscle sample. Free parvalbumin is separated from the bound $^{125}I$ parvalbumin by an excess of gamma-globulin, which precipitates the labelled complex. Radioactivity in the immunoprecipitant is counted on a gamma counter and the percent-binding is plotted as a function of the amount of competition added.

# RIA




Antigen & Antibody
in
muscle sample

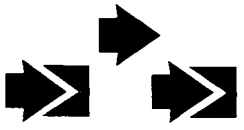

Incubation

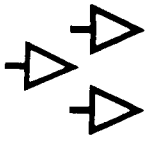

Add Radioactive Label ($^{125}I$)

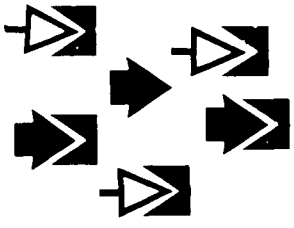

Incubation

Separate bound and free fraction
with $2^{\circ}$Ab

Count radioactivity bound to
immunoprecipitate

All assays were performed in triplicate in 10x75 cm glass tubes kept on ice. All dilutions were made in the RIA buffer prepared as follows. The stock barbital buffer contained 8 g of barbituric acid dissolved in 1000 ml of distilled water, while heating, to which 41.2 g of sodium barbital were added and the volume was brought to 2000 ml with distilled water (pH 8.2-8.5). The working buffer was then prepared by mixing 250 ml of stock barbital buffer with 6 g/L BSA, 1 mM EDTA and 0.02% sodium azide. The reaction mixture contained 700 µl of buffer, 100 µl of antiserum (1:400), and 100 µl of either standard or sample. The dilution series used for the PV standard (rat skeletal muscle from Calbiochem) ranged from 80 ng/100µl to 0.156 ng/100µl. CaBP was used in a dilution series of 240 to 7.5 ng/100 µl. Calmodulin was used in dilutions of 1 µg/100 µl to 31.25 ng/100 µl.

Maximum binding was measured in tubes containing 800 µl of buffer and 100 µl of either standard or sample. Tubes for nonspecific binding (NSB) measures contained only buffer. The assays were incubated overnight at 4°C followed by addition of 100 µl of labelled parvalbumin (10,000 cpm/tube). The assay was then returned to the cold (4°C) for 24 hr. For the RIA designed to test cross-reactivity of the antiserum the standards and label were added on the same day and incubated overnight at 4°C. Bound and free fractions were separated by the addition of 100 µl of bovine gamma globulin (8 mg/ml saline) and 1 ml of PEG (20% in $dH_20$). The assay tubes were vortex mixed until they appeared cloudy and then centrifuged at 4000 x g and 4°C for 30 min. The supernatant was drained by inversion of the tubes over a sink. The tubes were washed gently with a stream of tap water while inverted and allowed to dry prior to detection of $^{125}I$ on a Beckman model 1180 gamma counter. Standard curves showing the relationship between percent binding and the amount of unlabelled parvalbumin were plotted on semi-logarithmic paper. Percent binding was calculated as:

$$\frac{\text{counts (standard or sample) - NSB x 100}}{\text{total counts}}$$

## SPECIFIC METHODS

### Immunohistochemistry

Normal (+/+) and dystrophic ($dy^{2J}/dy^{2J}$) mice at 2 and 32 weeks of age were killed by cervical dislocation. The 2 week dystrophic animals were obtained by the amputation procedure described above. In an attempt to correlate muscle fiber-type and parvalbumin content, the fast-twitch extensor digitorum longus (EDL) and slow-twitch soleus muscles were dissected out, cut through the mid-belly regions and each half was processed separately either for immunohistochemical or histochemical staining procedures. Due to the high solubility of parvalbumin, the use of unfixed or postfixed cryostat sections was unsuitable for immunohistochemistry. Many fixation and embedding procedures were initially investigated as outlined in Table IV. Some of the tissue was embedded in Epon, and alternate semi-thick (1 µm) and thin (gold to silver) plastic-sections were stained for PV in an attempt to correlate the ultrastructural and immunohistochemical localization of this protein. Penetration of the antibody in the semi-thick plastic-sections was poor and the staining was unreliable, so that this method was not pursued any further. The most precise localizations of parvalbumin were achieved with a somewhat cumbersome and lengthy freeze-substitution fixation protocol (Feber and Sidman, 1958; Pearse, 1968, 1980) followed by paraffin embedding.

A preliminary test of the antisera titer (dilution range from 1:10 to 1:3200) was conducted on mouse cerebellum which is known to be positive for parvalbumin (Celio and Heizmann, 1981). A suitable antisera concentration was chosen based on this screening and on the ELISA test. The immunohistochemical method used was a modification of the unlabeled antibody enzyme-linked technique of Sternberger (1979). Muscle halves were frozen in isopentane cooled by liquid nitrogen and then immediately immersed into a vial of 1% picric/ethanol fixative kept at -70°C. The vials were surrounded by dry ice and then stored at -70°C for 2 weeks. The tissue was slowly dehydrated for paraffin embedding according to the following steps: (a)

three changes in ethanol over 12-24 hr at 4°C, (b) immersion for 6-12 hr in chloroform at 4°C, (c) immersion for 1 hr in chloroform at room temperature. Paraffin sections (10 µm thick) were collected on albumin-coated glass slides, and dried either for 2 hr at 60°C or for 24-48 hr at 40°C. After deparaffinization and subsequent rehydration in a graded series of ethanol, the sections were blocked in 10% $H_2O_2$ for 15 min, washed for 30 min in PBS, and then incubated in 5% normal goat serum (NGS) (Miles) for 30 min to reduce non-specific staining. The antiserum against mouse parvalbumin was applied to the sections at a 1:400 dilution in antibody buffer at pH 7.3 (PBS, 0.3% Triton X-100, 3% NGS) and incubated overnight in a moist chamber at 4°C. After the sections were washed in PBS for 15 min, they were incubated in a moist chamber at room temperature for 90 min in the second antibody, goat anti-rabbit (GAR) IgG (1:100, Miles). After another 15 min wash in PBS, sections were incubated with the rabbit peroxidase anti-peroxidase (PAP) complex (1:100, Cappel) for 90 min in a moist chamber at room temperature. Both the GAR and PAP were prepared in the antibody buffer containing normal goat serum. Final washes in PBS were followed by a rinse in 5 mM Tris-HCl buffer (TB) at pH 7.6. The enzyme reaction was developed with diaminobenzidine/$H_2O_2$ (Sigma), 30 mg/100 ml PBS containing 100 µl 3% $H_2O_2$, for about 10 min, after which the sections were rinsed in TB to stop the reaction.

The sections were then dehydrated through an ascending series of ethanol, cleared in xylene, and coverslipped with Cytoseal 60 (Stephens Scientific). Control slides were processed identically and simultaneously with preimmune serum from the same animal. Antiserum preabsorbed overnight with purified rat muscle parvalbumin was also used as a control. Sections were examined and photographed on a Leitz Orthoplan photomicroscope using Technical Pan 2415 Kodak film.

Histochemistry

A modified method for myosin ATPase staining was adopted because of its ease of

application (Doriguzzi et al., 1983). This method has the advantage of being less time consuming than previously published protocols. It also eliminates the use of ammonium sulfide, and all three extrafusal fiber types could be distinguished simultaneously with this procedure using the same pH.

The respective halves of the EDL and soleus muscles, corresponding to those processed for immunohistochemistry, were embedded in fresh mouse liver and frozen in isopentane cooled by liquid nitrogen, and stored at -70°C until required for sectioning. Serial cryostat-sections (10 µm thick) were collected on glass coverslips and air dried to room temperature before staining. The sections were stained for myofibrillar calcium-ATPase at pH 4.6 according to the method of Doriguzzi (1983). The coverslips were preincubated at room temperature for 5-6 min at pH 4.6, and then washed twice for 60 sec (two changes) in the basic medium. After a 20 min incubation at 37°C in the ATP basic medium, the sections were rinsed in 1% toluidine blue for 20 sec and then rinsed well with distilled water. Coverslips were then rinsed in ascending ethanol (70, 90 and 100%) for 2 min each, cleared in xylene, and mounted in Cytoseal 60 (Stephens Scientific). Photographs were taken on a Leitz Orthoplan photomicroscope using Technical Pan 2415 Kodak film.

Statistical Analysis

Muscle fibers were categorized and counted after PV immunohistochemical and myosin ATPase staining. They were designated light (L), dark (D), or intermediate (I) fiber-types using a Camera Lucida attachment to a Leitz bright field microscope. In the case of the myosin ATPase staining, this nomenclature corresponds to the more commonly used classifications (Brook and Kaiser, 1970; Peter et al., 1972): D = type 1/slow-twitch oxidative (SO), L = type 2A/fast-twitch, glycolytic (FG), and I = type 2B/fast-twitch, oxidative-glycolytic (FOG). Analysis of the data generated from these fiber counts included parametric analysis of variance (ANOVA) and Tukey's procedure for intercomparisons of normal and dystrophic group means. The statistical computer

programs in the "Stats Plus" and ANOVA packages supplied by Human System Dynamics were used for computations according to standard statistical procedures (Klugh, 1974).

Determination of Parvalbumin Content

i) Protein Determination. Total soluble protein (TSP) concentrations were determined in muscle extracts corresponding to those used for the RIA by the Bio-Rad method using porcine gamma globulin as a standard. Both the 32-week and 2-week normal samples were run on the standard (20-140 µg) Bio-Rad assay, while the 2-week dystrophic samples required the Bio-Rad microassay (1-20 µg). All standards and samples were made up in Tris saline buffer at pH 7.4 (100 mM NaCl, 20 mM Tris base, 1 mM EDTA, 1 mM DTT, 0.02% sodium azide). The assay tubes were shaken on a vortex, without frothing, and were allowed to sit at room temperature for 30 min. The protein concentration was determined, at optical density at 595 ($O.D._{595}$), on a Philips PV 8600 spectrophotometer and the TSP concentration was read from the standard curve (Figs. 21 and 22).

ii) Radioimmunoassay. The parvalbumin content in 32 and 2 week EDL and soleus muscles was measured by radioimmunoassay. Rabbit anti-mouse parvalbumin antiserum was developed in our laboratory. The parvalbumin used as a standard in the assay was from two sources. Purified rat skeletal muscle parvalbumin was purchased from Calbiochem and used at an initial dilution of 80 ng PV/100 µl buffer. In addition, an initial dilution of 32 µl/ml of a whole muscle homogenate from mouse fast-twitch muscle was also used as a standard. This dilution represented a PV concentration of 160 ng/ 100 µl buffer. In a preliminary assay, the standard curve produced using this initial dilution was found to compare favourably to that of the purified rat parvalbumin.

The muscle samples that were originally homogenized in a 20 times volume of Tris buffer were further diluted to 50 times volume in the Tris saline buffer used for the

Figure 21

Standard curve for the Bio-Rad Protein assay (20-140 µg), O.D.595. Total soluble protein values for all the 32-week muscle samples were extrapolated from this curve.

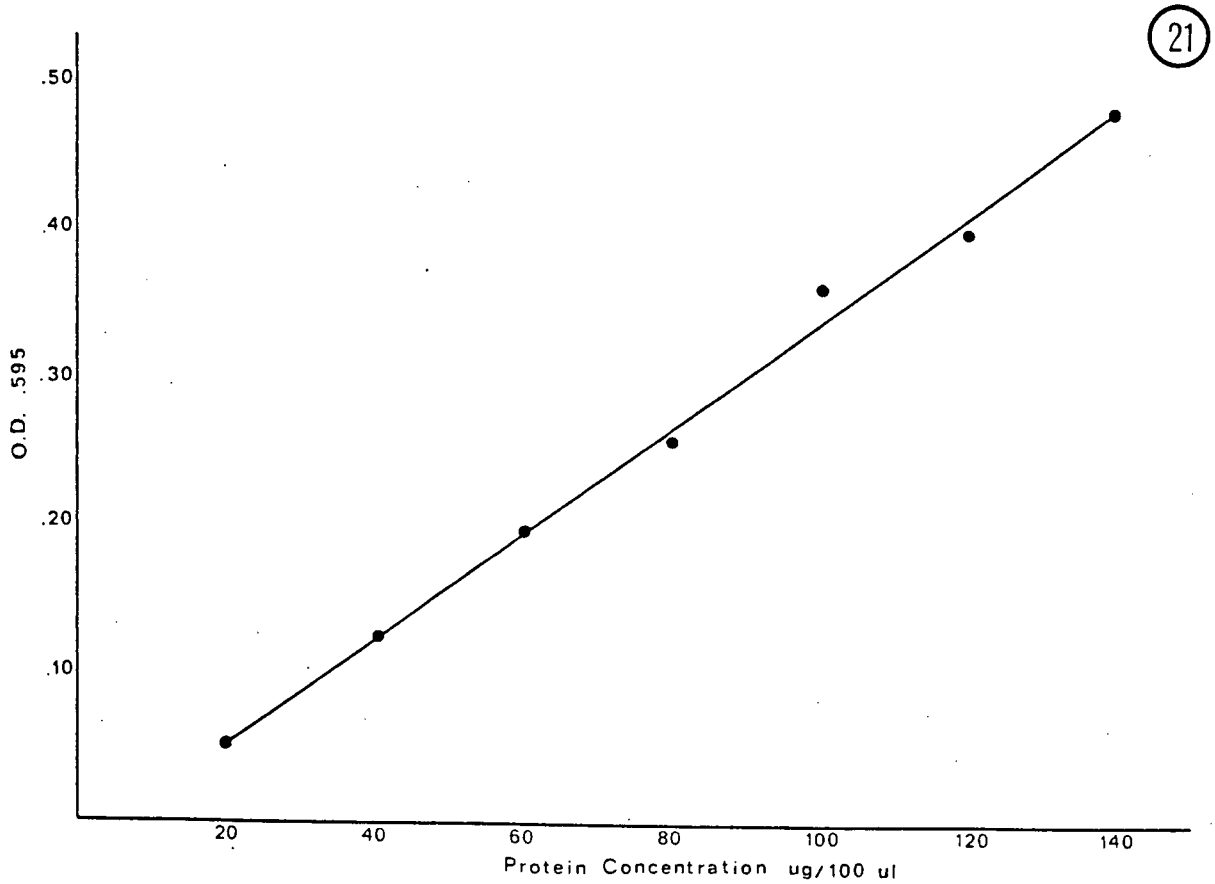
21
.50
.40
.30
.20
.10
O.D. .595
20
40
60
80
100
120
140
Protein Concentration ug/100 ul

Figure 22

Standard curve for the Bio-Rad Protein microassay (1-20 µg) used to calculate the total soluble protein in normal and dystrophic 2-week muscle samples.

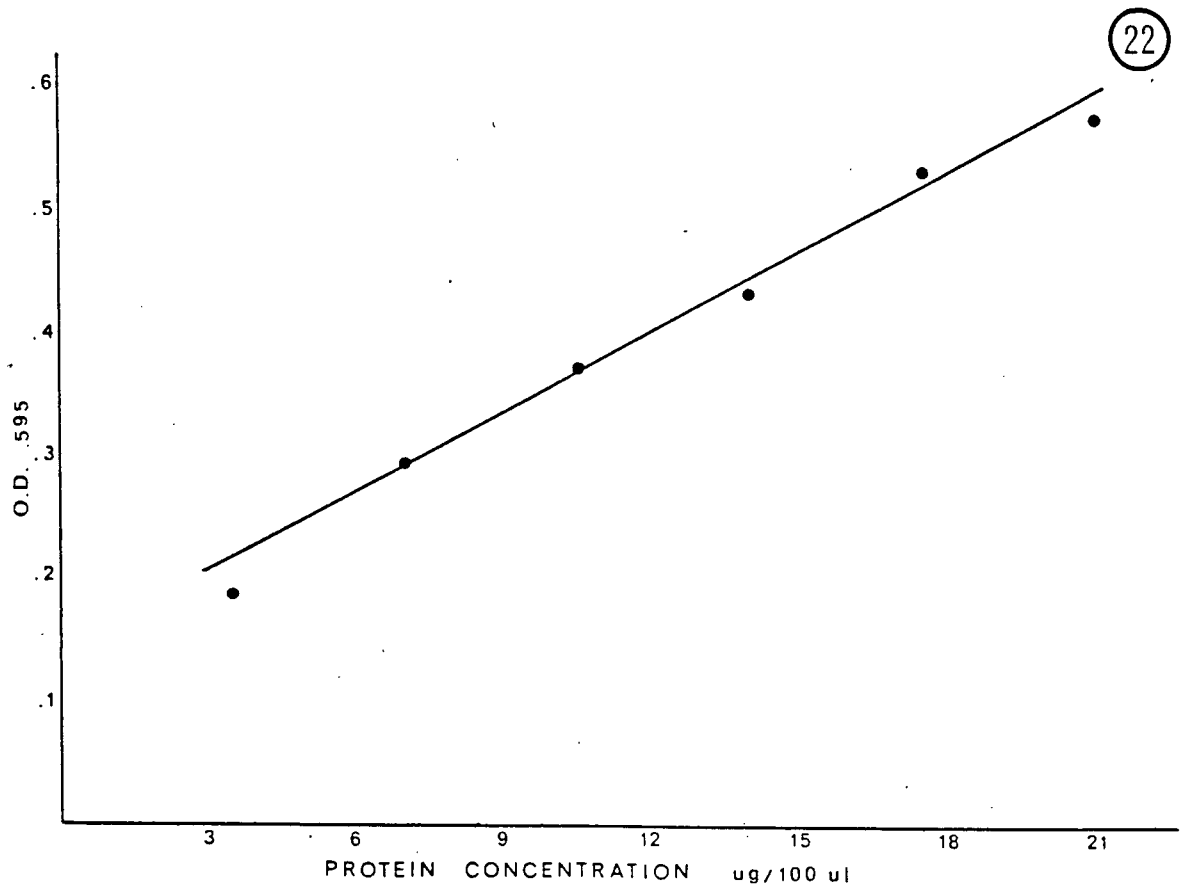
22
.6
.5
.4
.3
.2
.1
O.D. 595
3
6
9
12
15
18
21
PROTEIN CONCENTRATION ug/100 ul

protein assay. The samples were further diluted in RIA buffer and tested in the following concentrations:

| | |
|---|---|
| Normal 32 week EDL | 1:100, 1:200 |
| Dystrophic 32 week EDL | 1:25, 1:50 |
| Normal 32 week soleus | 1:5, 1:10 |
| Dystrophic 32 week soleus | 1:10, 1:20 |
| All 2 week samples | 1:5 - 1:160 |

All assays were run in triplicate as described under the general methods section for the RIA.

Parvalbumin content in the muscle sample was calculated by extrapolating a ng/100 µl value for parvalbumin at a given percent binding from the standard curve, and multiplying that by the appropriate dilution factor.

TABLE IV. Summary of fixation and sectioning methods investigated for the immunohistochemical localization of parvalbumin.

| Fixation | Embedding/ Sectioning | Morphology Status | Permeability to Antibody | Staining |
|---|---|---|---|---|
| 10% Ca++-Formalin acetate<br>- perfusion fixed<br>- post-fixed | cryostat, -floating and adhered to slides | -a | + | + |
| | - paraffin | -a | + | - |
| fresh tissue<br>- acetone or ethanol post-fixed | cryostat | - | + | - |
| 5% acrolein in PBS buffer | cryostat | -a | ++ | + |
| | paraffin | - | + | + |
| | Epon | +b | + | + |
| 2.5% glutaraldehyde in 0.1 M Sorensen's buffer | Epon | -b | - | - |
| 0.5% Benzoquinone in PBS buffer | cryostat | - | + | - |
| | paraffin | - | + | - |
| | Epon | - | - | - |
| Bouin's fixative | paraffin | - | + | - |
| | vibratome | + | +c | + |
| 4% paraformaldehyde/ 0.1% glutaraldehyde in 0.1 M Sorensen's buffer | cryostat | - | - | - |
| | Epon | + | - | - |
| | vibratome | + | -c | - |
| freeze-dried/ acrolein vapour-fixed | paraffin | - | - | - |
| freeze-substitution 1% picric acid in ethanol at -70°C | paraffin | +d | ++ | ++ |

- poor, + mediocre, ++ good
a shrinkage of the tissue upon final dehydration
b wrinkles in the Epon due to etching procedure
c problems mounting and stabilizing small tissue blocks: sections too thick
d some tissue artifact caused by either too slow freezing or allowing tissue to dry out before embedding

# RESULTS

## Characterization of Parvalbumin

The electrophoretic properties of mouse skeletal muscle parvalbumin have been shown to be similar to those of rat skeletal muscle parvalbumin (Heizmann, et al., 1982; Heizmann, 1984). The comigration experiments of pure rat skeletal muscle parvalbumin with normal EDL muscle samples, resolved on IEF gels (Fig. 23), showed that rat PV comigrates with the protein band identified as PV in a previous report (Jasch and Moase, 1985). In addition, rat PV comigrated with the band in the dystrophic soleus samples that was also believed to be PV (Fig. 24A). This band was not evident in muscle samples from the normal adult soleus (Fig. 24C).

Comparison of normal and dystrophic whole muscle samples by IEF (Fig. 25) showed a definite decrease in the density of the PV band in the dystrophic EDL at 32-weeks of age. A dramatic increase above normal levels was noted in this band in the adult dystrophic soleus at the same age. A number of other muscle proteins were altered in the dystrophic muscles but these have been identified and discussed in detail in a previous study (Jasch and Moase, 1985). By comparison, similar IEF experiments of the 2-week normal and dystrophic muscle samples (Fig. 26) showed no difference in the protein distribution between normal and dystrophic animals at this stage. In particular, the PV band was prominent in both EDL samples regardless of genotype, but it was undetectable in either the normal or dystrophic soleus muscle samples.

The positions of the mouse skeletal muscle proteins have been characterized on two-dimensional gels by other investigators (Crow and Kushmerick, 1982; Jasch and Moase, 1985). Comparison of our gels to those published was the basis for identifying the proteins labelled in Figures 27 - 30 of the 2-week samples. Examination of the 2-week samples confirmed that PV migrates as a single band to the 14 KD molecular weight range. This band was confirmed to be PV by RIA as described in the methods.

Figure 23

Isoelectric focusing (IEF) tube gels comparing normal mouse EDL muscle protein (1) to pure rat muscle parvalbumin (2). The protein band (PV) in the mouse migrates to the same isoelectric point as pure rat parvalbumin. Complete comigration studies of these samples have been reported earlier by Jasch and Moase (1985). IEF gels are oriented with the basic end to the left and the acidic end to the right. Mouse muscle samples are from normal 32-week-old animals.

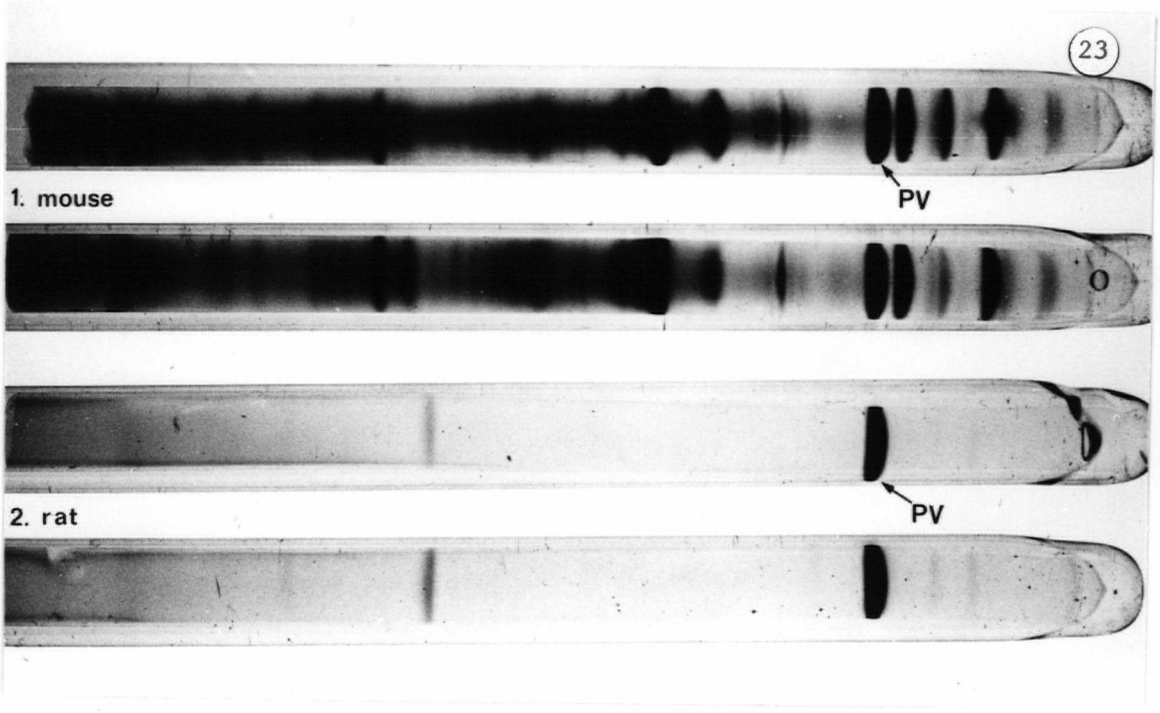
23
1. mouse
PV
O
2. rat
PV

Figure 24

Isoelectric focusing tube-gels comparing adult dystrophic (DY) and normal (N) soleus muscle proteins. Authentic rat muscle parvalbumin (PV) comigrates (A) with a protein band that appears in the dystrophic sample (B) but not in the normal sample (C), as indicated by the arrow. All gels contain proteins from 32 week mice. Acidic end to the left, basic end to the right.

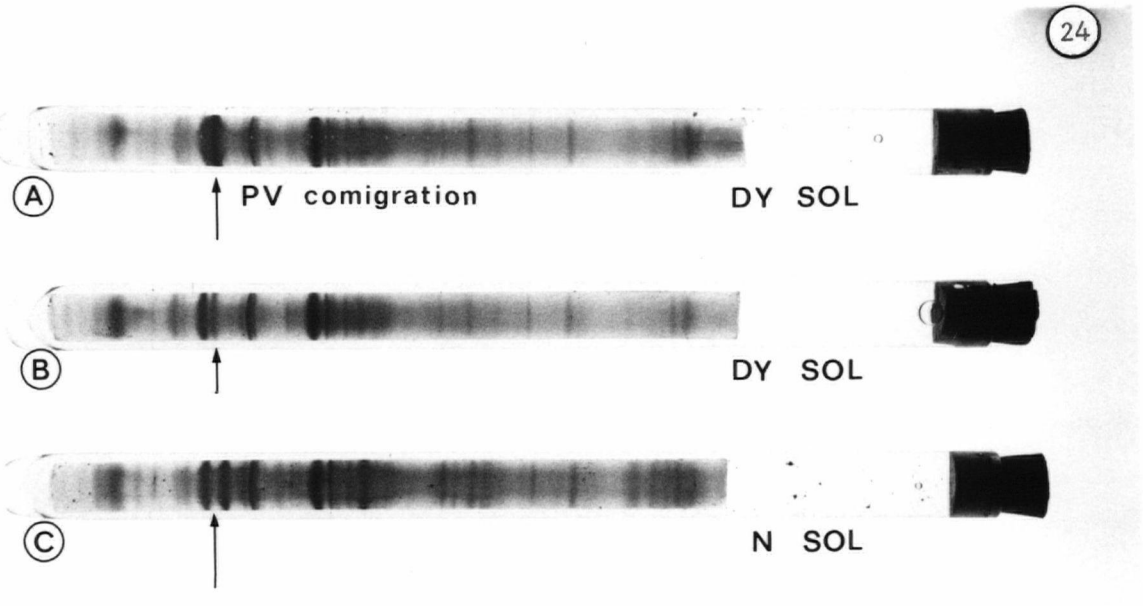
24
A
PV comigration
DY SOL
B
DY SOL
C
N SOL

Figure 25

Protein bands of normal (N) and dystrophic (DY) adult EDL and soleus (SOL) muscles separated according to their isoelectric point on isoelectric focusing tube-gels. The parvalbumin (PV) band is identified by an arrow. Note the appearance of this band in the dystrophic soleus and the decreased density of the PV band in the dystrophic EDL. IEF gels are oriented with the acidic end to the left and the basic end to the right.

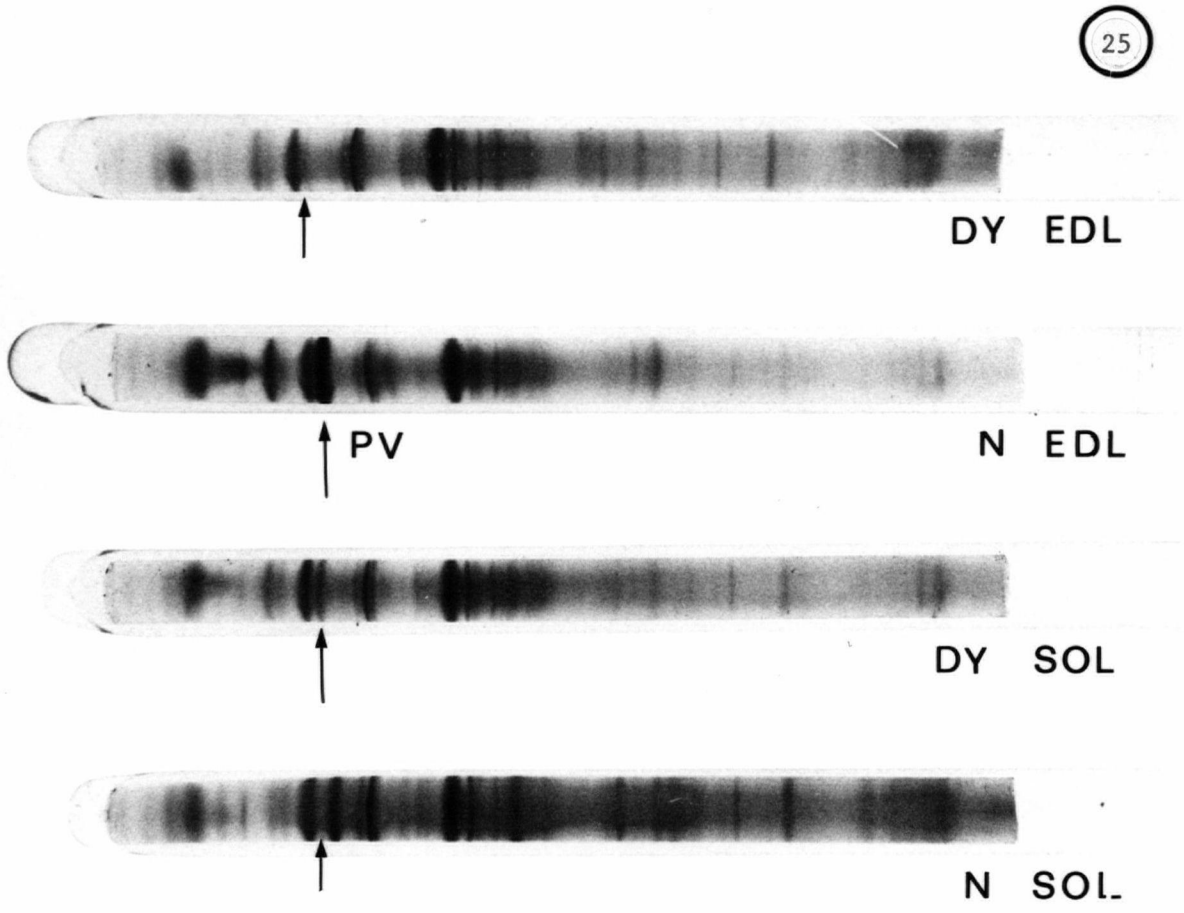
25
DY EDL
PV
N EDL
DY SOL
N SOL

Figure 26

Whole muscle protein distribution, isolated by isoelectric focusing tube gel electrophoresis, for normal (N) and dystrophic (DY) 2-week EDL and soleus (SOL) samples. The position of the parvalbumin band (PV) is indicated by the arrow for each gel. At 2 weeks of age only the EDL samples contain detectable quantities of parvalbumin. The density of the band appears to be similar for normal and dystrophic samples.

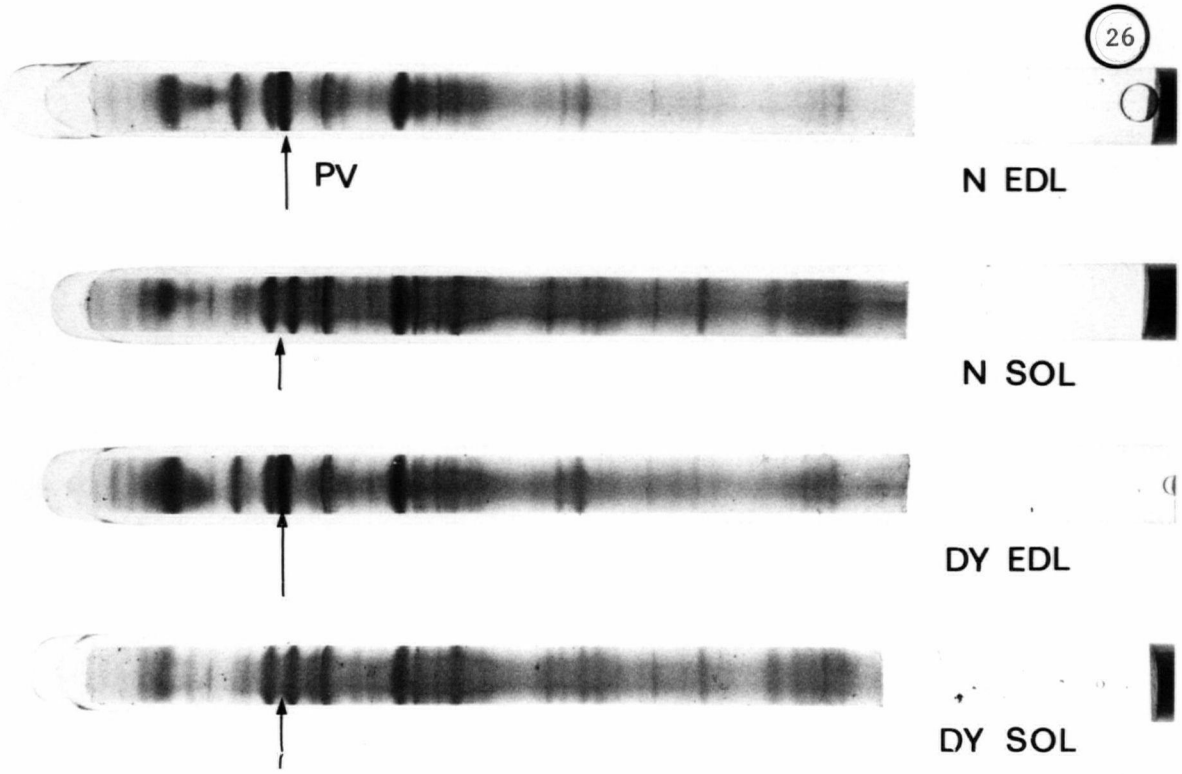
26
PV
N EDL
N SOL
DY EDL
DY SOL

The PV spot was prominent in the gels of normal and dystrophic EDL samples (Figs. 27 and 28) but barely detectable in either of the soleus extracts (Figs. 29 and 30). The distribution of proteins at 2 weeks of age was similar to that reported for the adult muscles (Jasch and Moase, 1985). This would indicate that the adult profile has been attained by 2 weeks of age; however, the adult protein concentrations are probably achieved later during postnatal development.

Characterization of the Antibody

The titre of the antisera against mouse PV was tested by ELISA procedures, as described in the methods, and the monospecificity by immunoblotting and RIA. The soluble muscle proteins were initially resolved by one-dimensional SDS electrophoresis (Fig. 31a) and then they were transferred to nitrocellulose paper for immunoblotting. As can be seen in Figure 31b, all of the low molecular-weight proteins transferred from the gel to the nitrocellulose. The left-hand lane in Figure 31a contained molecular weight markers; however, the corresponding lane in the half of the gel that was transferred (Fig. 31b) contained 25 µg of rat muscle PV.

As illustrated in Figures 32 and 34a, PV antisera did not react with any other proteins present in the muscle extract. In the adult samples, the PV antisera reacted most intensely to the rat muscle PV control, the normal gastrocnemius which was also used as a control, and the normal EDL (Fig. 32). As expected, the staining was less intense for the dystrophic EDL and soleus samples. Even though PV was undetected in the normal soleus by one-dimensional electrophoresis (Figs. 31a), the antisera reaction indicated the presence of trace amounts of the protein in the slow-twitch muscles regardless of genotype (Fig. 32).

The results of the RIA designed to test the cross-reactivity of the anti PV serum with CaBP and calmodulin, and thus its monospecificity, are depicted as standard curves in Figure 33. Only the PV standard resulted in complete displacement

Figures 27 and 28

Two-dimensional electrophoresis patterns of total muscle proteins separated according to their isoelectric points (IEF) and molecular weights (SDS), for 2-week normal (N) and dystrophic (DY) EDL muscle samples. Each IEF gel contained proteins derived from 5 mg wet weight muscle. IEF was run with the basic end to the left and the acidic end to the right. The prominent parvalbumin band (PV) appears in both normal and dystrophic samples at approximately 14 KD. Actin (A), tropomyosin (TM) and myosin light chains (LC) are also indicated.

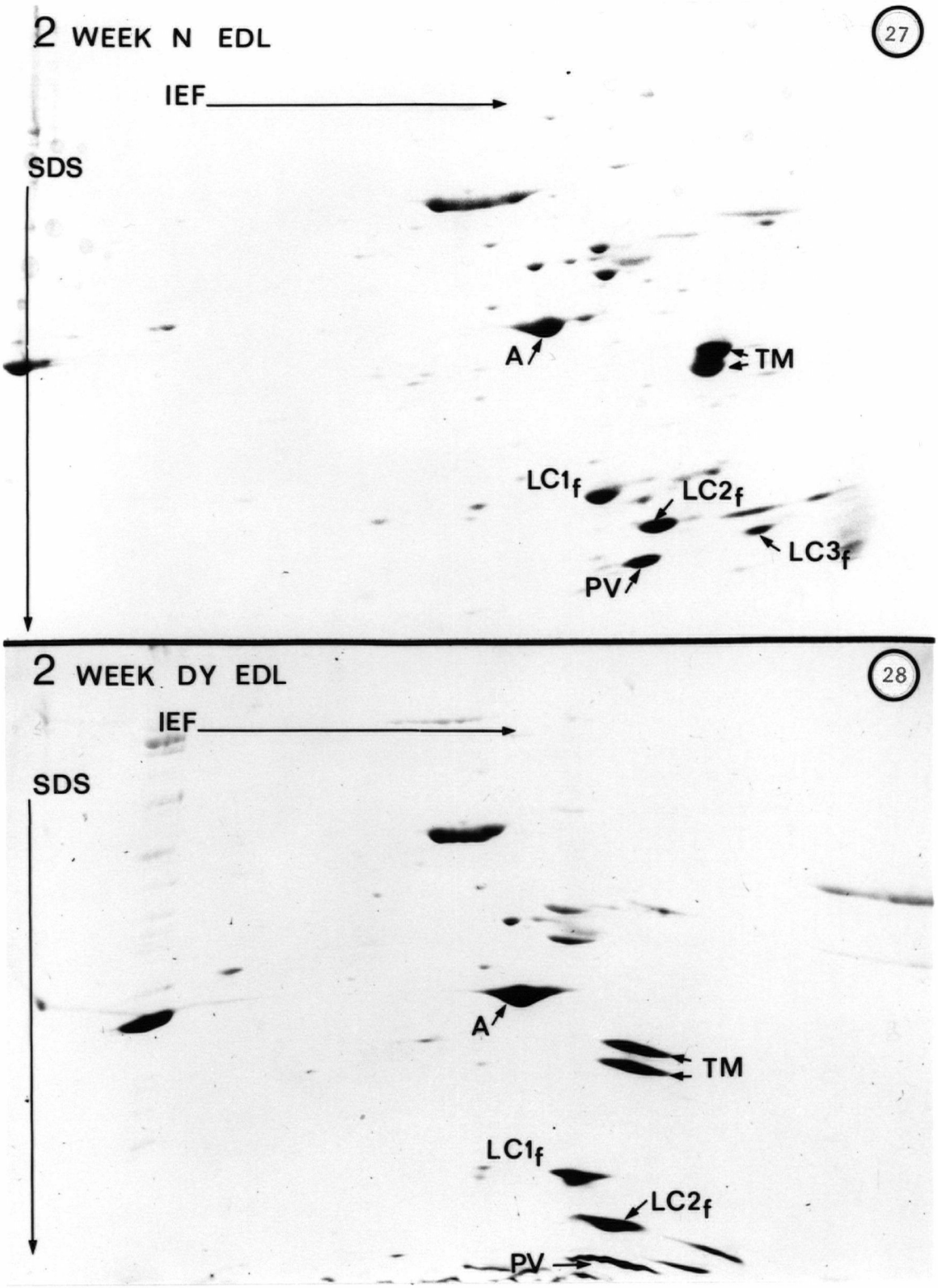
2 WEEK N EDL
27
IEF
SDS
A
TM
LC1f
LC2f
LC3f
PV
2 WEEK DY EDL
28
IEF
SDS
A
TM
LC1f
LC2f
PV

Figures 29 and 30

Two-dimensional patterns of total muscle proteins from normal (N) and dystrophic (DY) 2-week soleus, separated on 3 x 125 mm IEF tube-gels and on gradient SDS-PAGE according to O'Farrell (1975). IEF was from left (basic) to right (acidic). The parvalbumin band (PV) is barely visible in both normal and dystrophic electrophoretic patterns.

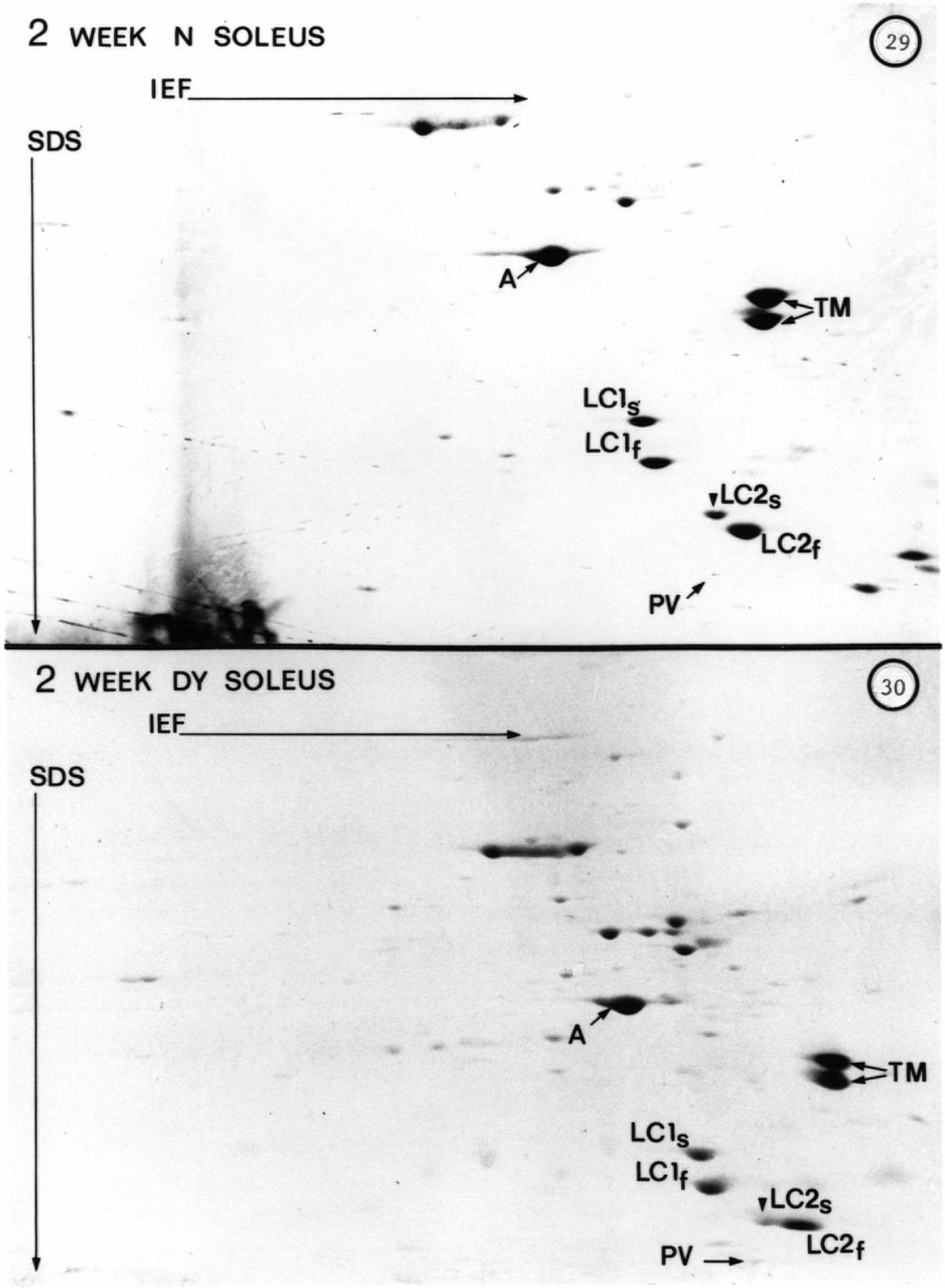
2 WEEK N SOLEUS
29
IEF
SDS
A
TM
LC1s
LC1f
LC2s
LC2f
PV
2 WEEK DY SOLEUS
30
IEF
SDS
A
TM
LC1s
LC1f
LC2s
LC2f
PV

Figures 31

A gradient 1-D SDS-PAGE (Fig. 31b) of adult muscle samples from which the proteins were transferred to nitrocellulose paper (Fig. 32), as described in Methods. The slab gel in Fig. 31a represents the corresponding half of the gel that was stained with Coomaisse Blue R250. The arrow indicates the parvalbumin band and the lanes are identified as follows: a) normal gastrocnemius; b) dystrophic EDL; c) normal EDL; d) dystrophic soleus; e) normal soleus.

Figure 32

Immunoblot (Fig. 32) of normal and dystrophic adult muscle homogenate samples, transferred from the SDS slab gels (Fig. 31b) The immunoblot is reversed to the pattern shown in Fig. 31a, with one exception. The extreme left-hand lane in Figure 31a contains molecular weight markers while the corresponding lane in Figure 32 contains pure rat parvalbumin. Only the normal (N) EDL, gastrocnemius (GAST), and parvalbumin control (PV) are heavily stained by the anti-mouse parvalbumin antisera.

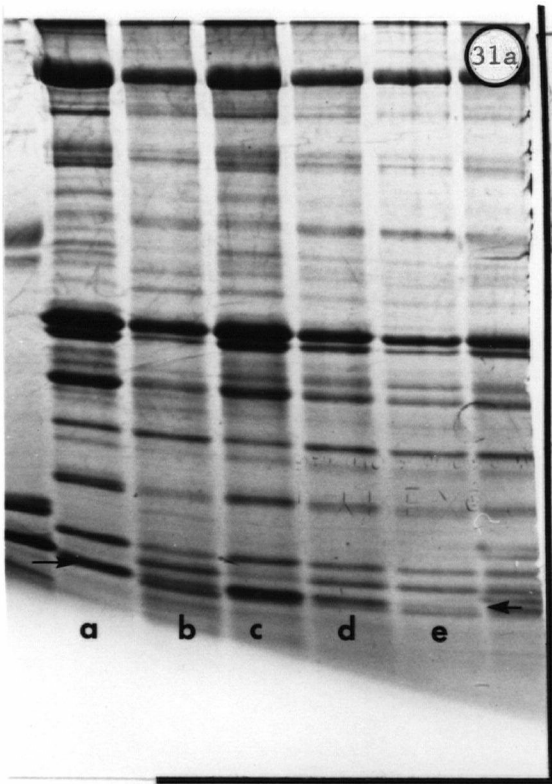
31a
a
b
c
d
e

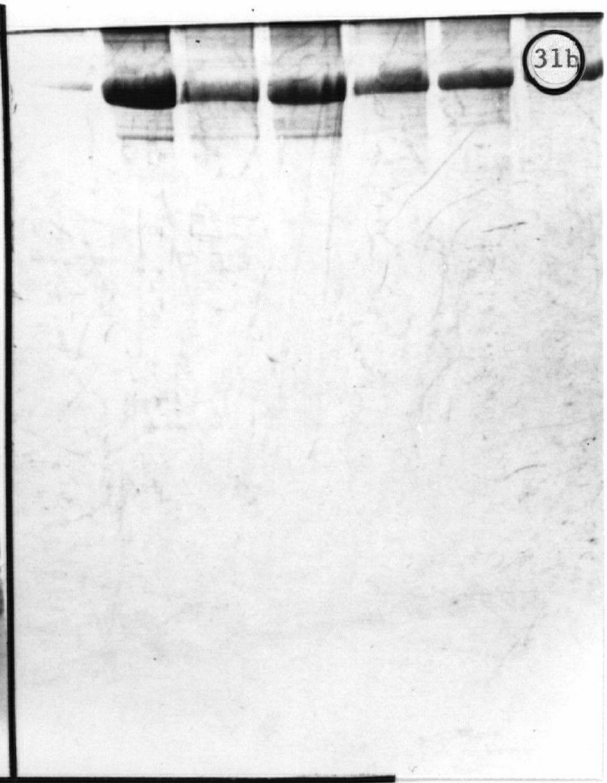
31b

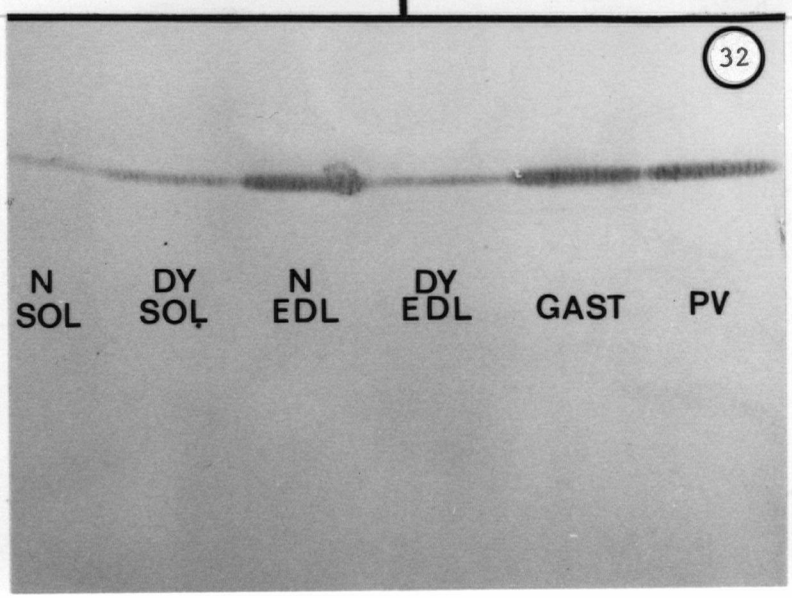
32
N SOL
DY SOL
N EDL
DY EDL
GAST
PV

of $^{125}$I-PV binding to the antiserum. No cross-reactivity with CaBP or calmodulin was observed.

The distribution of some of the higher molecular weight soluble-proteins was also altered in the dystrophic muscle at 32 weeks of age. Figure 34 shows the banding pattern for the adult muscle samples. Upon close examination of this gel, it is evident that the distribution of proteins (arrowheads) in the dystrophic EDL is similar to that of the normal soleus. Although less obvious, the pattern in the dystrophic soleus resembles that of the fast-twitch muscles with respect to particular protein bands. Only PV was identified on the gels. The other prominent bands were not characterized in the present study, but probably represent the various myosin light-chains, tropomyosin, troponin and actin.

Whereas definite changes in PV and some of the other muscle proteins could be seen in the adult preparations, the SDS gels and corresponding immunoblots of the 2-week extracts revealed identical features when comparing normal and dystrophic samples. Although differences could be seen between fast and slow-twitch muscles, no differences resulted due to genotype. The PV band was clearly identifiable in both EDL samples (Fig. 35b), and reacted positively to the antisera after immunoblotting (Fig. 35a). Parvalbumin was undetectable in either of the soleus samples by SDS-PAGE (Fig. 35b), but was faintly evident after immunoblotting (Fig. 35a).

Immunohistochemistry

The distribution of PV in muscle fibers was investigated by PAP methods using the antiserum against mouse skeletal muscle PV, on paraffin sections of muscle tissue fixed by freeze-substitution. Parvalbumin immunoreactivity was categorized into three groups of staining intensity: light (L), dark (D), and intermediate (I). The dark fibers were considered PV positive, whereas the light fibers were assumed to have no immunoreactivity to PV. A summary of the mean percentage of fibers in each category is given in Table V. Muscles were also fiber-typed for myofibrillar ATPase

Figure 33

Standard curve for the radioimmunoassay of rat skeletal muscle parvalbumin (--o--o--), bovine cerebellum CaBP (--●--●--), and bovine brain calmodulin, CaM, (--x--x--). No cross-reactivity between parvalbumin, CaBP or calmodulin was observed. A separate abscissa has been drawn for the two brain calcium-binding proteins.

(33)

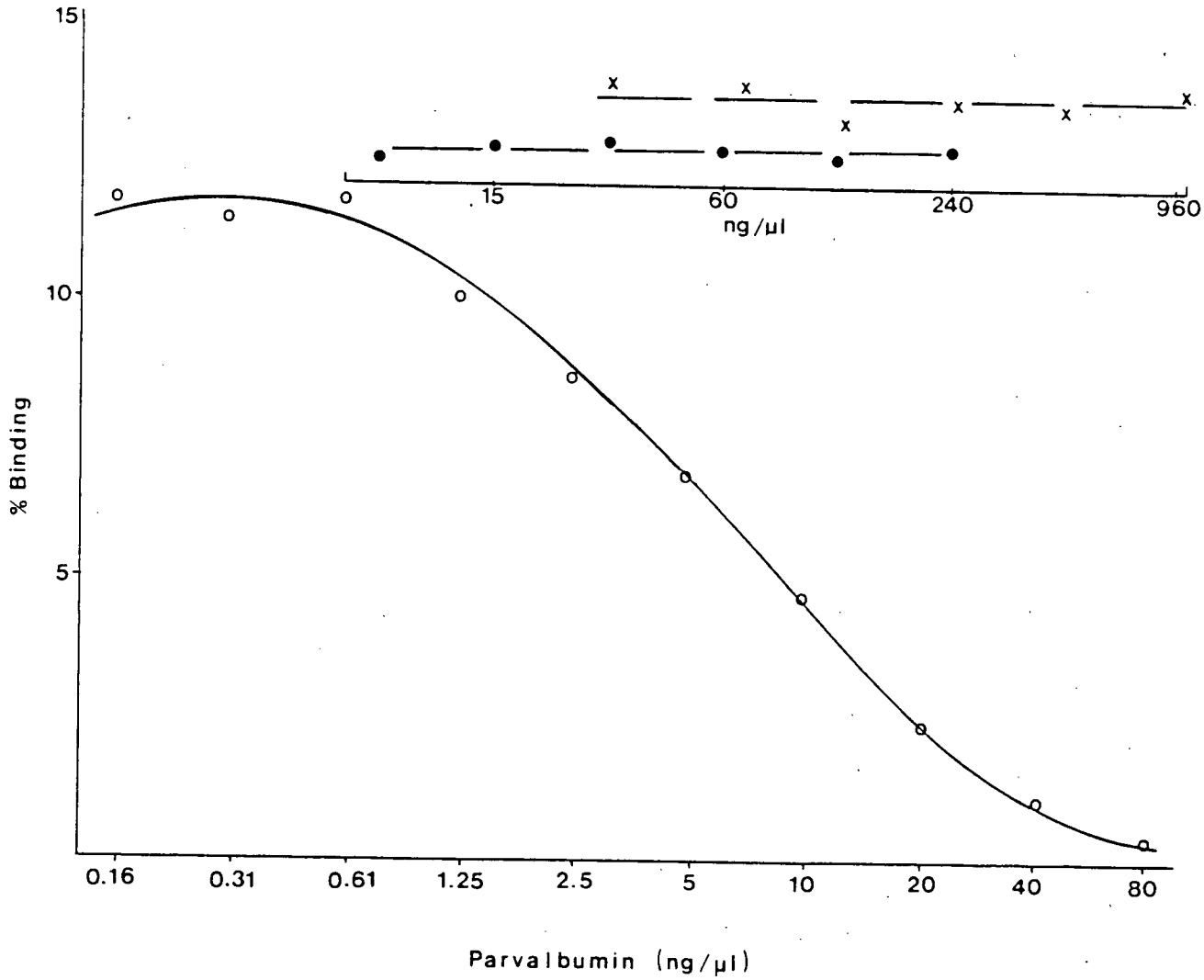
15
10
5
% Binding
0.16
0.31
0.61
1.25
2.5
5
10
20
40
80
Parvalbumin (ng/µl)
0
15
60
240
960
ng/µl

Figure 34

Gradient (5-22%) one-dimensional SDS-PAGE of 32-week normal (N) and dystrophic (DY) muscle proteins for gastrocnemius (GAST), EDL and soleus. The parvalbumin band (PV), approximately 14 KD, is indicated by the arrow. This gel corresponds to the immunoblot in Figure 31. Differences in the protein distribution between the normal and dystrophic, and fast-twitch vs slow-twitch muscles can also be seen in some of the higher molecular weight protein bands (arrowheads). None of which bands reacted with the parvalbumin antisera on the immunoblot. Molecular weight markers are indicated in kilodaltons (KD) in the extreme left column.

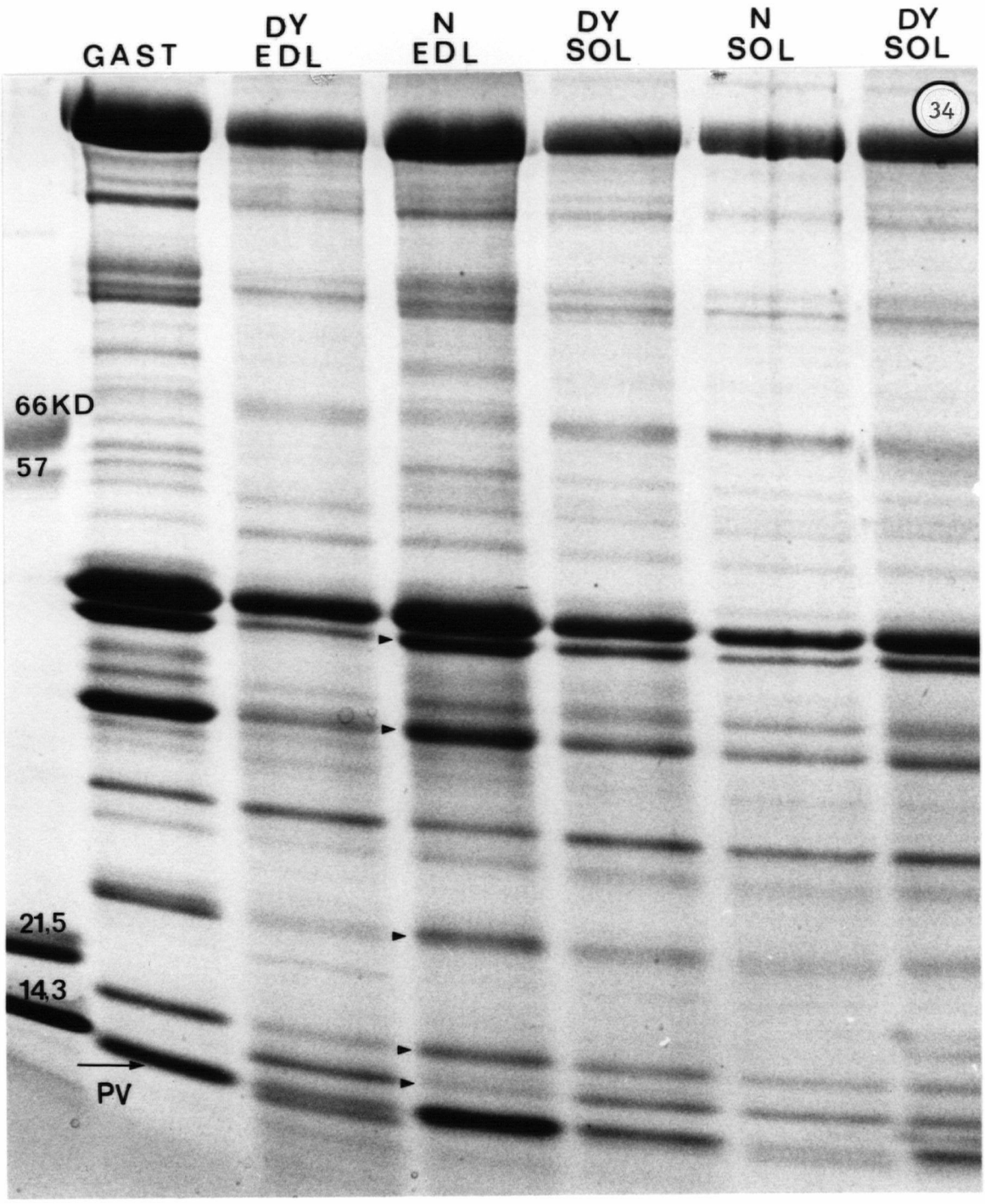
GAST
DY EDL
N EDL
DY SOL
N SOL
DY SOL
34
66KD
57
21,5
14,3
PV

Figure 35

Immunological analysis of 2-week normal (N) and dystrophic (DY) whole muscle homogenates after separation on SDS-PAGE (Fig. 35b) and electrophoretic transfer to nitrocellulose paper (Fig. 35a). Authentic rat parvalbumin was run on the half of the gel to be blotted, as a control for the antisera. The banding pattern shown on the nitrocellulose membrane (Fig. 35a) is reversed to that seen in the slab gel. Nitrocellulose was incubated with anti-mouse parvalbumin antiserum. The parvalbumin band is indicated by the arrow. Both normal and dystrophic samples show similar protein distributions at 2 weeks of age. Molecular weight markers are indicated in kilodaltons (KD), in the far right column of (Fig. 35b).

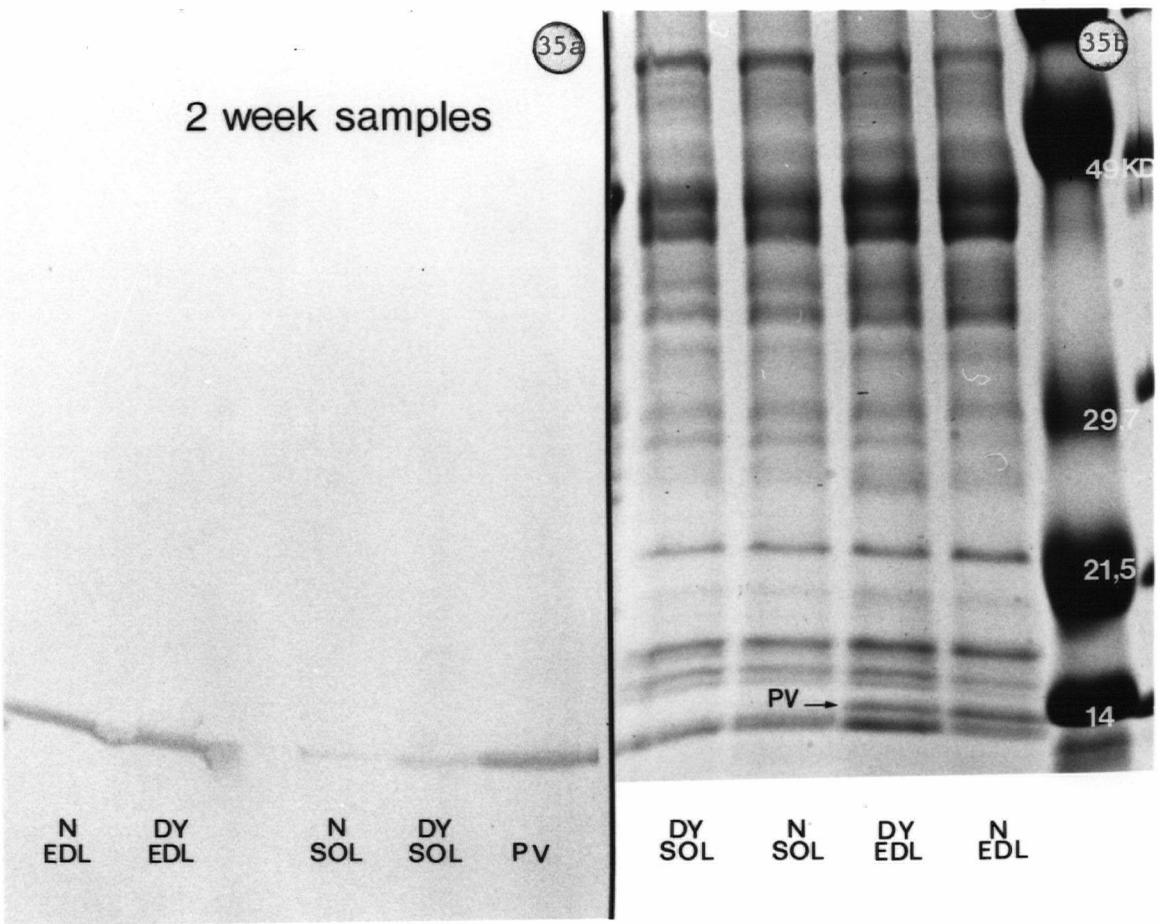
35a
2 week samples
N EDL
DY EDL
N SOL
DY SOL
PV
35b
49KD
29,7
21,5
14
PV
DY SOL
N SOL
DY EDL
N EDL

and divided into L, D, and I staining groups. These results are given in Table VI.

The original intent in using corresponding halves of each muscle was to simultaneously type the same fibers for PV immunoreactivity and myosin ATPase. Unfortunately due to problems with tissue shrinkage, freezing artifacts, and loss of sections, fiber typing from serial sections of corresponding halves of each muscle was not possible. However, the fiber typing was performed on sections from the same muscle for each staining procedure and expressed as the mean percentage of fibers in each group.

i) Adult EDL. Sections from the normal EDL muscles contained a heterogeneous mosaic pattern of PV immunoreactivity (Fig. 36). Three major extrafusal fiber types could be identified that varied according to PV immunoreactivity and cross-sectional diameters. The largest diameter and darkest fibers constituted the highest percentage of extrafusal fiber types (48.92%). There was also a population of small fibers (15.17%) that were non-reactive to the antisera. The remaining extrafusal fibers (35.78%) were intermediate in both staining intensity and cross-sectional diameter. A gradient of staining intensities could be observed in these intermediate fibers; however, this group was not further subdivided. This pattern of staining was in agreement with that reported in the rat (Celio and Heizmann, 1982) and ICRZ mouse (Heizmann et al., 1982). Celio and Heizmann (1982) categorized the PV-positive fibers as type 2-fast fibers, the light fibers of the type 1-slow variety, and the intermediate fibers as type 2-fast fibers with fatigue-resistant characteristics.

When this immunoreactivity profile was compared to the dystrophic EDL (Fig. 37) both the number of darkly-stained fibers (31.42%) and the intensity of staining had decreased. The proportion of non-reactive or light fibers (24.17%) was increased as was the percentage of fibers in the intermediate group (44.55%). The dystrophic EDL therefore, showed an overall decrease in PV immunoreactivity. In addition, there was a greater variability in fiber size in the sections from dystrophic muscle. Parvalbumin immunoreactivity was not specific to fiber size as in the normal EDL. As

Figures 36 and 37

Immunohistochemical demonstration of parvalbumin in normal (Fig. 36) and dystrophic (Fig.37) EDL muscles from 32-week-old mice. Muscles were fixed by freeze-substitution, embedded in paraffin, and processed as described in Methods. Three prominent staining intensities can be identified: large diameter, dark fibers (D), fibers of intermediate size and staining (I), and small non-reactive or light fibers (L). There are a greater number of light fibers in the dystrophic EDL, and an alteration in fiber diameter when compared to its normal counterpart. Peripheral nerve fascicles did not stain. x400

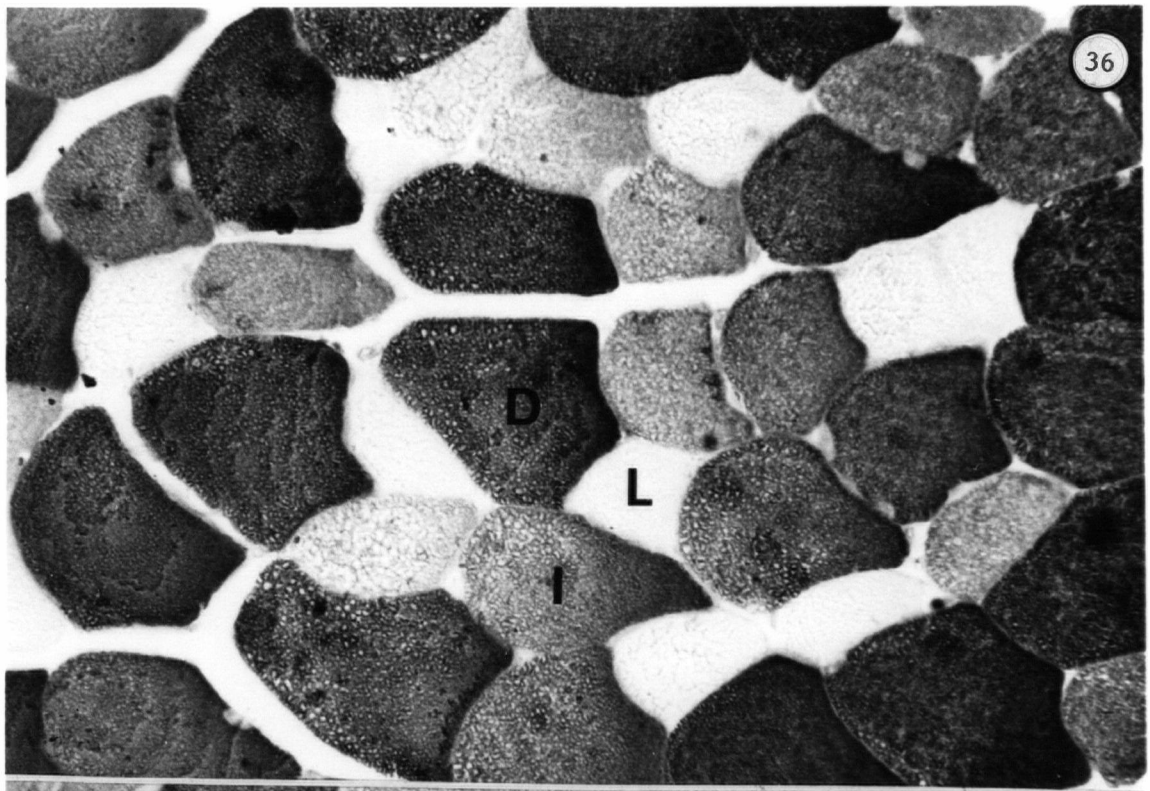
36
D
L
I

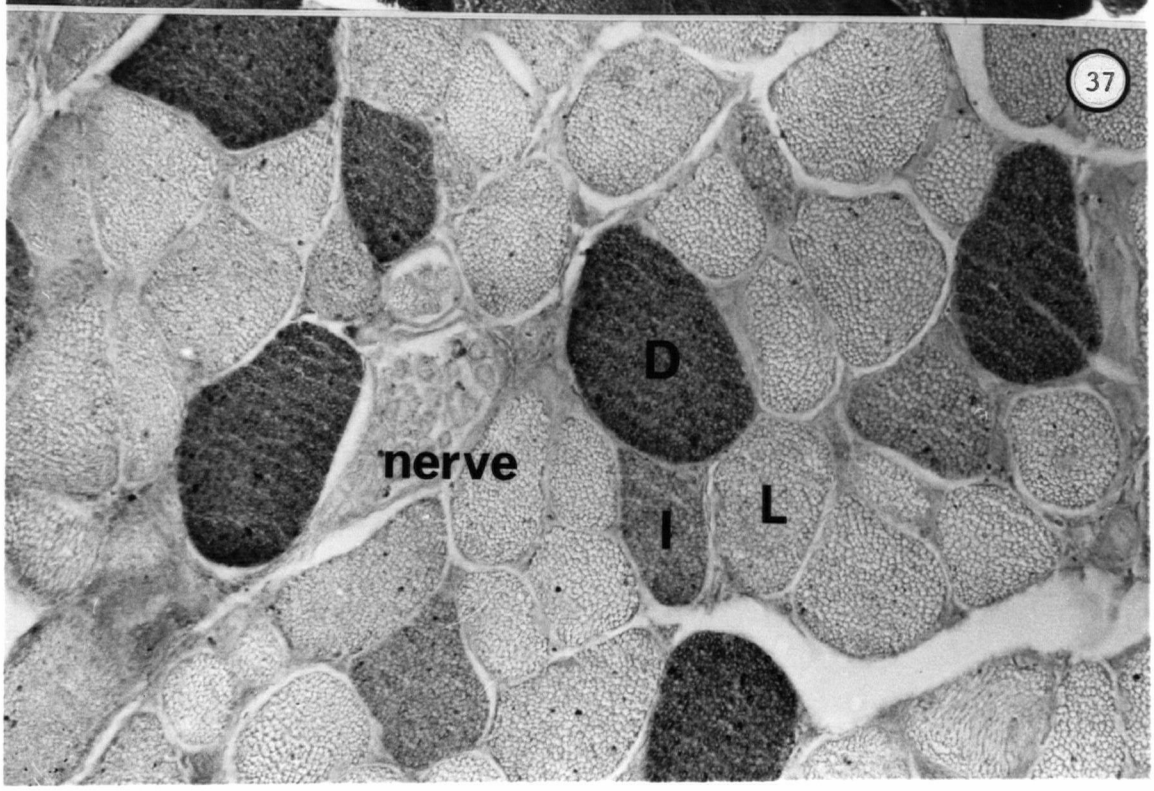
37
D
nerve
I
L

can be seen in Figure 37, small-diameter fibers may be either L, D, or I in staining for PV. The Tukey's statistical analysis procedure for intercomparisons indicated a significant interaction effect between genotype and PV staining pattern for the EDL sections.

These fiber groupings corresponded to the myofibrillar ATPase staining profile (Figs. 38 and 39) in which the largest and palest fibers were type 2-fast fibers, the intermediate fibers were type 2 fibers with both fast and slow characteristics, and the smallest and darkest fibers were of the slow variety. The myofibrillar ATPase staining pattern was almost a reverse to that seen with the PV immunohistochemistry (Table VII). The large fast type fibers were dark after PV antisera treatment and light after myosin ATPase. The small type 1 slow fibers were non-reactive for PV but were darkly stained by the myosin ATPase procedure.

In this study there was not a complete correlation between PV immunoreactivity and myosin ATPase staining. All type 2 fast fibers contained PV whereas there was a gradation of PV intensities in the second class of type 2 fibers ranging from non-reactive to intense. None of the small type 1 slow fibers contained PV. It was evident when comparing the percentages obtained from both the PAP and myosin ATPase staining procedures (Tables V and VI, respectively) that the extrafusal fibers could not be categorized into three distinct fiber types based on their PV immunoreactivity. When typing the fibers according to PV localization, a greater percentage of fibers fell into the I/type 2 and L/type 1 groups and a lower percentage into the D/type 2 group than was observed using the corresponding myosin ATPase reactivity as a basis for comparison. In other words, based on PV distribution, the normal and dystrophic EDL appear to be slower types of muscles than is indicated by the myosin ATPase localization.

The adult dystrophic EDL (Fig. 39) showed an increase in the number of I/type 2 fibers and a concomitant decrease in the number of L/type 2 extrafusal fibers when typed according to myosin ATPase. Although not visible in Figure 39, there was also

Figures 38 and 39

Histochemical demonstration of myofibrillar ATPase at pH 4.6 in frozen sections of normal (Fig. 38) and dystrophic (Fig. 39) adult EDL muscles. Three staining intensities are noted in the extrafusal fibers: light (L), dark (D) and intermediate (I). The outer capsule and Bag2 intrafusal fiber (asterisk) of a muscle spindle cut through the polar region (arrow) appear darkly stained in the dystrophic EDL. Also note the central nucleation and variation in extrafusal fiber diameters in the dystrophic muscle. x650

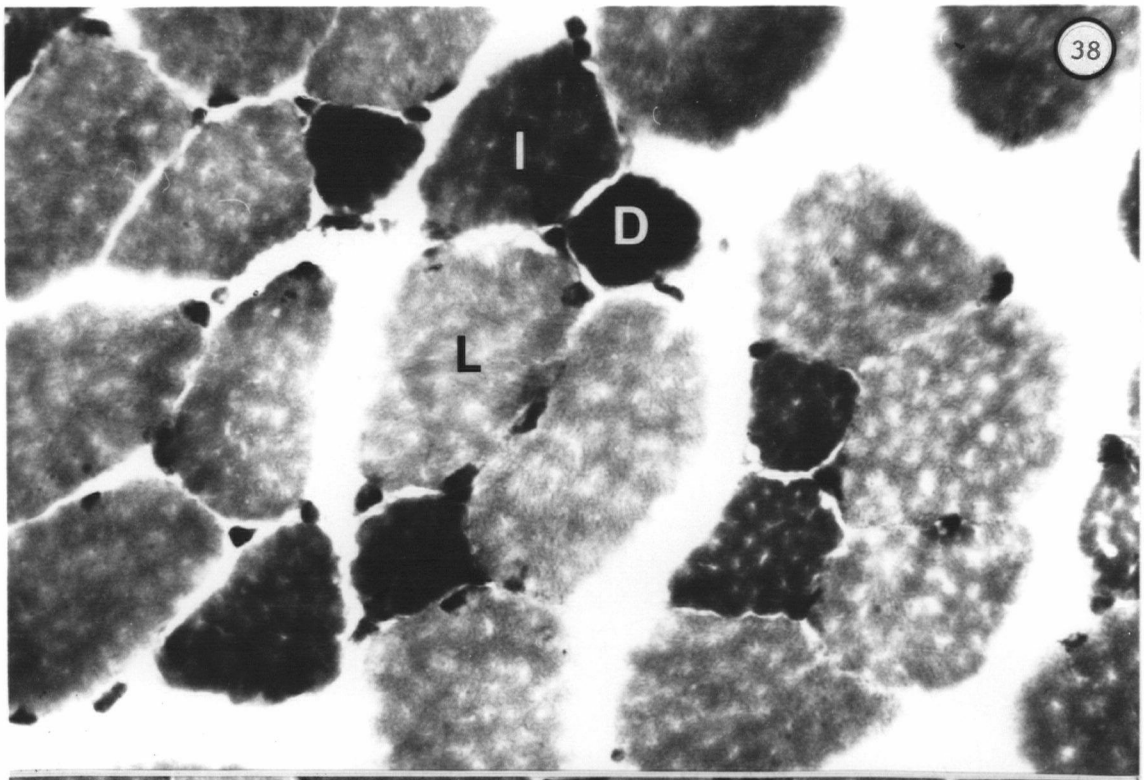
38
I
D
L

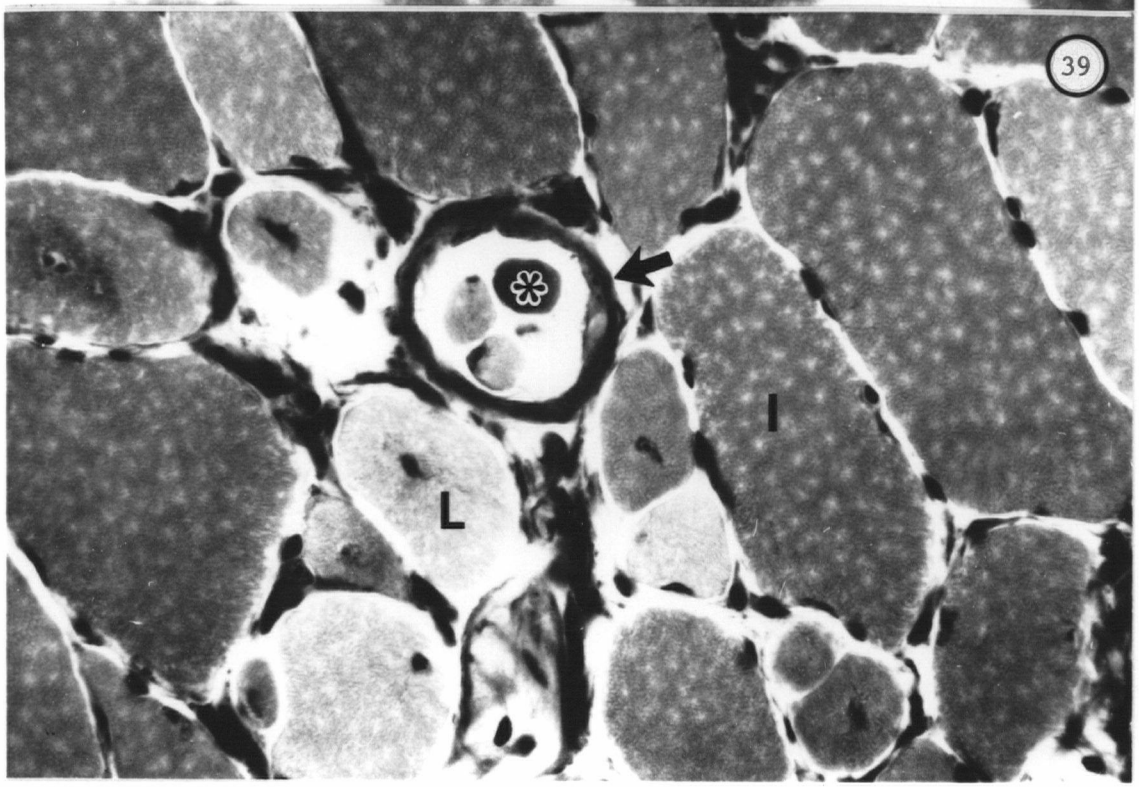
39
I
L

an increase in the number of D/type 1 fibers. An increase in the proportion of intermediate fibers was consistent with the PV results. One of the intrafusal fibers of muscle spindles, presumably the bag2 fiber, was darkly stained for myosin ATPase reactivity as was the thick outer capsule (Fig. 39).

ii) Adult Soleus. Muscle sections of the normal adult soleus treated with the PV antisera (Fig. 40) were predominantly made up of large non-reactive fibers (76.73%) and a small population of both intermediately (14.60%) and darkly (8.39%) stained extrafusal fibers. In the dystrophic soleus (Fig. 41), a significant ($p < .01$) decrease in the percentage of light fibers (26.64%), and an increase in the percentage of both dark (35.11%) and intermediate (44.34%) fibers were observed when compared to the normal soleus. There appeared to be a greater number of smaller-diameter fibers in the sections from the dystrophic muscle, and these small fibers were usually PV-positive. Overall, there was a greater proportion of fibers positive for PV in the dystrophic soleus than in the normal soleus.

The most striking observation was the similarity in the PV localization in the extrafusal fibers of the dystrophic soleus and the dystrophic EDL. The mean percentage of fibers categorized into each of the staining groups was virtually identical. Unlike their normal counterparts, the distribution of extrafusal muscle fibers either positively or negatively stained for PV was evenly dispersed in the sections from the dystrophic EDL and soleus (Table V).

This trend to a more homogeneous population of extrafusal fiber types in the 32-week dystrophic soleus was also observed in the myosin ATPase staining. It is evident from both Figures 42 and 43, as well as from Table VI, that the dystrophic soleus has a greater proportion of intermediate fibers than its normal counterpart. In addition to the conversion in staining intensities there was a greater variability in the extrafusal fiber diameters in the section of the dystrophic soleus than in the section of the normal tissue. A correlation between fiber size and fiber type could not be

Figures 40 and 41

Paraffin sections of freeze-substituted muscles from normal (Fig. 40) and dystrophic (Fig. 41) adult soleus muscles. Sections were processed for parvalbumin immunohistochemistry as described in the Methods. Three staining intensities are indicated, light (L), dark (D) and intermediate (I). There appears to be an increased number of intermediate fibers, and a greater variation in fiber size in the dystrophic soleus when compared to its normal counterpart. x650

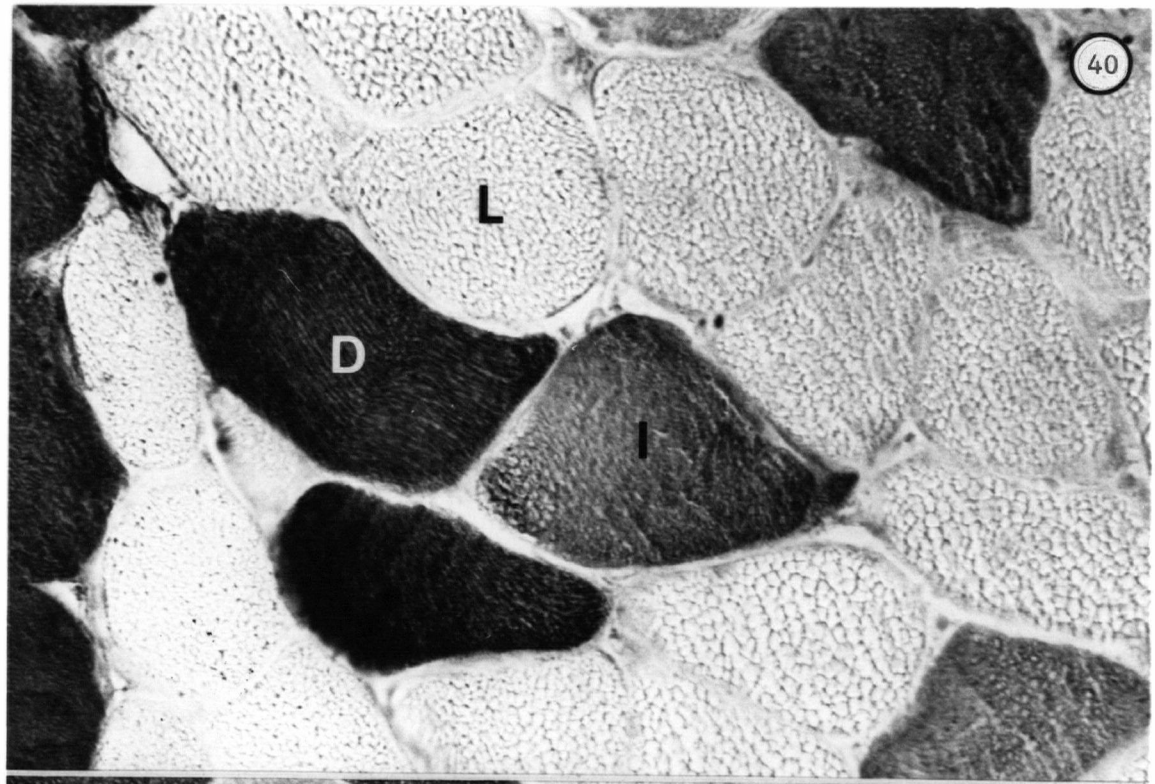
40
L
D
I

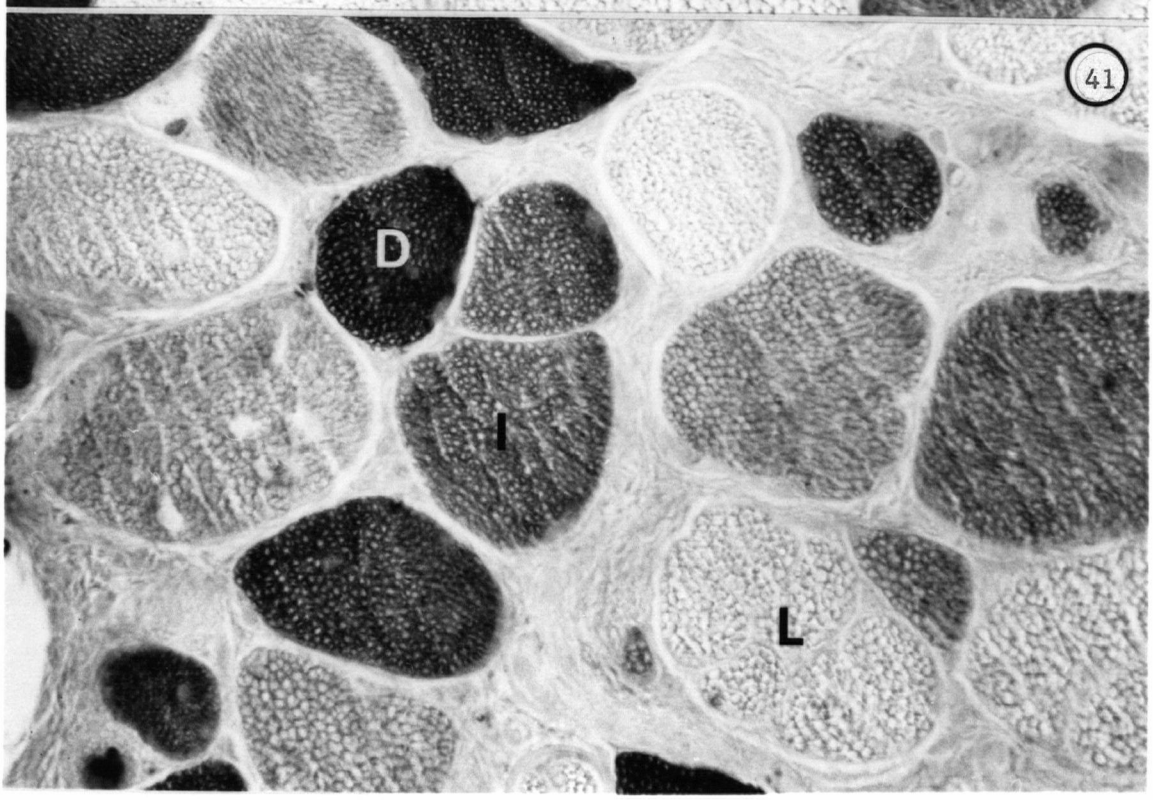
41
D
I
L

Figures 42 and 43

Frozen sections of normal (Fig. 42) and dystrophic (Fig. 43) adult soleus muscles, stained for myofibrillar ATPase pH 4.6. The three staining intensities are labelled light (L), dark (D) and intermediate (I). The dystrophic soleus contains many small diameter extrafusal fibers which vary in staining intensity. Overall there appears to be fewer dark fibers and more light fibers than observed in the normal soleus. A polar muscle spindle (arrows) is indicated in both sections. The Bag2 intrafusal fiber (asterisks) stains darkly in both normal and dystrophic muscles, however, only the outer capsule of the spindle in the dystrophic section is heavily stained. x650

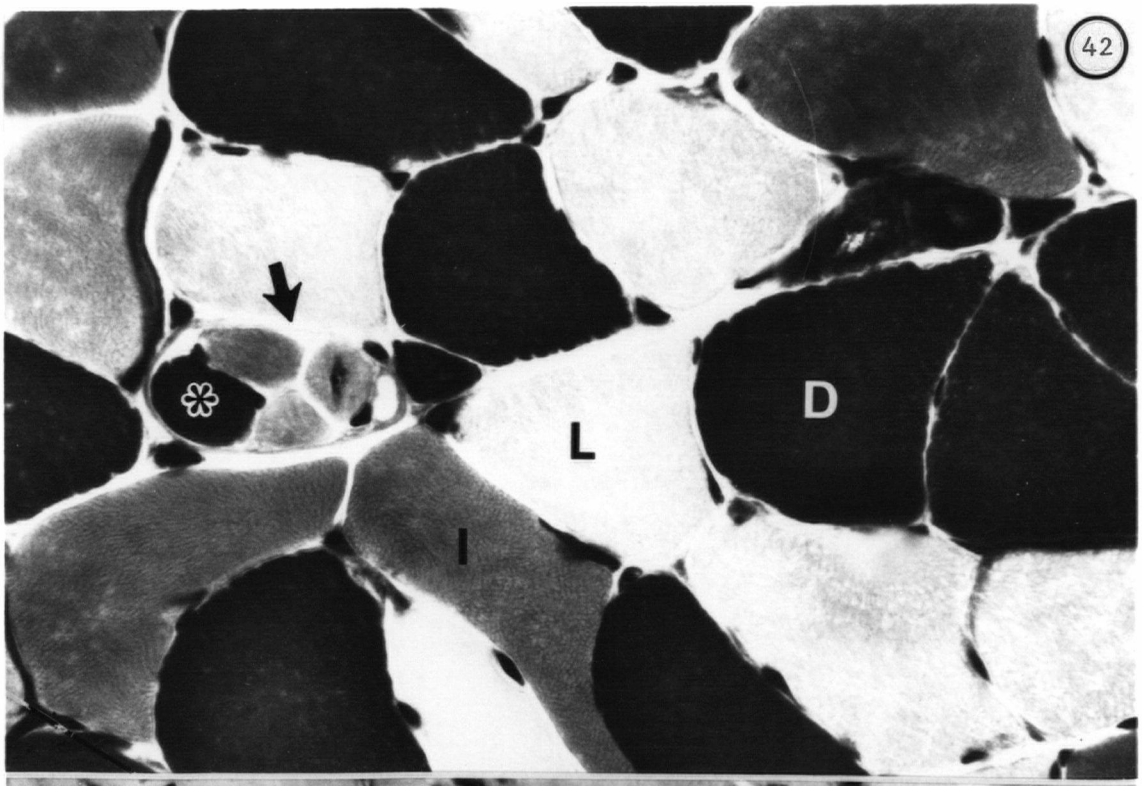
42
D
L
I

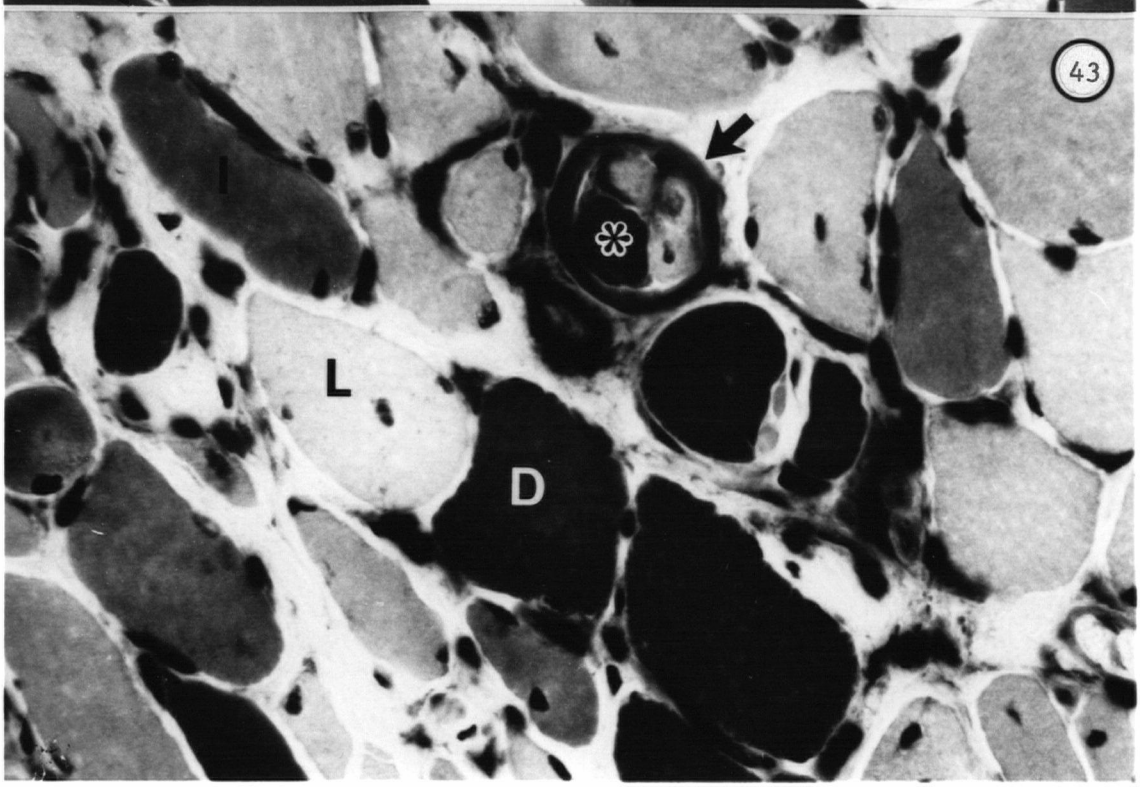
43
I
L
D

made since all three staining intensities were observed regardless of the diameter of the myofiber.

Generally, muscle spindles were less evident in the sections from the adult muscles using PAP immunohistochemistry than with myosin ATPase histochemistry. As in the 32-week EDL, one of the intrafusal fibers in the sections of the soleus muscles was darkly stained for myosin ATPase activity (Figs. 42 and 43). The thick outer capsule of muscle spindles was also darkly stained (Fig. 43); however, this was only observed in the dystrophic tissue. The intrafusal fibers typically had no PV immunoreactivity in either normal or dystrophic animals, however, an occasional positively-stained intrafusal fiber was observed in some spindles. Immunohistochemical staining of serial sections taken throughout the length of a muscle spindle were not performed . It is possible that regional differences in PV immunoreactivity may exist in the intrafusal fibers as was seen in Chapter 1 with the myosin ATPase staining.

iii) Two week EDL. The distribution of PV was similar in the 2-week-old normal EDL (Fig. 44) and dystrophic EDL (Fig. 45), although the sections from the dystrophic EDL showed a slightly greater percentage of light fibers (27% compared to 19%) as outlined in Table V. The majority of extrafusal fibers in both the normal and dystrophic EDL were positive for PV (50% and 41%, respectively). As can be seen in Figure 45, the overall background level of staining was higher in the dystrophic EDL sections. The PV distribution in the neonatal fast-twitch muscles resembled that seen in the normal adult EDL. At 2 weeks of age, these muscles did not show the variation in fiber diameters observed in the adult muscles.

Intrafusal fibers that stained positively for PV were often observed in polar regions of muscle spindles of the 2-week sections (Figs. 45 and 49). Spindles sectioned through the equatorial and juxtaequatorial regions revealed no PV immunoreactivity in the intrafusal fibers (Figs. 44 and 48). Judging by the size of the intrafusal fibers that were positive for PV, it appeared that one of the nuclear bag fibers contained PV (Fig. 49) as well as all of the nuclear chain fibers. This finding

is contrary to that reported in the adult EDL of the rat (Celio and Heizmann, 1982).

The distribution of extrafusal muscle fibers typed according to myosin ATPase activity (Table VI) was similar in the normal (Fig. 46) and dystrophic (Fig. 47) EDL. Approximately 86% of the extrafusal fibers were lightly stained and therefore of the fast (type 2) variety. Few intermediately-stained fibers were observed in either the normal or dystrophic 2-week EDL. Sections from the normal EDL often stained darker overall than those from the dystrophic muscles. When compared to the adult tissue sections, the myosin ATPase staining pattern of the 2-week samples differed with respect to the distribution of intermediate and dark muscle fibers. The proportion of these two groups of fibers was reversed from that seen in the adult. In the sections from the younger animals, there was a greater percentage of dark or slow fibers and a lower percentage of intermediate fibers than calculated for the adult EDL.

Intrafusal fibers in polar regions of muscle spindles in either the normal (Fig. 46) or dystrophic (Fig. 47) 2-week EDL stained according to that described in Chapter 1 for myosin ATPase under acid preincubation conditions. The small diameter intrafusal fibers, presumably chain fibers, were unstained while the large-diameter intrafusal fibers were darkly or intermediately stained.

iv) Two Week Soleus. The majority of the extrafusal muscle fibers in both the normal (Fig. 48) and dystrophic (Fig. 49) soleus were non-reactive for PV. There was a small population of extrafusal fibers, however, that stained positively for PV. The results for the soleus muscles are compiled in Table V. No significant differences were noted in the staining pattern between the normal and dystrophic soleus at 2 weeks of age. The distribution of PV in the extrafusal fibers was very similar to that noted in the normal adult soleus, but it was dramatically different from that observed in the dystrophic adult soleus. Parvalbumin immunoreactivity in the normal muscle, therefore, varies little after 2 weeks of age in the soleus. In the dystrophic soleus,

Figures 44 and 45

Immunohistochemical localization of parvalbumin in freeze-substituted paraffin-sections of normal (Fig. 44) and dystrophic (Fig. 45) neonatal EDL muscles. The three major types of fibers are labelled light (L), dark (D), or intermediate (I) in staining. Muscle spindles (arrows) are indicated in both sections. Note that intrafusal fibers in the dystrophic spindle appear positive for parvalbumin. Three more spindles (not labelled) are present at the lower edge of Fig. 30. There appears to be a relatively large proportion of lightly stained extrafusal fibers in both the normal and dystrophic EDL at 2 weeks. x650

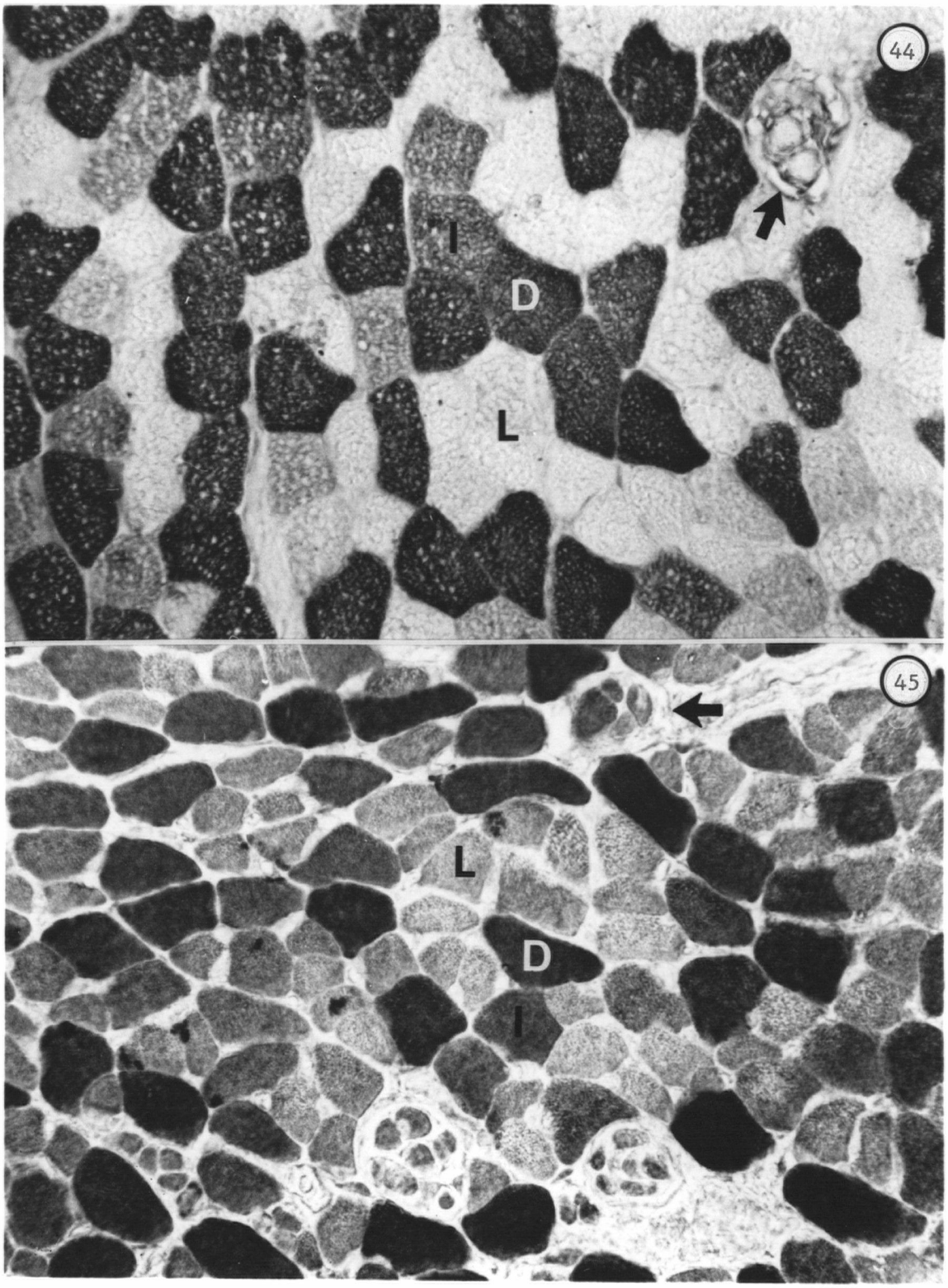
44
I
D
L
45
L
D
I

Figures 46 and 47

Frozen sections of normal (Fig. 46) and dystrophic (Fig. 47) neonatal EDL muscles, stained for myofibrillar ATPase pH 4.6. The majority of the extrafusal fibers at this age appear to be light (L) in staining. The Bag2 intrafusal fiber (asterisks) is darkly stained in the muscle spindle (arrows) of both the normal and dystrophic EDL. x650

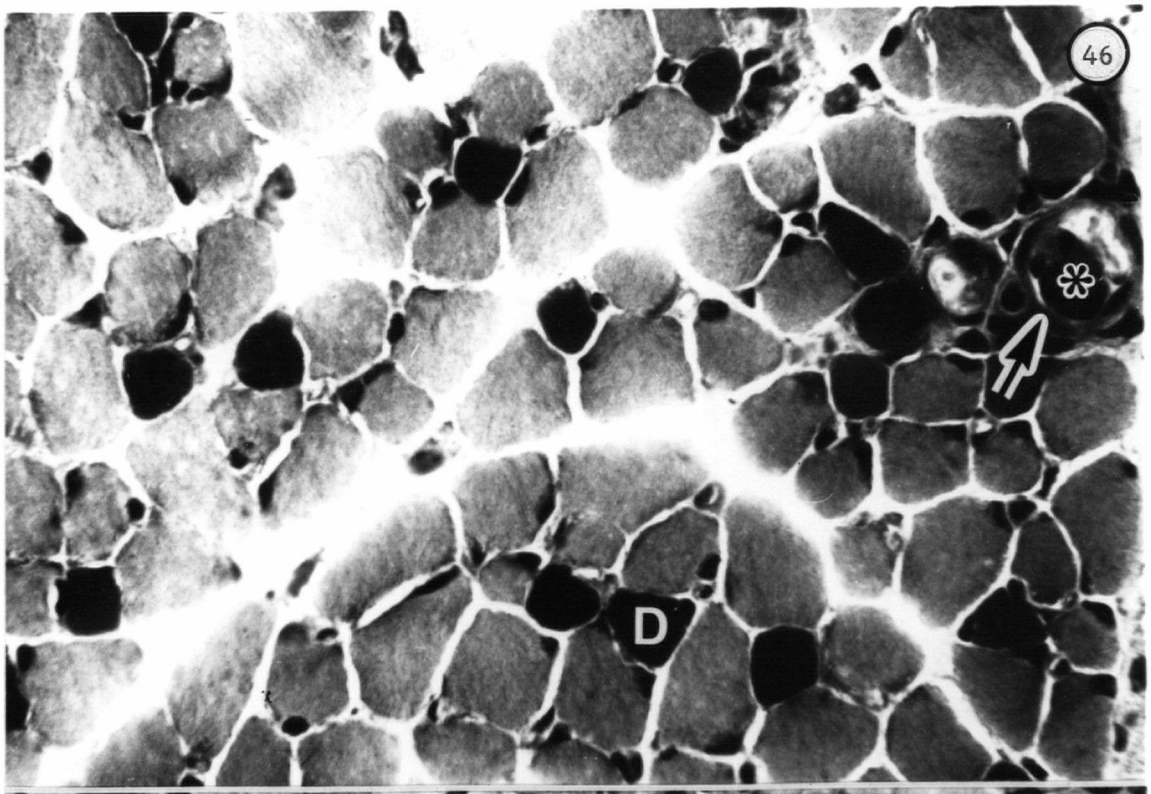
46
D

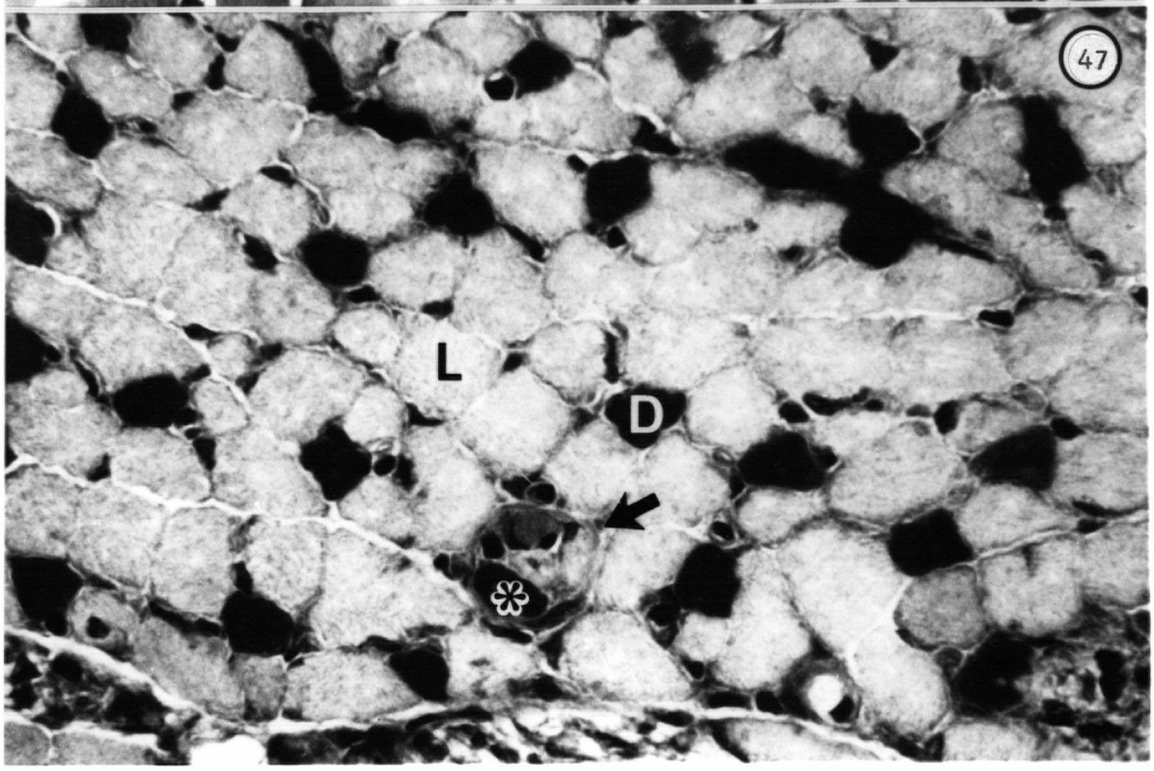
47
L
D

PV localization varied with age, indicating an interaction between staining pattern, age and genotype.

Intrafusal muscle fibers from the juxtaequatorial zone of muscle spindles did not stain for PV (Fig. 48). Polar regions of muscle spindles, however, contained intrafusal fibers which were positive for PV (Fig. 49). The diameters of these intrafusal fibers suggested that both nuclear bag and nuclear chain fibers may contain PV in the neonatal muscle. Interestingly, more PV was occasionally observed in one of the bag fibers than in the chain fibers (Fig. 49).

Extrafusal fibers in both the normal (Fig. 50) and dystrophic (Fig. 51) 2-week soleus could be categorized into the three staining groups according to myosin ATPase reactivity. Regardless of genotype, the predominant fiber classification was the L/type 2 variety (Table VI). The dystrophic soleus contained significantly more I/type 2 fibers than its normal counterpart but a similar mean percentage of the D/type 1 variety. The percentage of D/type 1 fibers was lower than that observed in the sections from the normal adult soleus. Intrafusal fibers stained in a similar fashion to that observed in the EDL at 2 weeks of age.

Summary of Immunohistochemical Results

The significant differences in PV and myosin ATPase staining were not due to a main effect of the stain but to an interaction of genotype, age and muscle ($p < .001$ according to the analysis of variance). The PV distribution pattern appears to vary according to genotype (more type I fibers in dystrophic muscles), muscle (more type D fibers in the EDL than in the soleus), and age. For a given muscle, the localization of PV appeared to vary according to genotype as well as age of the animal. These interaction effects were also observed in the myosin ATPase results.

Parvalbumin immunohistochemistry resulted in a gradation of staining intensities that made it difficult to type the extrafusal muscle fibers into the 3 distinct groups observed using the myosin ATPase method. No true correlation could be drawn

Figures 48 and 49

Light micrographs of paraffin sections of normal (Fig. 48) and dystrophic (Fig. 49) neonatal soleus muscles, stained for parvalbumin. Light (L), dark (D), or intermediate (I) fibers are common to both normal and dystrophic sections; however, the background staining is higher in Fig. 49. A muscle spindle in the juxtaequatorial zone is indicated in Fig. 48 (arrow) and a polar region spindle in Fig. 49. Note that one intrafusal fiber is darkly stained in the dystrophic spindle but those in the normal spindle are non-reactive. An intramuscular nerve in the upper right-hand corner of Figure 49 also shows some immunolabelling. x650

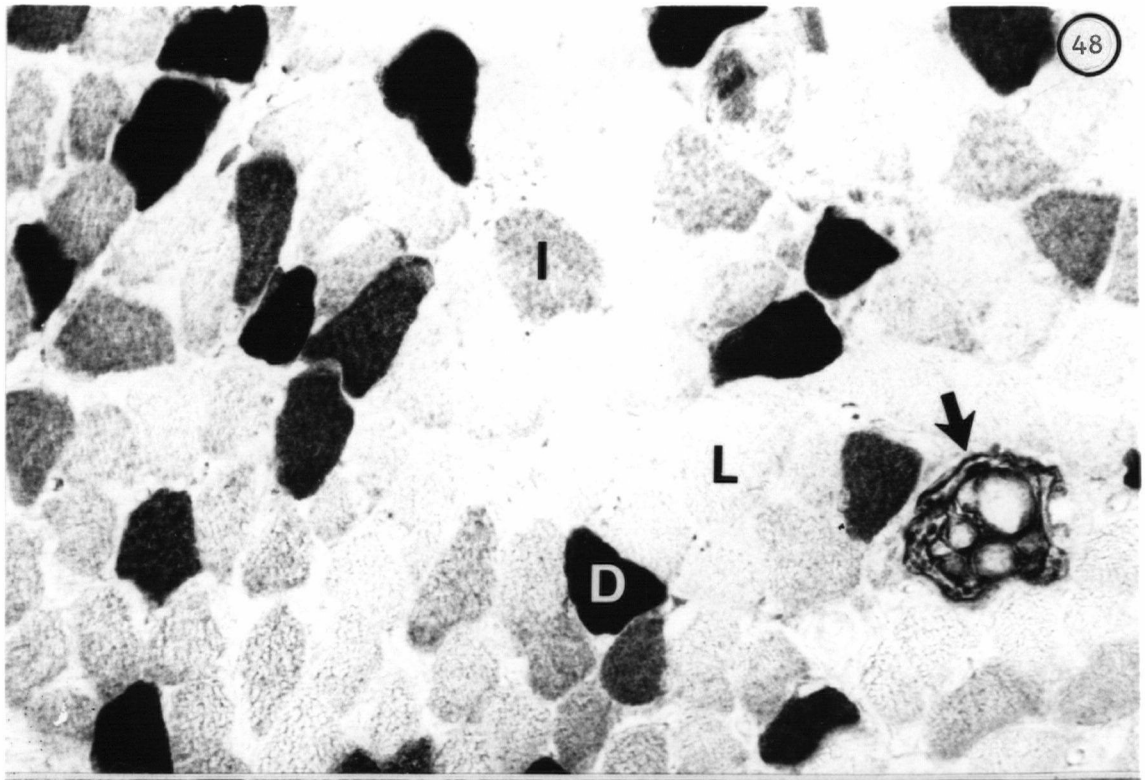
48
I
L
D

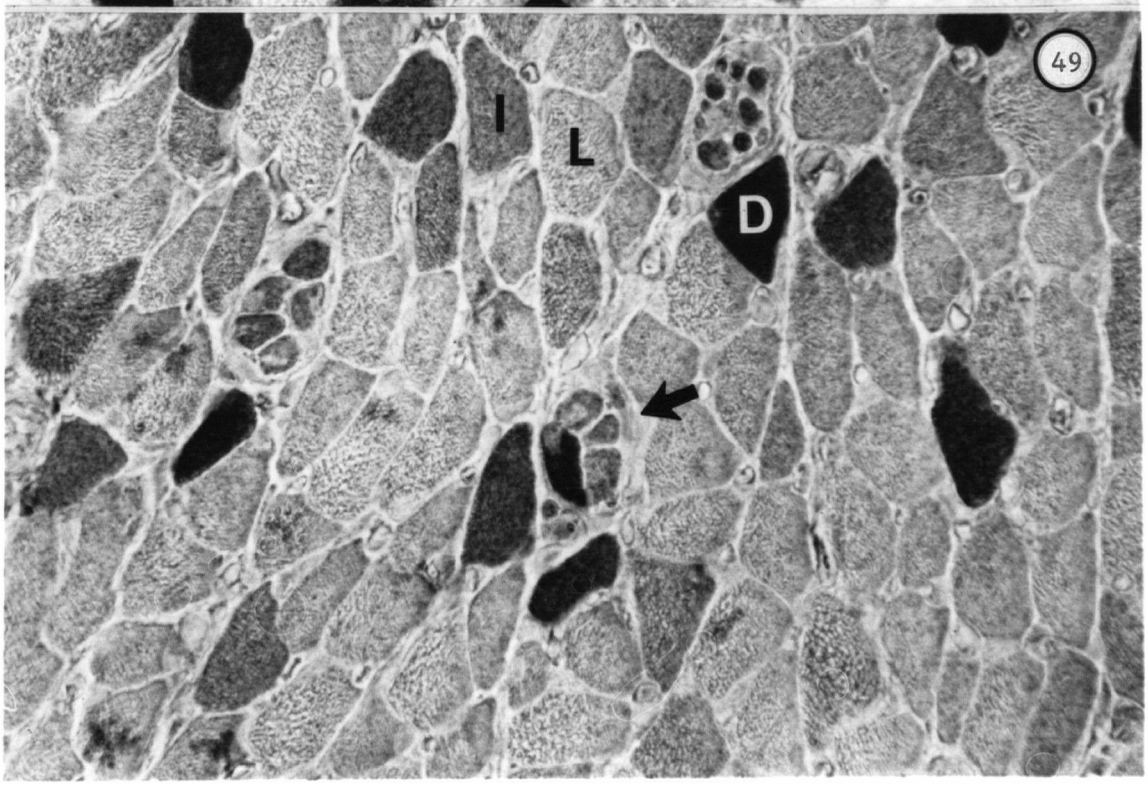
49
I
L
D

Figures 50 and 51

Light micrographs of frozen sections of normal (Fig. 50) and dystrophic (Fig. 51) neonatal soleus muscles, stained for myofibrillar ATPase pH 4.6. Three types of muscle fibers are identified, light (L), dark (D), or intermediate (I), as well as a muscle spindle (arrow). There appears to be more intermediately-stained fibers in the dystrophic soleus at 2 weeks of age when compared to its normal counterpart. x650

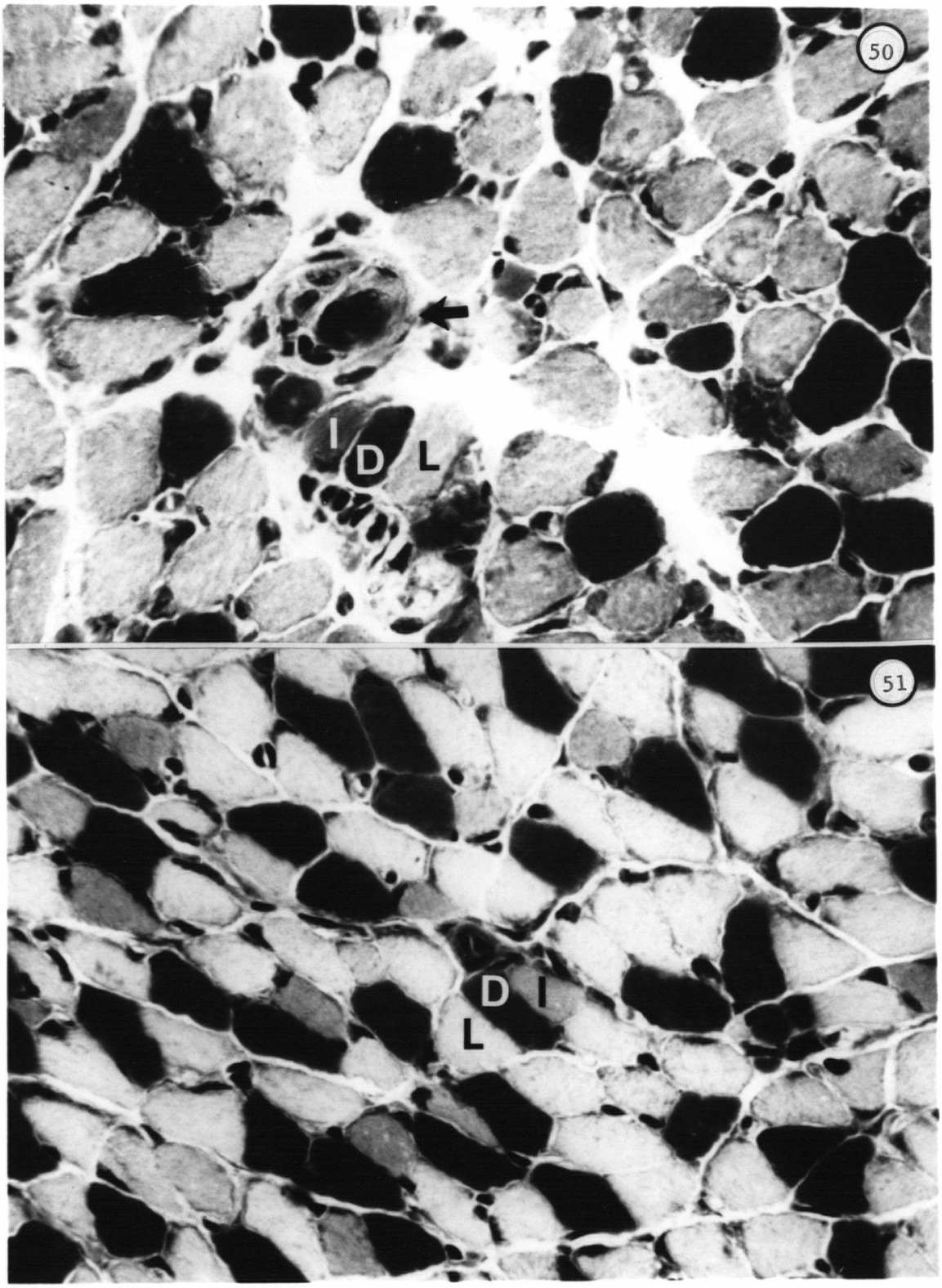
50
I
D
L
51
D
I
L

TABLE V. Distribution of fiber types according to parvalbumin immunoreactivity for normal (N) and dystrophic (DY) muscles at 32 and 2 weeks of age.

| | 32 Week | | | | 2 Week | | | |
|---|---|---|---|---|---|---|---|---|
| | EDL | | SOLEUS | | EDL | | SOLEUS | |
| | N | DY | N | DY | N | DY | N | DY |
| Light | 15.17 | 24.17 | 76.73b | 26.64 | 19.00 | 27.07 | 68.72 | 73.34 |
| Dark | 48.92a | 31.42 | 8.39b | 35.11 | 50.00a | 41.00 | 10.50 | 9.46 |
| Inter-mediate | 35.78 | 44.55 | 14.60b | 44.34 | 30.75 | 31.98 | 21.13 | 15.99 |

a Indicates statistical significance between normal and dystrophic values at $p < 0.05$.

b Indicates statistical significance between normal and dystrophic values at $p < 0.01$.

TABLE VI. Distribution of fiber types according to myosin ATPase reactivity for normal (N) and dystrophic (DY) muscles at 32 and 2 weeks of age.

| | 32 Week | | | | 2 Week | | | |
|---|---|---|---|---|---|---|---|---|
| | EDL | | SOLEUS | | EDL | | SOLEUS | |
| | N | DY | N | DY | N | DY | N | DY |
| L/type2 | 69.88b | 17.60 | 50.25b | 18.60 | 85.38 | 86.03 | 68.28 | 54.52 |
| D/type1 | 1.50 | 5.10 | 42.37b | 15.09 | 11.36 | 13.28 | 27.95 | 32.15 |
| 5/type2 | 28.62b | 77.27 | 7.33b | 66.33 | 3.21 | 0.63 | 4.08 | 13.30 |

a Indicates statistical significance between normal and dystrophic values at $p < 0.05$.
b Indicates statistical significance between normal and dystrophic values at $p < 0.01$.

TABLE VII. Correlation of extrafusal fiber classifications for parvalbumin and myosin ATPase staining procedures.

| | Light | Dark | Intermediate |
|---|---|---|---|
| Parvalbumin | non-reactive<br>slow | high<br>fast/type2 | medium<br>fast or slow |
| Myosin ATPase | fast<br>type2 | slow<br>type1 | fast-oxidative<br>type2 |

between PV and myosin ATPase reactivity. The distribution of type 1 and type 2 fibers typed according to myosin ATPase differed from the distribution of non-reactive and reactive fibers determined by the PV staining. When the extrafusal muscle fibers were categorized according to PV immunoreactivity, both the EDL and soleus contained an overall higher proportion of slow fiber types than was observed using the myosin ATPase stain. This observation is based on the fact that fibers of the type 1/SO variety had no PV immunoreactivity (Celio and Heizmann, 1982). As expected, the EDL contained more fibers that were positive for parvalbumin than the soleus. Whereas the distribution of parvalbumin did not vary significantly with age in the normal muscles, a significant difference was observed in the localization of PV in the adult dystrophic muscles when compared to their normal counterparts. The PV staining pattern was very similar between the adult dystrophic EDL and dystrophic soleus.

Parvalbumin Content

Levels of PV were measured by RIA using anti-mouse skeletal muscle PV antiserum raised in the rabbit. Individual muscles were pooled from a number of animals in each group to obtain enough muscle extract in each sample for the immunoassay. Typical standard curves of the assay for PV for the adult and 2-week samples are shown in Figures 52 and 53, respectively. In the rat system the $^{125}$I-PV, antiserum and parvalbumin standard were all derived from rat skeletal muscle. When dilutions of mouse muscle homogenates were added to the rat system incomplete cross-reactivity occurred, indicating relative species specificity. Therefore, in order to determine the PV concentration in the mouse muscle samples, and in view of the fact that only pure rat PV was available for iodination, a heterogeneous assay was used. The iodinated rat PV was incubated with anti-mouse PV antiserum and a standard curve constructed using dilutions of the calibrated mouse muscle homogenate. Calibration of this sample was done by extrapolating the mid-point from the mouse

homogenate dilution curve to the mid-point of the rat standard curve. This value was used to determine the real concentration of PV at a given dilution. While this procedure may introduce some inaccuracies the relative differences are small. Dilution curves were made of muscle extracts so that the amount of PV present in each assay sample would fall in the linear portion of the standard curve. The concentration necessary for linearity ranged from 1:5 to 1:200 depending on muscle type.

Tables VIII and IX summarize the PV content in the various muscles of adult and 2-week samples, respectively. These values are also depicted in histograms in Figures 54 and 55. All the values are expressed as the mean PV content.

Normal adult EDL muscles contained high levels of PV (27.89 µg PV/mg TSP). The amount of PV in the normal EDL was 5.3 times greater than that found in the dystrophic EDL (5.27 µgPV/mg TSP). In contrast, very little immunoreactivity could be detected in the normal adult soleus muscle extracts (1.03 µgPV/mg TSP), and this value was 4.5 times less than the amount detected in the dystrophic samples. Of greater interest was the resemblance of the PV content of the adult dystrophic EDL with that in the soleus muscles. This dramatic conversion to similar concentrations of the protein is depicted in Figure 54. All of these reported differences were significant at $p < .001$. These results are consistent with the electrophoresis and immunoblot data, and they are in reasonable agreement with previous reports of PV content in normal and dystrophic skeletal muscle (Heizmann et al., 1982; Pette et al., 1985).

Developmental Changes

Parvalbumin levels were the highest in the EDL samples of the 2-week-old samples (Table IX). However, unlike the adult preparations, the mean PV content of the normal EDL at 2 weeks (19.74 µg PV/mg TSP) was virtually identical to that of the dystrophic EDL (18.99 µg PV/mg TSP) as illustrated in Figure 55. These values were slightly less than those observed for the normal adult EDL (70.8% of the adult

Figure 52

Standard curves for the radioimmunoassay of rat skeletal muscle parvalbumin (open stars) and mouse muscle homogenate (solid stars). The muscle homogenate was used at an initial dilution of 1:32 to simulate the purified rat parvalbumin. Values for parvalbumin content in the 32-week samples were calculated from this curve.

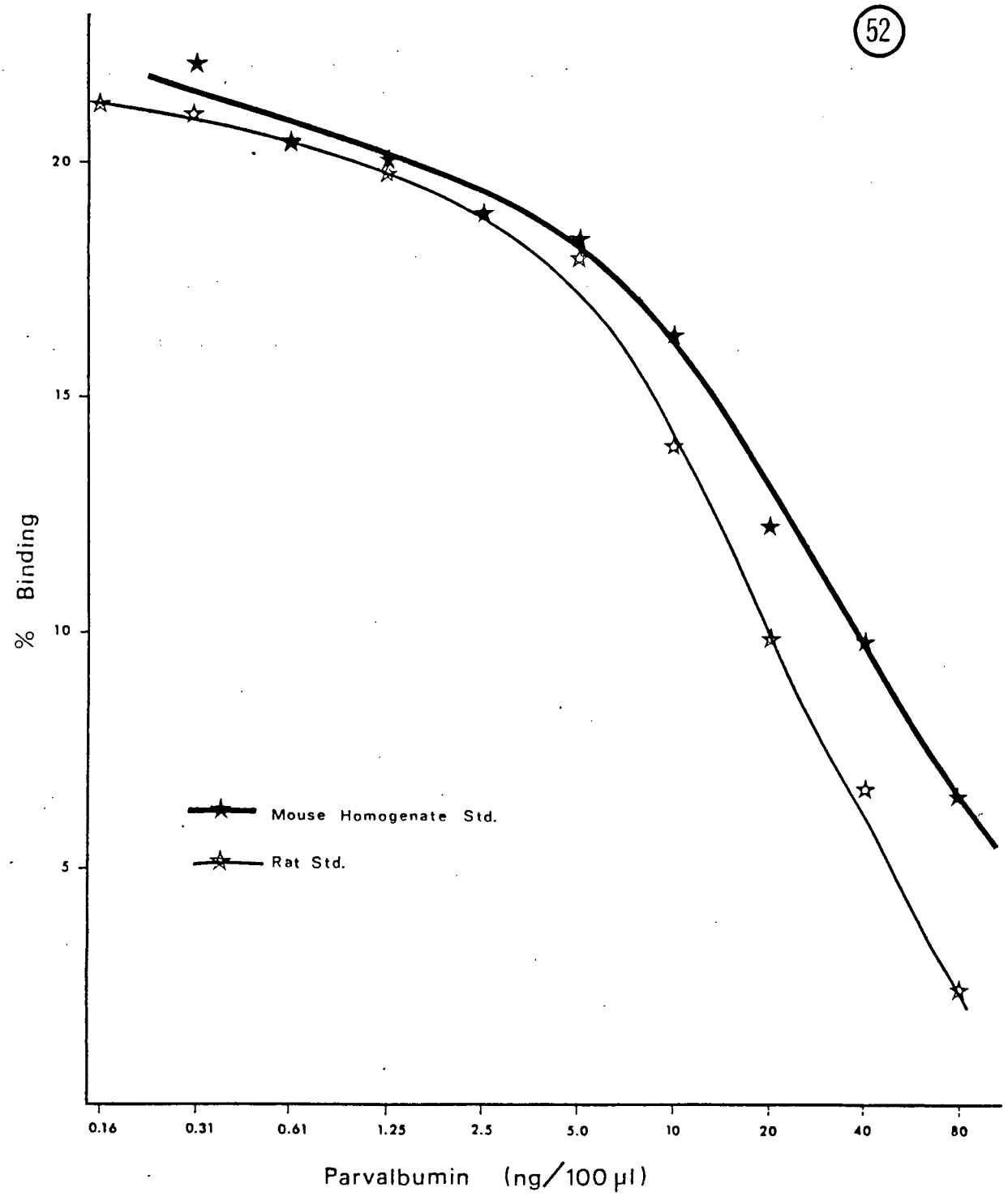
52
20
15
10
5
% Binding
Mouse Homogenate Std.
Rat Std.
0.16
0.31
0.61
1.25
2.5
5.0
10
20
40
80
Parvalbumin (ng/100 µl)

Figure 53

Standard curve for the radioimmunoassay of rat skeletal muscle parvalbumin (broken line) and mouse muscle homogenate (solid line). The muscle homogenate was used at an initial dilution of 1:32 to simulate the purified rat parvalbumin. Values for parvalbumin content in the 2-week samples were calculated from this curve.

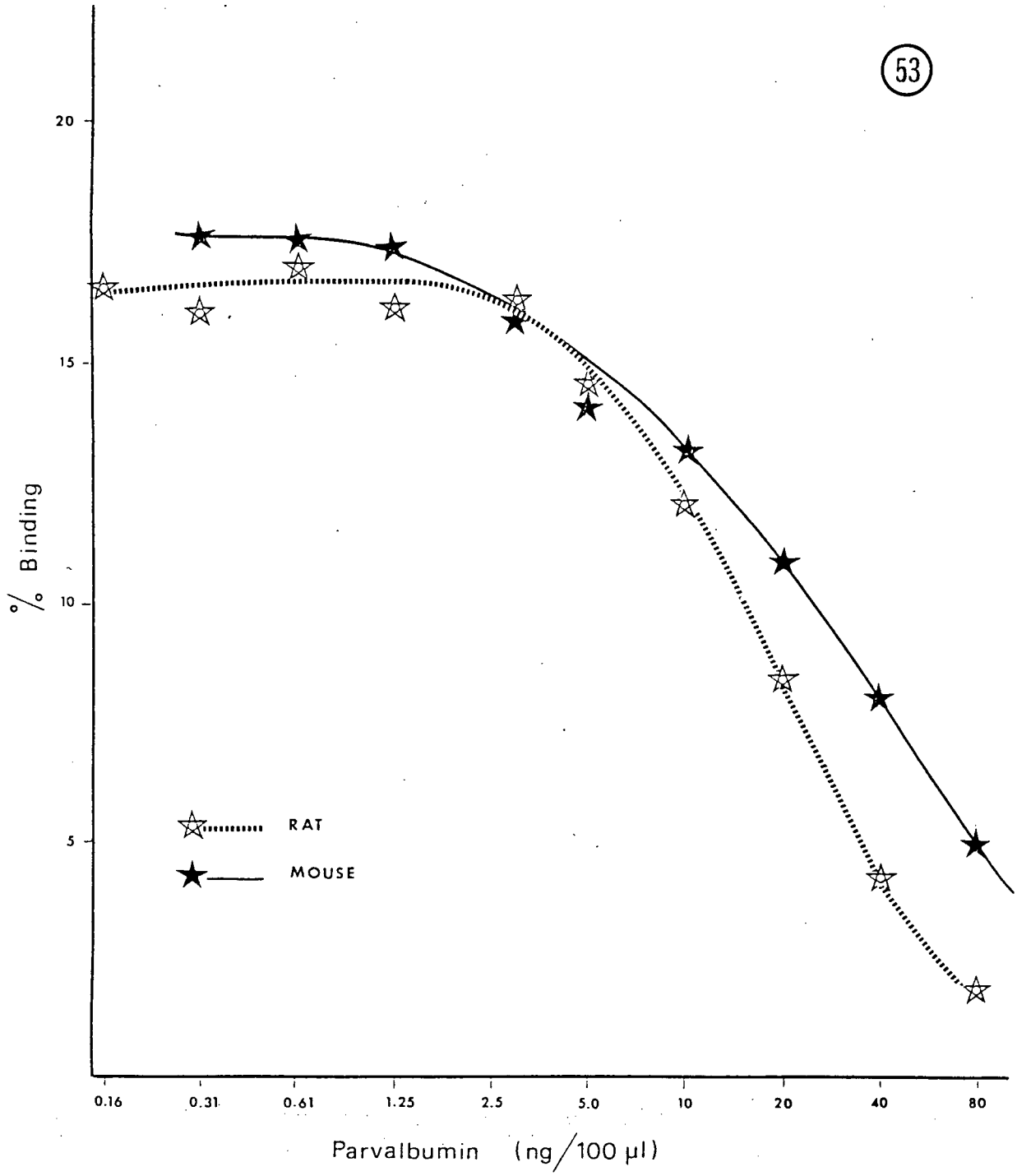
53
20
15
10
5
% Binding
RAT
MOUSE
0.16
0.31
0.61
1.25
2.5
5.0
10
20
40
80
Parvalbumin (ng/100 µl)

Figure 54

Histogram of the mean parvalbumin (PV) content determined by RIA, comparing normal (N) and dystrophic (DY) muscle samples from adult EDL and soleus (SOL) muscles. Both the dystrophic EDL and the dystrophic soleus show a dramatic change in mean PV content, approaching similar values to each other.

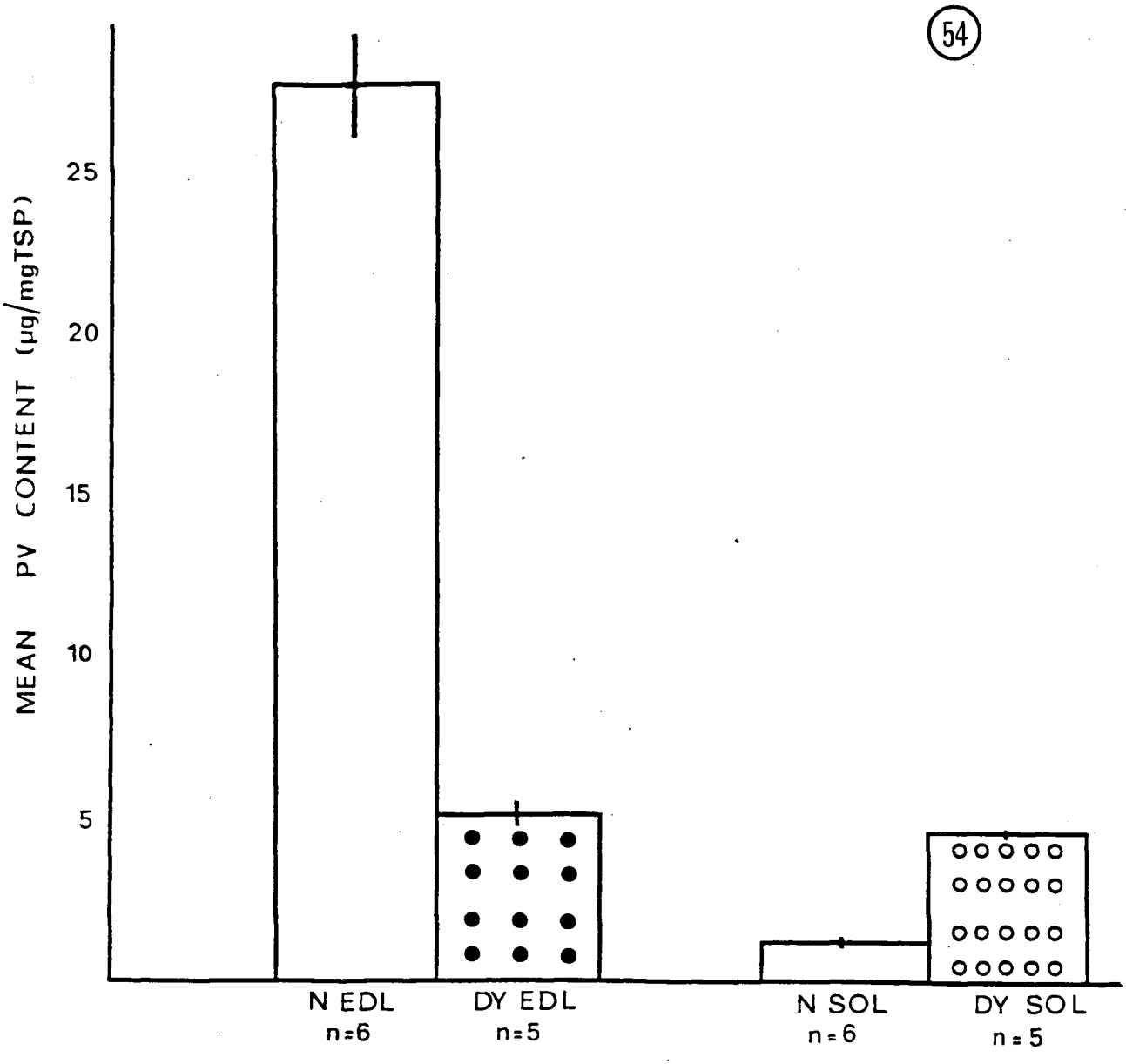
54
MEAN PV CONTENT (µg/mgTSP)
25
20
15
10
5
N EDL
n=6
DY EDL
n=5
N SOL
n=6
DY SOL
n=5

Figure 55

Histogram of the mean parvalbumin (PV) content as determined by RIA, comparing normal (N) and dystrophic (DY) muscle samples from 2-week EDL and soleus (SOL) samples. The amount of PV contained in both soleus samples was beyond the detectable limit of the assay and is therefore expressed as the minimal value detected. Mean parvalbumin content, determined by the RIA, is similar for normal and dystrophic samples at 2 weeks of age.

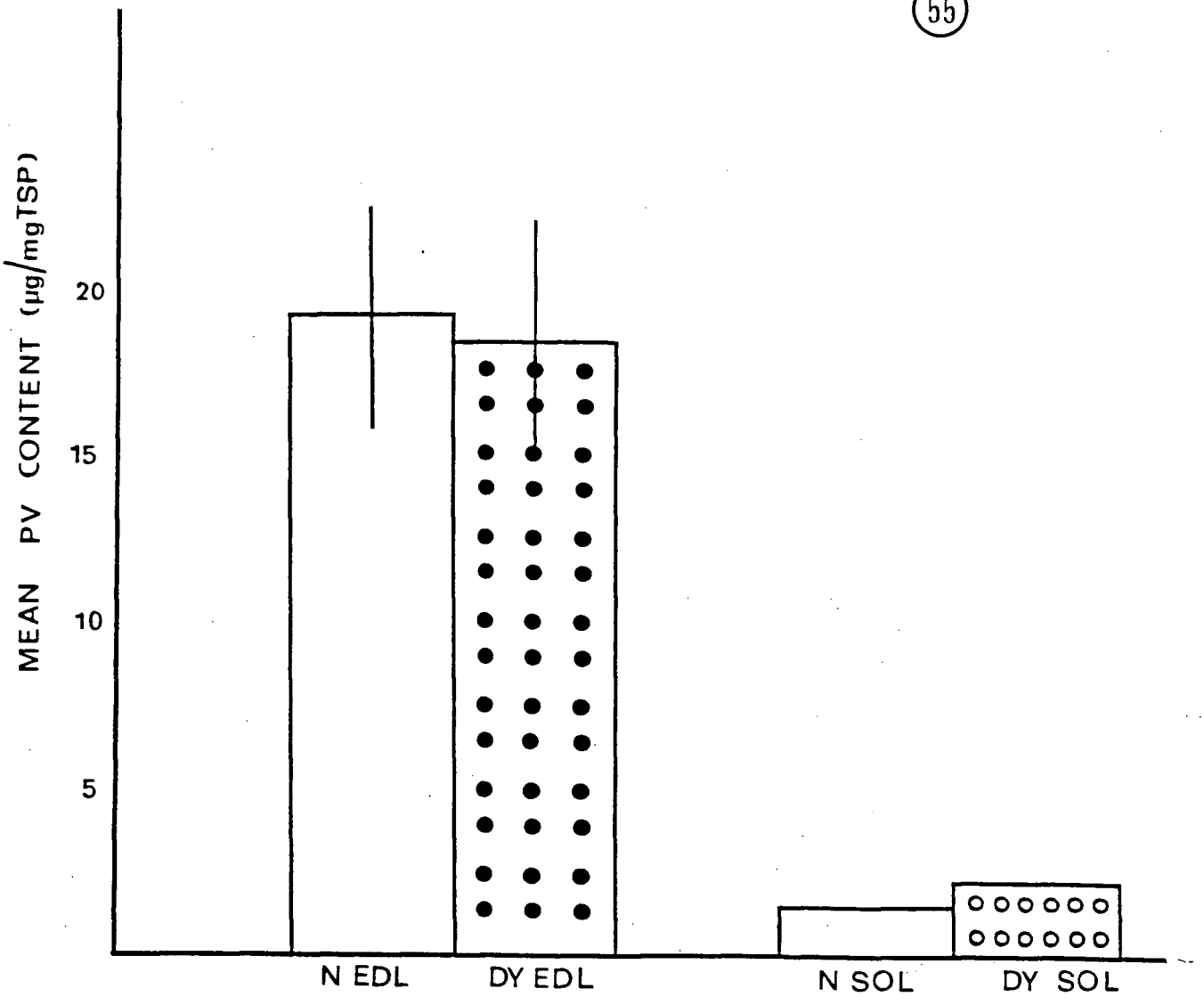
MEAN PV CONTENT (µg/mg TSP)
20
15
10
5
N EDL
DY EDL
N SOL
DY SOL

value) suggesting that synthesis of PV comparable to adult levels has not been attained by 2 weeks of age.

The RIA for the 2-week samples was not sensitive enough to detect significant amounts of PV in either the normal or dystrophic soleus preparations. These quantities were expressed as the minimum detectable value and not the mean PV content (Table IX). Based on these results, it would appear that postnatal maturation does not coincide with a significant increase in PV content in soleus muscles. Minimal levels of PV were detected in the normal soleus at both 32 and 2 weeks of age. The values for the dystrophic soleus at 2 weeks of age were virtually identical to those of the normal soleus (Fig. 55). Only the dystrophic adult soleus showed a change in mean PV content with age. These results are consistent with those obtained by different techniques to study the PV concentration in early development and maturation of skeletal muscle (Leberer and Pette, 1986a; Klug et al., 1983b).

Intergroup comparisons of the EDL muscles, conducted by Student's t-test, showed a significant difference ($p < .02$) between RIA results of the 32-week dystrophic EDL and the 2-week dystrophic EDL. The difference between normal 32-week and 2-week EDL assay results was not significant. Therefore, 2-week EDL muscles have almost reached their adult concentrations of PV. The normal or dystrophic soleus at 2 weeks of age did not differ significantly in PV content when compared to the normal adult soleus.

In summary the mean PV content varied in any given group according to genotype, age and muscle type. Although, at 2 weeks of age, genotype and age had less of an affect on mean PV content than did muscle type.

TABLE VIII. Mean values for parvalbumin content in 32 week normal (N) and dystrophic (DY) muscle samples.

| | | PARVALBUMIN CONTENT | |
|---|---|---|---|
| | | µg/mgTSP | µg/mg WET WT |
| N EDL | MEAN | 27.89 | 1.06 |
| n=6 | S.D. | 4.78 | 0.18 |
| | S.E.M. | 1.95 | 0.07 |
| DY EDL | MEAN | 5.27 | 0.15 |
| n=5 | S.D. | 0.62 | 0.024 |
| | S.E.M. | 0.28 | 0.011 |
| N SOL | MEAN | 1.04 * | 0.032 |
| n=6 | S.D. | 0.22 | 0.009 |
| | S.E.M. | 0.09 | 0.004 |
| DY SOL | MEAN | 4.64 | 0.124 |
| n=5 | S.D. | 0.24 | 0.032 |
| | S.E.M. | 0.11 | 0.014 |

* $p < .001$ between N and DY groups for both TSP and WET WT.

TSP = total soluble protein
WET WT = wet weight
S.D. = standard deviation
S.E.M. = standard error of the mean

TABLE IX. Mean values for parvalbumin content in 2 week normal (N) and dystrophic (DY) muscle samples.

| | | PARVALBUMIN CONTENT | |
|---|---|---|---|
| | | µg/mgTSP | µg/mg WET WT |
| N EDL | MEAN | 19.74 | 1.031 |
| n=5 | S.D. | 7.74 | 0.582 |
| | S.E.M. | 3.46 | 0.260 |
| DY EDL | MEAN | 18.99 | 0.622 |
| n=5 | S.D. | 8.48 | 0.291 |
| | S.E.M. | 3.79 | 0.130 |
| N SOL | LESS THAN | 1.62 | 0.094 |
| n=5 | | | |
| DY SOL | LESS THAN | 2.33 | 0.003 |

Values reported for the SOL are the minimum values detected for mean TSP and WET WT.

TSP = total soluble protein
WET WT = wet weight
S.D. = standard deviation
S.E.M. = standard error of the mean

# DISCUSSION

This work represents the first immunohistochemical study of PV in murine dystrophic tissue at both preclinical and postclinical stages of the disease. It is also the first study to compare the changes in PV distribution and content in fast and slow-twitch skeletal muscles of dystrophic mice.

## Immunohistochemistry

The immunohistochemical distribution data of PV in normal and dystrophic tissue does not provide new information regarding the function of PV in muscle. It is, however, consistent with the proposed role of PV as a soluble relaxing factor in fast-twitch muscle and correlates well with histochemical (Ovalle et al., 1983), biochemical (Jasch and Moase, 1985) and physiological (Bressler et al., 1983) data.

Muscles composed primarily of fast-twitch fibers generally have a high concentration of parvalbumin (Celio and Heizmann, 1982; Heizmann et al., 1982). This portion of the study was an attempt to simultaneously investigate the distribution of parvalbumin in the EDL and soleus of normal and genetically dystrophic mice, and the distribution of extrafusal fibers typed according to myosin ATPase. The present data supports these previous reports on the immunohistochemical distribution of parvalbumin. The highest percentage of parvalbumin-positive fibers was found in tissue sections from the normal EDL muscles (approximately 50%) and the lowest in the soleus (8-10%). There was a definite population of dark (parvalbumin-positive) and light (non-reactive) fibers which most likely corresponds to type 2/fast-twitch and type 1/slow-twitch fibers, respectively. Those muscle cells classified as intermediate fibers comprised a continuum of staining intensities. These intermediately-stained fibers probably represent a subgroup of fibers that cannot be categorized as either typical type 2 or type 1 fibers. When the fiber numbers are compared between the parvalbumin and myosin ATPase reactions (Tables V - VII) it is evident that not all

the non-reactive fibers for parvalbumin are of the type 1/slow variety. This was also noted by Celio and Heizmann (1982) who found that parvalbumin was localized exclusively in the type 2 fiber displaying degrees of staining intensity. These investigators also reported that some of the type 2A fibers were actually devoid of parvalbumin immunoreactivity and resembled the type 1 fibers. Therefore, a muscle typed solely according to parvalbumin immunoreactivity would be considered a slower muscle than if typed according to myosin ATPase reactivity. Hence, the results of this immunohistochemical study would suggest that there is not a true correlation between parvalbumin localization and myosin ATPase activity.

The continuum of staining intensities noted in PV may also reflect the recently described heterogeneous C fiber population noted between types 1 and 2A (Staron and Pette, 1986). These fibers were characterized by the co-existence, in varying ratios, of both type 1 slow-myosin heavy chains and type 2A fast-myosin heavy chains, but did not correlate with the myosin light chain complement. In the adult dystrophic tissue the increased proportions of intermediately stained fibers for PV may reflect a greater C fiber population. This would support the hypothesis that dystrophic muscle experiences a lack of differentiation as the disease progresses. It is also possible that since no true correlation between PV and myosin ATPase staining was observed in the present study, the PV localization may correlate more closely with the myosin light chain composition than the myosin heavy chain complement of particular fiber types.

Since PV is a water-soluble protein, artifactual redistribution during fixation is always a possibility. A redistribution may be responsible for the checkerboard staining pattern of the extrafusal fibers. This issue has been excluded by single muscle fiber analysis (Heizmann et al., 1982). Typed, single muscle fibers from freeze-dried samples of rat muscle were subjected to two-dimensional polyacrylamide gel electrophoresis and revealed PV to be present only in the type 2 fibers. In addition, two-dimensional gels of heat-stable extracts from homogeneous type 2B/FG

muscles resulted in very high concentrations of PV after HPLC analysis of the same extracts. These concentrations correlated well with the known contraction and half-relaxation times.

In the present immunohistochemical study, age was not a significant factor in the distribution of parvalbumin. No obvious changes were observed in the parvalbumin immunostaining pattern from 2 to 32 weeks of age in the normal muscles. Apparently then, the adult profile has almost been attained by 2 weeks of age in the normal mouse, and thereafter, PV localization varies with muscle type and not with age. However, there was some evidence that the 2-week muscles are still obtaining mature characteristics in that the 2 week EDL had a slightly higher percentage of non-reactive muscle fibers than its adult counterpart. In addition, the 2-week soleus showed a slightly higher percentage of PV-positive fibers. In contrast, myosin ATPase reactivity was age-dependent in both the EDL and soleus. The 2-week EDL exhibited more slow muscle-fiber characteristics whereas the soleus more closely resembled fast-twitch muscle than did the 32 week samples. Therefore, the rate of synthesis of PV would appear to plateau before the transition of the isoforms of myosin has been completed. This finding is consistent with recent reports that have shown that changes in enzyme profiles, PV, and in the SR occur in advance of those observed for myosin, in response to chronic nerve stimulation and increased muscular activity (Klug et al., 1983a; Green et al., 1984). Since the transitions of the various systems seem to follow a distinct time course, PV immunoreactivity may be a useful indicator of muscle maturity.

The most dramatic finding observed in this portion of the study was the similarity in the localization of PV in the adult dystrophic EDL with that in the soleus muscles. The trend toward a more even distribution was brought about by a preponderance of intermediately-stained fibers in both the fast and slow dystrophic muscles. This trend was also noted in the myosin ATPase staining profiles of these muscles. It is likely that these "intermediate" fibers may represent not only type

2/FOG fibers but also regenerating, degenerating, or immature extrafusal fibers. This classification of intermediate fibers may therefore include those fibers referred to as "atypical", "transitional", or "abnormal" by other investigators (Dribin and Simpson, 1977; Ovalle et al., 1983).

This trend in the alteration of PV-specific proportions was not noted in the muscles of 2-week-old mice. Other than slight distribution variations, the localization of PV was unaffected by dystrophy at this preclinical stage. Not only was the distribution of PV similar in normal and dystrophic groups at 2 weeks, but it also resembled that of the adult muscles. Thus, PV immunostaining appears to be established by 2 weeks of age in the mouse, and its distribution is not affected during the incipient stages of murine muscular dystrophy. At least with respect to PV and myosin ATPase reactivity, dystrophy does not seem to alter the normal development of muscle; however, it may disturb the maturation process. Although the presence of fetal myosin (Fitzsimons and Hoh, 1983) and type 2C fibers (Dubowitz and Brooke, 1973) in dystrophic muscle may indicate a failure in complete muscle maturation or a regression back to a more immature state, PV distribution in the adult dystrophic EDL and soleus does not adopt the staining pattern observed in the 2-week-old mice. However, the concentration of PV in the adult dystrophic muscles may indicate a more immature state despite the differences in the staining profile from the neonatal muscles. The immunohistochemical results suggest that the dystrophic muscles do not become more fetal-like in their PV localization but, rather, show a diminution in PV staining due to the increased number of dystrophic fibers. It would be of interest to ascertain whether those muscle fibers that have been shown to contain fetal myosin are also those that stain intermediately for PV, and have been described as "transitional" or "abnormal" by other investigators.

i) Muscle Spindles

Because serial sections along the lengths of individual muscle spindles were not

performed in the present study, very little can be concluded about the localization of PV in intrafusal muscle fibers. It is likely that regional differences exist in the distribution of PV in intrafusal fibers, similar to those noted in myosin ATPase reactivity as discussed in Chapter 1. Regardless of genotype, in polar regions of muscle spindles sections of adult muscles occasionally contained chain fibers that were positively stained for PV. On the other hand, chain and bag fibers in the 2-week muscles of both normal and dystrophic mice were immunoreactive in polar regions. No staining of the intrafusal fibers, however, was observed in equatorial and juxtaequatorial zones of muscle spindles in either of the age groups. Since most of the contractile apparatus of an intrafusal fiber is found within the polar region of the spindle it may not be surprising that PV would also be concentrated here. However, if PV is a truly cytoplasmic protein with no affinity for intracellular structures, this result may represent evidence for some particular intracellular localization.

PV immunoreactivity has been reported in one of the chain fibers of muscle spindles in adult rat EDL and soleus muscles but not in the nuclear bag fibers (Celio and Heizmann, 1982). These investigators reported that the immunostaining was unequivocal in spindles of the soleus but not in those of the EDL. It is known that mammalian chain fibers have faster relaxation properties than bag fibers (Boyd and Smith, 1984) Although this may account for the positive reaction of the chain fiber to PV (Celio and Heizmann, 1982), it is of interest that only one of the chain fibers shows immunoreactivity. Myosin ATPase reactivity appeared identical in the two intrafusal chain fibers as described in Chapter 1. As in the extrafusal fibers, it would appear that neither PV immunoreactivity nor myosin ATPase staining can be used separately as a means of determining intrafusal fiber types since there is no true correlation between the two.

The presence of PV in nuclear bag fibers of muscle spindles in the 2-week muscles may be a sign of immaturity in the synthesis of this protein. However, the fact that the synthesis of PV generally proceeds that of myosin isoforms, and that

adult myosin ATPase staining patterns are established by 2 weeks of age in murine intrafusal fibers (see Chapter 1), it is unlikely that PV-positive reactivity of bag fibers is a developmental phenomenon. Bag2 intrafusal fibers have been described as fast nuclear bag fibers due to their rapid contraction and relaxation times when compared to bag1 fibers (Boyd and Smith, 1984). It is possible that the unique physiological properties of intrafusal fibers may also correlate the immunolabelling observed in this study. Why PV was not observed in bag fibers of the adult muscles is unknown.

Parvalbumin Content

Although immunocytochemical staining procedures may specifically localize PV in a particular cell, they do not provide very quantitative information. Determining the cellular content of this protein by the intensity of the stain is a very subjective exercise. The immunohistochemical results in this study revealed dramatic differences in PV distribution not only between muscles, but also between individual fiber types and age groups. More noteworthy were the alterations in the localization of PV in the dystrophic samples. It was therefore of interest to quantify these changes and thereby determine whether the immunohistochemical results could be substantiated biochemically.

The biochemical findings presented here support the results of the preceding immunohistochemical experiments. The presence of PV, as determined by gel electrophoresis and immunoblotting, and the PV content determined by RIA were consistently shown to be more prevalent in the EDL than in the soleus. This is true for the tissue sampled at both 2 and 32 weeks of age in the normal population, and in the 2-week dystrophic age group. Parvalbumin values were approximately 27 times greater in the adult EDL than in the adult soleus, and approximately 12 times greater in the EDL than in the soleus of the younger animals. This difference in the concentration of PV between fast-twitch and slow-twitch muscles is consistent with

similar trends reported previously in other species (Leberer and Pette, 1986a,b; Heizmann, 1984; Heizmann et al., 1982). Collectively, these results support the hypothesis that PV content is fiber type specific (Celio and Heizmann, 1982), in that muscles composed predominantly of type 2 fibers have a higher PV concentration than muscles that are primarily type 1 in composition.

The sensitivity of radioimmunoassay depends on the specificity of the antiserum, optimal dilution ratios of antibody and antigen, and the purity of the antigen used for the iodination (Cooper, 1979). It should be remembered that the immunochemical approach is an indirect one in which the observed competition may be the result of a small amount of competitor whose identity is the same as the standard antigen, or a larger quantity of material that has a similar antigenic determinant (Cooper, 1979). The PV values obtained by the RIA in the present study are low compared to previously published reports (Heizmann et al., 1982; Klug et al., 1985; Endo et al., 1986b). A possible source for this discrepancy is the fact that the antiserum had a low titre of 1:400-500. The affinity of the antisera may have been masked by the presence of various other antibodies in the serum. As well, Heizmann heat treats his samples such that the TSP values are lower than ours and the TP over TSP values are greater than ours.

The immunohistochemical data showed that the overall distribution of PV in the 2-week normals was not significantly different from that of the adult muscles. The concentration of PV in the EDL, however, is age dependent. By 2 weeks of age the PV content is 70% of that found in the normal adult EDL. Soleus concentrations between age groups were virtually identical to each other. Therefore, although the pattern of PV distribution has been established by 2 weeks of age, the synthesis of PV within the positively-stained fibers has not reached its peak.

The present findings are in agreement with previous developmental studies that have detected PV by postnatal day 4 or 5 in the EDL of the rat (Celio and Heizmann, 1982; Berchtold and Means, 1985; Leberer and Pette, 1986b). In one-week-old mice,

the PV content represents 5-13% of that found in the adult (Klug et al., 1985). The initial synthesis and time course of the increases in PV appear to occur asynchronously in various fast-twitch muscles (Leberer and Pette, 1986b; Le Peuch et al., 1979). While mature levels of PV have been noted in the gastrocnemius and psoas of the rabbit by 9 weeks after birth, similar levels in the EDL have not been obtained after 17 weeks (Leberer and Pette, 1986b). By 8-12 weeks of age, adult levels of PV in the EDL of the mouse have been achieved (Jasch et al., 1982, Jasch and Moase, 1985; Klug et al., 1985). In a more recent developmental study of the rat gastrocnemius muscle, PV mRNA was first detected at day 5 postnatally, and subsequently increased 15 to 20-fold by day 20 to achieve its maximum levels (Berchtold and Means, 1985). In the chick embryo, other investigators have shown that active synthesis of PV begins 2 days before hatching in muscles of the leg, followed by its synthesis in the pectoralis muscle 4-5 days after hatching, reaching maximal levels by day 7 (Le Peuch et al., 1979). Results from these studies, therefore, indicate that PV synthesis in skeletal muscles is developmentally regulated.

The developmental regulation of PV in these various muscles appears to correlate with the differentiation processes which lead to the formation of fast-contracting and rapidly-relaxing extrafusal muscle fibers (Berchtold and Means, 1985; Heizmann, 1984). These include a decrease in relaxation time after a twitch or tetanus, and the synthesis of elements of the calcium cycle, in particular the SR calcium pump and myosin light chain kinase (Le Peuch et al., 1979). This has recently been supported by a study designed to see if PV is involved in the role of tissue differentiation, cell migration and the events of early embryo development (Kay et al., 1987). Using isolated cDNA segments encoding a PV of tadpoles, and available antibodies as molecular probes it was found that PV and its mRNA is absent during early development. The first demonstrable appearance of PV occurred at the time of somite differentiation when muscle cells were active in expression of the contractile apparatus. It was suggested that the coordinated expression of PV and contractile

proteins also supports the belief that PV plays a role in the contraction-relaxation events of skeletal muscle.

The biochemical data in the present study (Table VIII) showed that the adult dystrophic EDL contains significantly less PV than the normal EDL, consistent with the observed immunohistochemical changes. An 81% diminution from normal values was noted in the 32 week dystrophic EDL. This reduction is larger than the 40% decrease in PV reported previously for various fast-twitch dystrophic muscles at 15 weeks of age (Klug et al., 1985). Both of these findings are, however, consistent with published data on changes in protein distributions in mouse muscle during progressive postnatal stages of the disease (Jasch et al., 1982). Normalized data from scans of these IEF gels indicate that there is a gradual depletion of PV from 12 to 32 weeks of age in the EDL of the dystrophic mouse. Therefore, the 81% drop noted in the present study is probably due to the advanced stage of the disease resulting from a degradation of PV as the expression of extrafusal fiber types change.

On the other hand, a similar trend was not observed in the soleus muscles. In fact, the concentration of PV in the adult dystrophic soleus surpassed that of the normal soleus to levels approaching those of the dystrophic EDL. Hence, these results support our data on the immunohistochemical distribution of PV in the fast and slow muscles of the dystrophic animals. It would appear, then, that the EDL and soleus are becoming more alike with respect to content and distribution of PV, as well as in their pattern of soluble muscle proteins as noted in the gels.

The results from our experiments on the normal soleus muscles were also noteworthy. Parvalbumin was undetectable by gel electrophoresis, barely evident on the immunoblots, and only minimal values could be obtained with the RIA. However, the immunohistochemical data indicated that, taken collectively, 22% of the extrafusal fiber population in the normal soleus contained some level of PV. A possible explanation for this may lie in the fact that all the biochemical data was collected on whole muscle homogenates and not from single fibers, whereas the

immunohistochemical staining identified PV in sections of individual muscle cells. In addition, even though there is a relatively high percentage of positive fibers indicating the presence of PV, the actual PV concentration within these fibers may not be in sufficient amounts to be detected by gel electrophoresis or RIA.

It is obvious that muscular dystrophy does not affect the concentration of PV during the preclinical stages of the disease in the $dy^{2J}$ mouse (see Table IX). A noteworthy feature emerges when a comparison of the preclinical and postclinical values for both the dystrophic EDL and soleus muscles are made. The content of PV in the adult EDL has diminished beyond that of the 2-week EDL, whereas the values for the soleus have increased significantly above those of the 2-week muscle. These findings suggest that the two muscles are adapting to an intermediate form that more closely resembles the muscles in the preclinical stages of dystrophy. These alterations in PV support the hypothesis that dystrophy may reflect an immature state or an alteration in the differentiation process with respect to the calcium regulatory system (Klug et al., 1985; Pette et al., 1985).

As illustrated in Figure 34, PV was not the only soluble muscle protein that was altered by murine dystrophy. Of particular interest are a number of bands in the 16-20 KD range. Those bands characteristic of the slow muscles now appear in the dystrophic fast muscle. A reciprocal phenomenon occurs in the dystrophic soleus. Some, or all, of these higher molecular-weight proteins may also be either calcium-binding or calcium-regulated proteins. According to the position of these bands it is quite probable that they represent the various myosin light chains (LC1-fast, 22.5 KD; LC2-fast, 18 KD; LC3-fast, 16.5 KD; LC1-slow, 27 KD; LC2-slow, 19 KD), troponin-C, 18 KD and calmodulin, 16.7 KD. An alteration in the myosin LC composition in murine dystrophy may also reflect a loss of the normal differentiation process. It is noteworthy that not all the myosin LC's are similarly affected in murine dystrophy (Fitzsimons and Hoh, 1983; Jasch and Moase, 1985). It is not known what the interrelationship is between these proteins and PV. Further speculation should not be

made until the identity of these proteins is known. A critical follow-up to the present study would be to determine whether the other major calcium-binding proteins, namely calmodulin and troponin-C, are affected in a similar fashion by the dystrophic process.

Besides the various enzyme activator activities of calmodulin, such as the physiological $Ca^{2+}$-dependent regulation of myosin light chain kinase in all three muscle types (Walsh et al., 1980), calmodulin can effectively substitute for troponin-C in restoring $Ca^{2+}$-sensitivity to actomyosin ATPase. And, although calmodulin does not stimulate $Ca^{2+}$-uptake in the SR of either fast or slow muscle (Eibschutz et al., 1984) calmodulin may be involved in $Ca^{2+}$-release from skeletal SR (Chiesi and Carafoli, 1982). Although the role of calmodulin in the regulation of skeletal muscle SR and $Ca^{2+}$-transport remains to be determined, it appears that this protein may be involved in the calcium-regulation of muscle contraction. However, it is possible calmodulin could also substitute for PV in the relaxation phase of the cycle. If the function of calmodulin is altered in dystrophy this may also contribute to the changes in the physiological response of muscle in murine dystrophy.

Extracts from dystrophic chicken muscle pretreated with calcium-activated neutral protease exhibit a decrease in troponin-I and troponin-C with a relative preservation of troponin-T (Sugita et al., 1980). Studies of skeletal muscle from hamsters have demonstrated no detectable differences between the calmodulin content of normal and dystrophic animals; therefore, no apparent correlation exists between the calcium accumulation observed in dystrophic muscle and the recorded changes in calmodulin content (Klamut et al., 1983).

Although the decrease in muscle proteins in dystrophy is largely attributed to an increased rate of protein degradation (Garber et al., 1980), it appears that, despite close similarities in proteins such as calmodulin, troponin-C and PV, each one may be affected differently by the same disease. In murine dystrophy, the alterations observed in PV content are largely due to a conversion in the phenotypic expression

of extrafusal fiber types. This conversion to an intermediate type or perhaps an immature state may be a consequence of the degradation process triggered by a defect in calcium metabolism.

# GENERAL DISCUSSION

It was not unexpected that no alterations were observed in the neonatal intrafusal fibers and muscle spindles in the dystrophic mice. However, this observation is in itself interesting when one considers the complex innervation pattern to these sensory receptors and the alterations which have been described in both the sensory and motor nerve supply to dystrophic muscle. It is possible that complexity of the muscle spindles polyneuronal innervation is its own safeguard mechanism. It is also tempting to speculate that the intrafusal fiber may be governed by neurotrophic influences which are different from those of its neighbouring extrafusal fibers, and which are spared the dystrophic gene expression. As well, the actual combination or composition of various myosin heavy chains and myosin light chains within the intrafusal fibers may in fact mask any histochemical changes which may occur as a result of the disease.

Although PV may be a useful indicator of a muscle's state of maturity, and perhaps a marker for early neuromuscular disturbances, significant changes in PV localization could not be detected in the intrafusal fibers. However, without a more rigorous investigation into the actual distribution of PV throughout the entire length of the intrafusal fibers, nothing conclusive can be said about its appearance in dystrophy with regards to the spindle.

The data presented in Chapter 2 of this thesis indicates that a decrease in parvalbumin content occurs in the extrafusal fibers of the dystrophic EDL whereas an increase in parvalbumin content occurs in the dystrophic soleus with age. These alterations are consistent with the known changes that occur in the fast-twitch muscles in half-relaxation times. This study also provides further indirect evidence for the proposed role of parvalbumin as a soluble relaxation factor in fast-twitch skeletal muscle.

In both the dystrophic EDL and soleus there appears to be a conversion of

extrafusal fiber types to a more intermediate form than that seen in normal age-matched muscles. This intermediate form of myofiber does not completely resemble neonatal muscles at 2 weeks of age in either the content or the distribution of parvalbumin. The concentration of parvalbumin found in these dystrophic muscles does, however, resemble the levels reported in more immature muscle. The slight increase in parvalbumin in the adult dystrophic soleus and the appearance of higher molecular-weight protein bands in the dystrophic EDL resembling those observed in the slow-twitch muscle, also support the hypothesis that dystrophy in some way alters the differentiation process and the subsequent maturation of regenerating fibers. The changes observed in this disease in both parvalbumin content and the distribution of fiber types may reflect an immature state of dystrophic muscle. This is consistent with the reported conversions in extrafusal fiber types, isomyosins and $Ca^{2+}$ metabolism to a neonatal stage of development. Interestingly, parvalbumin maturation parallels that of the SR and other calcium-regulated entities. Muscular dystrophy, therefore, appears to influence the maturation or differentiation of normal fast muscle fibers, particularly the elements involved in the $Ca^{2+}$ cycle.

There are several indications that skeletal muscle maturation is prolonged or altered in murine dystrophy. Normal differentiation of fast muscle includes the withdrawal of polyneuronal innervation, the switching off of slow-twitch muscle myosin, an increase in the activity of glycolytic enzymes and the uptake-capacity of the SR for $Ca^{2+}$, and a decrease in contraction and half-relaxation times (Vrbova, 1983; Dhoot, 1985). Synthesis of these elements that are part of the $Ca^{2+}$ cycle, correspond with the synthesis of parvalbumin (Celio and Heizmann, 1982; Berchtold and Means, 1985). Analysis of native myosin isoenzyme and myosin light chain distribution in fast-twitch murine dystrophic muscle (Fitzsimons and Hoh, 1983; Jasch and Moase, 1985) has shown an alteration in these components when compared to their normal counterparts. The dystrophic muscle is characterized by an increase in slow and intermediate myosin, and a decrease in the proportion of myosin light chain

3 (fast) and myosin light-chain 2 (fast-phosphorylated). Samaha and Thies (1979) investigated the myosin light chains in dystrophic human muscle and found no alterations in the type or mobility of LC1 and LC2 when compared to normal muscle. However, a more diverse composition of myosin light chains has been detected in type 1 fibers of DMD patients than in control muscle (Takagi et al., 1982). In particular, the fast-type LC3 was noted in 55% of these slow type fibers. In a study of human skeletal isomyosins, Fitzsimons and Hoh (1981) found large amounts of fetal myosin in muscle from Duchenne patients and suggested that the presence of this isoform reflects muscle regeneration or immaturity. The percentage of fetal myosin in muscle affected with Duchenne dystrophy was estimated by these workers at 1-12% of the total amount of myosin.

A more recent immunofluorescence study (Schiaffino et al., 1986) also reported the existence of myosin isoforms that were indistinguishable from fetal myosin in human dystrophic muscle. These workers observed many small extrafusal fibers that stained positively for anti-fetal myosin, and estimated the percentage of reactive fibers to be between 20% and 41%. They suggested that fetal myosin in dystrophic muscle are confined to a population of newly formed fibers resulting from successive cycles of necrosis and regeneration. Alternatively, muscle fiber maturation that is normally accompanied by the cessation of fetal myosin synthesis may be delayed in the dystrophic process. Parry and Desypris (1983) also demonstrated with immunohistochemical methods the presence of slow myosin in fast-twitch hindlimb muscles of dystrophic mice. In addition to these findings, similarities in enzyme and isoenzyme patterns of anaerobic metabolism in both adult dystrophic mouse muscle and immature normal muscle have recently been demonstrated (Petell et al., 1984; Reichmann and Pette, 1984). An increased synthesis and accelerated degradation of many other muscle proteins in dystrophic muscle (Garber et al., 1980) may account for the presence of immature muscle characteristics. These abnormalities correlate well with the contractile and histochemical changes just mentioned, indicating a

transformation in extrafusal fibers to a more immature or intermediate state.

For a more complete study of this maturation issue, it would have been useful to include in this study tissue samples from 1-week-old dystrophic mice and those from another developmental stage, such as 8-12 weeks of age. These age groups would have provided data on a more immature stage of development and may have revealed transformations in PV distribution during a transitional stage of 8-12 weeks. Due to the difficulties in obtaining adequate numbers of young dystrophic animals, and in the time constraints, such an extensive study was not undertaken.

Why is there a reduction in PV in the dystrophic fast-twitch EDL muscle concomitant with an increase in this calcium-binding protein in the slow-twitch soleus, and what are the functional implications of these alterations? A decrease in the parvalbumin content is not merely related to a depletion of the protein but to a conversion in fiber types to a population of muscle fibers that contain less parvalbumin. These myofibers are not necessarily type 1/SO or type 2/FOG fibers but perhaps either atypical, regenerating or degenerating fibers that display low parvalbumin immunoreactivity. Parvalbumin localization and its content in fast-twitch skeletal muscles respond rapidly to experimentally induced fiber type transformations (Klug et al., 1983a; Green et al., 1984; Stuhlfauth et al., 1984; Müntener et al., 1985). It has been established as one of the earliest and most sensitive markers of activity-induced fast-to-slow conversions in developing skeletal muscle (Klug et al., 1983a,b). Because an altered parvalbumin content has also been observed in response to electrical stimulation, cross-reinnervation and denervation, it is more likely that the changes observed in the dystrophic murine muscle are secondary effects and a consequence of a conversion in the phenotypic expression of extrafusal myofiber types.

We cannot speak of muscle fiber transitions based on one parameter alone, such as myosin ATPase fiber type or PV content. The transformation must be considered at the level of specific systems, not merely as a single entity with respect to the

muscle fiber. It has been observed that fiber type transitions involve changes in enzyme profiles, sarcoplasmic reticulum, myosin isoforms, and PV (Green et al., 1984). These alterations follow an ordered time course as they are developmentally regulated. Thus, it would appear that murine dystrophy induces, in a graded fashion, the observed modifications of the various functional systems of the extrafusal muscle fiber similar to the plasticity described in response to other neuromuscular conditions (Pette, 1980).

The changes in fiber distribution in the dystrophic muscles observed in the present study, and in previous reports, may in fact play a crucial role in the decreased calcium uptake of the SR, in addition to the alterations in PV. Type 2 fast fibers have a more highly developed SR than type 1 slow fibers. As dystrophic muscle acquires a more intermediate fiber type distribution, it is possible the calcium uptake ability of this tissue mirrors the phenotypic expression in fiber types. An increase in the relative amounts of intermediate or slow muscle fibers, adipose tissue, and connective tissue would naturally affect the muscle's overall calcium metabolism. This in turn would be reflected in the prolonged half-relaxation times and time-to-peak tension that are characteristic features of the dystrophic process in the $dy^{2J}/dy^{2J}$ strain of mouse (Bressler et al., 1983; Parry and Desypris, 1983). The delayed physiological reactions have been attributed to the presence of slow myosin in fast-twitch muscle (Parry and Desypris, 1983). However, these changes also correlate well with the decreases in PV content. Thus dystrophy appears to induce numerous asynchronous changes in the differentiation process as a consequence of an unknown genetic defect.

Although the changes in PV content in the dystrophic fast muscle mirrors the prolonged half-relaxation time of this muscle, an increased PV content in the slow muscle is not paralleled by a decrease in its half-relaxation time by 32 weeks of age (Bressler et al., 1983). A similar finding was observed in a recent cross-reinnervation study of fast and slow muscle of the rat (Müntener et al., 1986).

Cross-reinnervated fast muscle with a slow nerve had similar histochemical and physiological characteristics to those of the normal slow muscle. However, the PV content was 30-80 times greater than the slow muscle. Thus a slow contracting/slow relaxing muscle may contain more PV than a fast contracting/fast relaxing muscle in the face of a disturbance to its normal nerve-muscle interaction (Müntener et al., 1986). This might suggest that PV is a useful marker for early changes in neuromuscular disturbances as well as an indicator of abnormal changes in muscle transformations. These observations also support the hypothesis that murine dystrophy may suffer from an altered nerve-muscle interaction.

At the present time it is not clear whether the different muscle proteins are dysfunctional in any way in the dystrophic tissue. It is possible that the changes seen in PV localization and content in the present study may be the result of an alteration in the antigenicity of the protein due to chemical or structural changes. In light of this, it might be useful to run an amino acid analysis and HPLC profile on PV extracted from typed single fibers of dystrophic muscle.

It is difficult to determine what effect an alteration in the parvalbumin concentration may have on the intracellular $Ca^{2+}$-buffering system of skeletal muscle. Certainly a diminished protein content would alter the $Ca^{2+}$-buffering capacity of the muscle fiber, and perhaps lead to an activation of $Ca^{2+}$-dependent proteases, which in turn can lead to the irreversible cell destruction typical of this disease. Klug and coworkers (1985) have estimated a 360 μmole/kg of muscle reduction in the sarcoplasmic $Ca^{2+}$-binding capacity in dystrophic tissue. However, it is not known whether the levels observed in dystrophic fast-twitch muscle are significantly reduced to be responsible for the increased intracellular calcium concentrations noted in these muscles. In the dystrophic state, it now seems plausible that the sarcoplasmic free calcium concentration rises in response to: (1) an altered membrane permeability, (2) an impaired functioning of the SR $Ca^{2+}$-uptake and sequestering system, and (3) a decrease in PV.

A decrease in the number of PV-positive extrafusal fibers, concomitant with a prolonged half-relaxation time, have also been observed in several neuromuscular disturbances. Studies on the mutant mouse "arrested development of righting response" as well as those on cross-reinnervation and denervation of rat muscles, indicate that the expression of PV in fast skeletal muscle is dependent on a nerve-muscle interaction (Stuhlfauth et al., 1984; Müntener et al., 1985, 1986). It has been suggested that PV is under neural regulation by fast-type motor-neuron activity since concentrations of PV are suppressed in presumptive fast-twitch muscle by denervation, whereas slow-twitch muscle appears unaffected by denervation (Leberer and Pette, 1986b). Denervation of developing fast-twitch muscle results in a rapid decay in PV compared to that of adult fast muscle which exhibits a delayed suppression in PV concentrations. This difference in the rate of PV reduction was attributed to the higher turnover of proteins in the developing muscle (Leberer and Pette, 1986a). These findings suggest that the changes observed in dystrophic muscle may have important implications. The alterations in PV may reflect a loss of the acquired state of differentiation of the affected muscles, evidenced by a transformation in fiber types. This in turn may be due to a failure of the normal nerve-muscle interaction in postnatal development as suggested by Jasch and Moase (1985).

In a study of the trophic influences of nerve and muscle in the $dy^{2J}$ mouse Saito and coworkers (1983) found that the dystrophic muscle fibers underwent degeneration inspite of complete reinnervation by a normal nerve, and normal muscle could not prevent degeneration of the dystrophic nerve. No myotrophic influences were observed. It appeared that both nerve and muscle were genetically programmed to degenerate in murine dystrophy and both could do so to some extent independent of each other. Muscle degeneration was the additive effects of the dystrophic gene expression and abnormal neurotrophic influences. Nerve degeneration, on the other hand, was influenced by dystrophic gene expression alone. In light of this, abnormal neurotrophic influences may, in part, be responsible for the altered PV expression in

dystrophic tissue, as well as the changes in the SR and fiber composition which arise as secondary features governed by the unknown primary defect.

Although the physiological role of PV in nervous tissue is not known, PV in this tissue is believed to function in the $Ca^{2+}$-regulated release of neurotransmitters and in axonal flow. The author of a recent report (Celio, 1986) has suggested that PV may function to shorten the refractory period and enable GABA neurons to fire in rapid succession. It was also proposed that the release of $Mg^{2+}$ by PV may trigger Mg-dependent enzymes within the GABA neurons, and thereby regulate both electrical and metabolic activity within nervous tissue. In light of the involvement of PV in neuronal processes and in skeletal muscle, parvalbumins are probably involved in the regulation of various $Ca^{2+}$-dependent systems. Even though the distribution and concentration of PV is altered in both the fast and slow muscles of the muscular dystrophic mice, it is unlikely that the function or conformation of the protein is modified. It would be of interest to study the response of PV in the nervous tissue of the dystrophic animals to determine whether the observed changes represent a more global alteration in PV or if they are specific to skeletal muscle. If parvalbumin is regulated by a neurogenic factor, which it appears to be, then changes in its content or distribution might also be expected in nervous tissue. A global effect on PV concentration would add credence to a disturbance in calcium regulation as a major defect in dystrophic skeletal muscle.

## BIBLIOGRAPHY


Ashley, C.C. 1983 Calcium in muscle. In: Calcium in Biology. T.G. Spiro, ed. John Wiley, New York, pp. 107-175.

Ashley, C.C., Griffiths, P.J. 1983 The effect of injection of parvalbumins into single muscle fibers from the barnacle Balanus hibilus. J. Physiol.(Lond), 345:105P.

Atwood, H.L., Kwan, I. 1978 Dystrophic and normal mice show age-dependent divergence of muscle sodium concentrations. Exp. Neurol., 60:386-392.

Bakker, G.J., Richmond, F.J.R. 1981 Two types of muscle spindles in cat neck muscles: a histochemical study of intrafusal fiber composition. J. Neurophysiol., 45:973-986.

Bandman, E. 1985 Continued expression of neonatal myosin heavy chain in adult dystrophic skeletal muscle. Science, 227:780-782.

Banker, B.Q., Hirst, N.S., Chester, C.S., Fok, R.Y. 1979 Histometric and electron cytochemical study of muscle in the dystrophic mouse. Ann. N.Y. Acad. Sci., 317:115-132.

Banks, R.W., Harker, D.W., Stacey, M.J. 1977 A study of mammalian intrafusal muscle fibers using a combined histochemical and ultrastructural technique. J. Anat., 123:783-796.

Barker, D. 1974 The morphology of muscle receptors. In: Handbook of Sensory Physiology. Vol. 111/2, Muscle Receptors. C.C. Hunt, ed. Springer-Verlag, Berlin, pp. 84-89.

Barker, D., Chin, N.K. 1960 The number and distribution of muscle spindles in certain muscles of the cat. J. Anat., 94:473-486.

Barker, D., Milburn, A. 1984 Development and regeneration of mammalian muscle spindles. Sci. Prog., 69:45-64.

Barnard, E.A., Bhargava, A.K., Hudecki, M.S. 1976 Postponement of symptoms of hereditary muscular dystrophy in chickens by 5-hydroxytryptamine antagonists. Nature, 263: 422-424.

Baron, G., Demaille, J. Dutruge, E. 1975 The distribution of parvalbumin in muscle and other tissues. FEBS Lett., 56:156-160.

Baylor, S.M., Chandler, W.K., Marshall, M.W. 1983 Sarcoplasmic reticulum calcium release in frog skeletal muscle fibers estimated from Arsenazo 111 calcium transients. J. Physiol.(Lond), 344:625-666.

Benzonana, G., Capony, J.P., Pechère, J.F. 1972 The binding of calcium to muscular parvalbumins. Biochim. Biophys. Acta, 278:110-116.

Benzonana, G., Chaponnier, C., Gabbiani, G. 1977 Immunofluorescent subcellular localization of muscle porteins. Experientia, 33:787.

Benzonana, G., Wnuk, W., Cox, J.A., Gabbiani, G. 1975 Cellular distribution of sarcoplasmic calcium-binding proteins by immunofluorescence. Histochemistry, 51:335-341.

Berchtold, M.W., Celio, M.R., Heizmann, C.W. 1984 Parvalbumin in non-muscle tissues of the rat: quantitation and immunohistochemical localization. J. Biol. Chem., 259:5189-5196.

Berchtold, M.W., Celio, M.R., Heizmann, C.W. 1985 Parvalbumin in human brain. J. Neurochem., 45:235-239.

Berchtold, M.W., Heizmann, C.W., Wilson, K.J. 1982a Primary structure of parvalbumin from rat skeletal muscle. Eur. J. Biochem., 127:381-389.

Berchtold, M.W., Heizmann, C.W., Wilson, K.J. 1983 $Ca^{2+}$-binding proteins: A comparative study of their behavior during high-performance liquid chromatography using gradient elution on reverse-phase supports. Anal. Biochem., 129:120-131.

Berchtold, M.W., Means, A.R. 1985 The $Ca^{2+}$-binding protein parvalbumin: molecular cloning and developmental regulation of mRNA abundance. Proc. Natl. Acad. Sci. USA, 82:1414-1418.

Berchtold, M.W., Wilson, K.J., Heizmann, C.W. 1982b Isolation of neuronal parvalbumin by high-performance liquid chromatography. Characterization and comparison with muscle parvalbumin. Biochem., 21:6552-6557.

Blum, H.E., Lehky, P., Kohler, L., Stein, E.A., Fischer, E.H. 1977 Comparative properties of vertebrate parvalbumin. J. Biol. Chem., 252:2834-2838.

Boyd, I.A., Smith, R.S. 1984 The muscle spindle. In: Peripheral Neuropathy, Vol. 1. P.J. Dyck, P.K. Thomas, E.H. Lambert, R. Bunge, eds. W.B. Saunders, Philadelphia, pp. 171-202.

Bray, G.M., Perkins, S., Peterson, A.C., Aguayo, A.J.1977 Schwann cell multiplication deficit in nerve roots of newborn dystrophic mice. J. Neurol. Sci., 32:203-212.

Bressler, B.H., Jasch, L.G., Ovalle, W.K., Slonecker, C.E. 1983 Changes in isometric contractile properties of fast-twitch and slow-twitch skeletal muscle of C57BL/6Jdy$^{2J}$/dy$^{2J}$ dystrophic mice during postnatal development. Exp. Neurol., 80:457-470.

Briggs, N. 1975 Identification of the soluble relaxing factor as a parvalbumin. Fed. Proc., 34:540.

Brooke, M.H., Kaiser, K.K. 1970 Muscle fiber types: How many and what kind? Arch. Neurol., 23:369-379.

Bulfield, G., Siller, W.G., Wight, P.A.L., Moore, K.J.1984 X-chromosome-linked muscular dystrophy (mdx) in the mouse. Proc. Natl. Acad. Sci., 81:1189-1192.

Butcher, L.A., Tomkins, J.K. 1986 Protein profiles of sarcoplasmic reticulum from normal and dystrophic mouse muscle. J. Neurol. Sci., 72:159-169.

Butler, J., Cosmos, E. 1977 Histochemical and structural analysis of the phenotypic expression of the dystrophic gene in the 129/ReJ dy/dy and the C57BL/6Jdy$^{2J}$/dy$^{2J}$ mice. Exp. Neurol., 57:666-681.

Butler, J.E., Feldbush, T.L., McGivern, P.L., Stewart, N. 1978 The enzyme-linked immunosorbent assay (ELISA): a measure of antibody concentration or affinity. Immunochem., 15:131-136.

Butler, R. 1979 A new grouping of intrafusal muscle fibers based on developmental studies of muscle spindles in the cat. Am. J. Anat., 156:115-120.

Butler, R. 1980 The organization of muscle spindles in the tenuissimus muscle of the cat during late development. Dev. Biol., 77:191-212.

Carafoli, E. 1982 The regulation of intracellular calcium. Adv. Exp. Med. Biol., 151:461-472.

Carafoli, E., Penniston, J.T. 1985 The calcium signal. American Scientific, 253:70-78.

Cave, A., Pages, M., Morin, P.L., Dobson, C.M. 1979 Conformational studies on muscular parvalbumins cooperative binding of calcium (II) to parvalbumins. Biochemie, 61:607-613.

Cazzato, G., Walton, J.N. 1968 The pathology of the muscle spindle: A study of biopsy material in various muscular and neuromuscular diseases. J. Neurol. Sci., 7:15-70.

Celio, M.R. 1986 Parvalbumin in most -aminobutyric acid-containing neurons of the rat cerebral cortex. Science, 231:995-997.

Celio, M.R., Heizmann, C.W. 1981 Calcium-binding protein parvalbumin as a neuronal marker. Nature, 293:300-302.

Celio, M.R., Heizmann, C.W. 1982 Calcium-binding protein parvalbumin is associated with fast contracting muscle fibres. Nature, 297:504-506.

Celio, M.R., Lutz, H., Jenny, E. 1981 Myosin isoenzymes in rat muscle spindles. J. Histochem. Cytochem., 29:894 (abst.).

Chiesi, M., Carafoli, E. 1982 The regulation of $Ca^{2+}$-transport by fast skeletal muscle sarcoplasmic reticulum. Role of calmodulin and the 53,000 dalton glycoprotein. J. Biol. Chem., 257:984-991.

Childers, S.R., Siegel, F.L. 1976 Calcium-binding proteins in electroplax and skeletal muscle. Comparison of the parvalbumin and phosphodiesterase activator protein of Electrophorus electricus. Biochim. Biophys. Acta, 439:316-325.

Cohen, P. 1980 The role of calcium ions, calmodulin and troponin in the regulation of phosphorylase kinase from rabbit skeletal muscle. Eur. J. Biochem., 111:563-574.

Cooper, S. 1960 Muscle spindles and other muscle receptors. In: The Structure and Function of Muscle. G.H. Bourne, ed. Academic Press, New York, pp. 381-420.

Cooper, T.G. 1979 The Tools of Biochemistry. John Wiley, New York, pp. 295-308.

Cox, J.A., Winge, D.R., Stein, E.A. 1979 Calcium, magnesium and the conformation of parvalbumin during muscular activity. Biochemie, 61:601-605.

Crow, M.T., Kushmerick, M.J. 1982 Myosin light chain phosphorylation is associated with a decrease in the energy cost for contraction in fast-twitch mouse muscle. J. Biol. Chem., 257:2121-2124.

Crowe, L.M., Baskin, R.J. 1982 Quantitative ultrastructural differences in the development of normal and dystrophic muscle. Exp. Neurol., 78:303-305.

Cullen, M.J., Mastaglia, F.L. 1980 Morphological changes in dystrophic muscle. Brit. Med. Bull., 36:145-152.

Dhoot, G.K. 1985 Initiation of differentiation into skeletal muscle fiber types. Muscle Nerve, 8:307-316.

Doriguzzi, C., Mongini, T., Palmucci, L., Schiffer, D. 1983 A new method for myofibrillar Ca++-ATPase reaction based on the use of metachromatic dyes: Its advantages in muscle fiber typing. Histochemistry, 79:289-294.

Dow, P.R., Ovalle, W.K. 1985 Muscle spindle morphology in advanced murine muscular dystrophy. Anat. Rec., 211:53A (abstr.).

Dow, P.R., Shinn, S.L., Ovalle, W.K. 1980 Ultrastructural study of a blood-muscle spindle barrier after systemic administration of horseradish peroxidase. Am. J. Anat., 157:375-388.

Dribin, L.B., Simpson, S.B. 1977 Histochemical and morphological study of dystrophic (C57BL/6Jdy$^{2J}$/dy$^{2J}$) and normal muscle. Exp. Neurol., 56:480-497.

Dubowitz, V., Brooke, M.H. 1973 Muscle Biopsy: A Modern Approach. W.B. Saunders, Philadelphia, p. 32.

Duncan, C.J.1978 Role of intracellular calcium in promoting muscle damage: A strategy for controlling the dystrophic condition. Experientia, 34:15531-1535.

Eibschutz, B., Wong, A.P.G., Lopaschuk, G.D., Katz, S. 1984 The presence and binding characteristics of calmodulin in microsomal preparations enriched in sarcoplasmic reticulum from rabbit skeletal muscle. Cell Calcium, 5:391-400.

Endo, T., Kobayashi, M., Kobayashi, S., Onaya, T. 1986a Immunocytochemical and biochemical localization of parvalbumin in the retina. Cell Tissue Res., 243:213-217.

Endo, T., Takazawa, K., Kobayashi, S., Onaya, T. 1986b Immunochemical and immunohistochemical localization of parvalbumin in rat nervous tissues. J. Neurochem., 46:892-898.

Engel, A.G. 1986 Duchenne dystrophy In: Myology. Chapter 37, A.G. Engel, B.Q. Banker eds. McGraw-Hill, New York, pp. 1185-1240.

Engvall, E., Perlmann, P. 1971 Enzyme-linked immunosorbent assay (ELISA) quantitative assay for immunoglobulin G. Immunochemistry, 8:871.

Feder, N., Sidman, R.L. 1958 Methods and principles of fixation by freeze-substitution. J. Biophysic. Biochem. Cytol., 4:593-602.

Fitzsimons, R.B., Hoh, J.F. 1981 Embryonic and foetal myosins in human skeletal muscle. J. Neurol. Sci., 52:367-384.

Fitzsimons, R.B., Hoh, J.F.Y. 1983 Myosin isoenzymes in fast-twitch and slow-twitch muscles of normal and dystrophic mice. J. Physiol.(Lond), 343:539-550.

Flaherty, L. 1981 Congenic strains. In: The Mouse in Biochemical Research, Vol. I. H.L. Foster, J.D. Small, J.G. Fox, eds. Academic Press, New York, pp. 215- 222.

Focant, B., Pechère, J.F. 1965 Contribution a l'etude des proteines de faible poids moleculaires des myogenes de vertebres inferieurs. Arch. Int. Physiol. Biochim., 73:334-354.

Garber, A.J., Schwartz, R.J., Seidel, C.L., Silvers, A., Entman, M.L. 1980 Skeletal muscle protein and amino acid metabolism in hereditary mouse muscular dystrophy. J. Biol. Chem., 255:8315-8324.

Gerday, C. 1982 Soluble calcium-binding proteins from fish and invertebrate muscle. Mol. Phys., 2:63-87.

Gerday, C., Gillis, J.M. 1976 The possible role of parvalbumins in the control of contraction. J. Physiol. (Lond), 258:96P-97P.

Gerday, C., Joris, B., Gerardin-Otthiers, N., Collin, S., Hamoir, G. 1979 Parvalbumins from the lungfish (Protopterus dolloi). Biochimie., 61:589-599.

Gerfen, C.R., Baimbridge, K.G., Miller, J.J. 1985 The neostriatal mosaic: Compartmental distribution of calcium-binding protein and parvalbumin in the basal ganglia of the rat and monkey. Proc. Natl. Acad. Sci. USA, 82:8780-8784.

Gillis, J.M. 1980 The biological significance of muscle parvalbumins. In: Calcium-Binding Proteins: Structure and Function. F.L.Siegel, E. Carafoli, R.H. Kretsinger, D.H. MacLennan, R.H. Wasserman, eds. Elsevier North-Holland, New York, pp.309-3ll.

Gillis, J.M., Lebacq, J., Piront, A. 1985 Quantification of the relaxing effect of muscle parvalbumins. J. Physiol.(Lond), 365:67P

Gillis, J.M., Piront, A., Gosselin-Rey, C. 1979 Parvalbumin distribution and physical state inside the muscle cell. Biochem. Biophys. Acta, 585:444-450.

Gillis, J.M., Thomason, D., Lefevre, J., Kretsinger, R.H. 1982 Parvalbumins and muscle relaxation: A computer stimulation study. J. Muscle Res. Cell Motil., 3:377-398.

Goodman, M., Pechère, J.F. 1977 The evolution of muscular parvalbumins investigated by the maximum parsimony method. J. Mol. Evol., 9:131-158.

Goodman, M., Pechère, J.F., Haiech, J., Demaille, J.G. 1979 Evolutionary diversification of structure and function in the family of intracellular calcium-binding proteins. J. Mol. Evol., 13:331-352.

Gosselin-Rey, C. 1974 Fish parvalbumins: Immunochemical reactivity and biological distribution. In: Calcium Binding Proteins. W. Drabikowski, H. Strzelecka-Golaszewska, E. Carafoli, eds. Polish Scientific Publishers, Warsaw, pp. 679-701.

Gosselin-Rey, C., Gerday, C. 1977 Parvalbumins from frog skeletal muscle (Rana temporaria L.). Isolation and characterization. Structural modifications associated with calcium binding. Biochim. Biophys. Acta, 492:53-63.

Gosselin-Rey, C., Piront, A., Gerday, C. 1978 Polymorphism of parvalbumins and tissue distribution. Characterization of component I, isolated from red muscles of Cyprinus carpio L. Biochim. Biophys. Acta, 532: 294-304.

Green, H.J., Klug, G.A., Reichmann, H., Sedorf, U., Wiehrer, W., Pette, D. 1984 Exercise-induced fiber type transitions with regard to myosin, parvalbumin, and sarcoplasmic reticulum in muscle of the rat. Pflugers Arch., 400:432-438.

Green, H.J., Reichmann, H., Pette, D. 1982 A comparison of two ATPase based schemes for histochemical muscle fiber typing in various mammals. Histochemistry, 76:21-31.

Greenwood, F.C., Hunter, W.M. 1963 The preparation of 131I-labelled human growth hormone of high specific activity. Biochem. J., 89:114-123.

Guth, L., Samaha, F.J. 1970 Procedure for the histochemical demonstration of actomyosin ATPase. Exp. Neurol., 28:365-367.

Haiech, J, Derancourt, J., Pechère, J.F., Demaille, J.G. 1979a Magnesium and calcium binding: Evidence for differences between parvalbumins and an explanation of their relaxing function. Biochemistry, 18: 2752-2758.

Haiech, J., Derancourt, J., Pechère, J.F., Demaille, J.G. 1979b A new large-scale purification procedure for muscular parvalbumins. Biochimie, 61:583-587.

Hamoir, G., Gerardin-Otthiers, N., Focant, B.,1980 Protein differentiation of the superfast swimbladder muscle of the toadfish Opsanus tau. J. Mol. Biol., 143:155-160.

Harris, J.B., Slater, C.R. 1980 Animal models: What is their relevance to the pathogenesis of human muscular dystrophy? Br. Med. Bull., 36:193-197.

Heilmann, C., Pette, D. 1979 Molecular transformations in sarcoplasmic reticulum of fast-twitch muscle by electro-stimulation. Eur. J. Biochem., 93:437-446.

Heizmann, C.W. 1984 Parvalbumin, an intracellular calcium-binding protein; Distribution, properties and possible roles in mammalian cells. Experientia, 40:910-921.

Heizmann, C.W., Berchtold, H.W., Rowlerson, A.M. 1982 Correlation of parvalbumin concentration with relaxation speed in mammalian muscles. Proc. Natl. Acad. Sci. USA, 79:7243-7247.

Heizmann, C.W., Celio, M.R. 1986 Localization of the $Ca^{2+}$ binding parvalbumin. Methods Enzymol., in press

Heizmann, C.W., Strehler, E.E. 1979 Chicken parvalbumin-like protein and three other components (Mr = 8,000 to 13,000). J. Biol. Chem., 254:4296-4303.

Henrotte, J.G. 1955 A crystalline component of carp myogen precipitating at high ionic strength. Nature, 176:1221-1223.

James, N.T., Meek, G.A. 1979 Ultrastructure of muscle spindles in C57BL/6Jdy$^{2J}$/dy$^{2J}$ dystrophic mice. Experientia, 35:108-109.

Jasch, L.G., Bressler, B.H., Ovalle, W.K., Slonecker C.E. 1982 Abnormal distribution of proteins in the soleus and extensor digitorum longus of dystrophic mice. Muscle Nerve, 5:462-470.

Jasch, L.G., Moase, E.A. 1985 Evidence for the identities of five proteins decreased in skeletal muscle of dystrophic mice. Muscle Nerve, 8:389-401.

Johnson, M.I., Ovalle, W.K. 1984 Neonatal development of muscle spindles in slow and fast muscles of genetically dystrophic mice. Anat. Rec., 208:83A (abst.).

Johnson, M.I., Ovalle, W.K. 1986 Alterations in parvalbumin content in murine dystrophic skeletal muscle. Anat. Rec., 214:62A (abst.).

Johnson, M.I., Ovalle, W.K. 1986 A comparative study of muscle spindles in slow and fast neonatal muscles of normal and dystrophic mice. Am. J. Anat., 175:413-427.

Johnson, J.D., Robinson, D.E., Robertson, S.P. 1981 $Ca^{2+}$-exchange with troponin and the regulation of muscle contraction In: The Regulation of Muscle Contraction:Excitation-Contraction Coupling. A.D. Grinnell and M.A.B. Brazier, eds. Academic Press, New York, pp. 241-259.

Jones, E., Krohn, P. 1960 Orthotopic ovarian transplantation in mice. J. Endocrinology, 20:135-146.

Kay, B.K., Shah, A.J., Halstead, W.E. 1987 Expression of the calcium-binding protein, parvalbumin, during embryonic development of the frog Xenopus laevis. J. Cell Biol., 104:841-847.

Kelly, B.S., Levy, J.G., Sikora, L. 1979 The use of the enzyme-linked immunosorbent assay (ELISA) for the detection and quantification of specific antibody from cell cultures. Immunology, 37:45-52.

Kennedy, W.R., Poppele, R.E., Quick, D.C. 1980 Mammalian muscle spindles. In: The Physiology of Peripheral Nerve Diseases. A.J. Sumner, ed. W.B. Saunders Co., Philadelpia. pp. 74-133.

Khan, M.A., Soukup, T. 1979 A histoenzymatic study of rat intrafusal muscle fibers. Histochemistry, 62:179-189.

Klamut, H.J., Lin, C.H., Strickland, K. 1983 Calmodulin content and Ca-activated protease activity in dystrophic hamster muscles. Muscle Nerve, 6:436-441.

Klug, G., Reichmann, H., Pette, D. 1983a Rapid reduction in parvalbumin concentration during chronic stimualtion of rabbit fast-twitch muscle. FEBS Letters 152:180-182.

Klug, G., Reichmann, H., Pette, R. 1985 Decreased parvalbumin contents in skeletal muscles of C57BL/6J(dy$^{2J}$/dy$^{2J}$) dystrophic mice. Muscle Nerve, 8:576-579.

Klug, G., Wiehrer, W., Reichmann, H., Leberer, E., Pette, D. 1983b Relationships between early alterations in parvalbumins, sarcoplasmic reticulum and metabolic enzymes in chronically stimulated fast-twitch muscle. Pflugers Arch., 399:280-284.

Klugh, H.E. 1974 Statistics: The essentials for research. John Wiley, New York, pp. 396-399.

Kozeka, K., Ontell, M. 1981 The three-dimensional cytoarchitecture of developing murine muscle spindles. Dev. Biol., 87:133-147.

et Kronnie, G., Donselaar, Y., Soukup, T., van Raamsdonk, W. 1981 Immunohistochemical differences in myosin composition among intrafusal muscle fibers. Histochemistry, 73:65-74.

et Kronnie, G., Donselaar, Y., Soukup, T., Zelena, J. 1982 Development of immunohistochemical characteristics of intrafusal fibers in normal and de-efferented rat muscle spindles. Histochemistry, 74:355-366.

Kucera, J. 1977 Histochemistry of intrafusal muscle fibers outside the spindle capsule. Am. J. Anat., 148:427-432.

Kucera, J. 1980 Myofibrillar ATPase activity of intrafusal fibers in chronically de-afferented rat muscle spindles. Histochemistry, 66:221-228.

Kucera, J. 1981 Histochemical profiles of cat intrafusal muscle fibers and their motor innervation. Histochemistry, 73:397-418.

Kucera, J., Dorovini-zis K. 1979 Types of human intrafusal muscle fibers. Muscle Nerve, 2:437-451.

Landon, D.M. 1972 The fine structure of the equatorial regions of developing muscle spindles in the rat. J. Neurocytol., 1:189-210.

Law, P.K., Saito, A., Fleischer S. 1983 Ultrastructural changes in muscle and motor end-plate of the dystrophic mouse. Exp. Neurol., 80:361-382.

Lazarides, E., Hubbard, B.D. 1976 Immunological characterization of the subunit of the 100 Angstrom filaments from muscle cells. Proc. Natl. Acad. Sci. USA, 73:4344-4348.

Leberer, E., Pette, D. 1986a Immunochemical quantification of sarcoplasmic reticulum Ca-ATPase, of calsequestrin and of parvalbumin in rabbit skeletal muscles of defined fiber composition. Eur. J. Biochem., 156:489-496.

Leberer, E., Pette, D. 1986b Neural regulation of parvalbumin expression in mammalian skeletal muscle. Biochem. J., 235:67-73.

Lehky, P., Blum, H.E., Stein, E.A., Fischer, E.H. 1974 Isolation and characterization of parvalbumins from skeletal muscle of higher vertebrates. J. Biol. Chem., 249:4332-4334.

Le Peuch, C.J., Ferraz, C., Walsh, M.P., Demaille, J.G., Fischer, E.H. 1979 Calcium and cyclic nucleotide dependent regulatory mechanisms during development of chick embryo skeletal muscle. Biochem., 18:5267-5273.

Madrid, R.E., Jaros, E., Cullen, M.J., Bradley, W.G.1975 Genetically determined defect of Schwann cell basement membrane in dystrophic mouse. Nature, 257:319-321.

Martonosi, A.N. 1982 Regulation of cytoplasmic calcium concentration by sarcoplasmic reticulum. In: Disorders of the Motor Unit. D.L. Schotland, ed. John Wiley, New York, pp.565-583.

Maynard, J.A., Cooper, R.R., Ionaeseu, V.V. 1977 An ultrastructure investigation of intrafusal muscle fibers in myotonic dystrophy. Virchows. Arch. A. Path. Anat. Histol., 373:1-13.

Meier, H. 1969 The muscle spindle in mice with hereditary neuromuscular diseases. Experientia, 25:965-968.

Meier, H., Southard, J.L. 1970 Muscular dystrophy in the mouse caused by an allele at the dy-locus. Life Sci., 9:137-144.

Mendell, J.R., Higgins, R., Sahenk, Z., Cosmos, E. 1979 Relevance of genetic animal models of dystrophy to human muscular dystrophies. Ann. N.Y. Acad. Sci., 317:409-430.

Michelson, A.M., Russell, E.S., Harman, P.J. 1955 Dystrophia muscularis: A primary myopathy in the house mouse. Proc. Nat. Acad. Sci. USA, 41:1079-1084.

Milburn, A. 1973 The early development of muscle spindles in the rat. J. Cell Sci., 12:175-195.

Monaco, A.P., Neve, R.L., Colletti-Feener, C., Bertelson, C.J., Kurnit, D.M., Kunkel, L.M. 1986 Isolation of candidate cDNAs for portions of the Duchenne muscular dystrophy gene. Nature, 323:646-650.

Montgomery, A., Swenarchuk, L.1978 Further observations on mylinated axon number in normal and dystrophic mice. J. Neurol. Sci., 38:77-82.

Mrak, R.E.1985 Muscular Dystrophy In: Muscle Membranes in Diseases of Muscle. R.E. Mrak ed. CRC Press Inc., Florida, pp. 23-80.

Mrak, R.E., Baskin, R.J. 1978 Calcium transport and phosphoenzyme formation in dystrophic mouse sarcoplasmic reticulum. Biochem. Med., 19:47-70.

Müntener, M., Berchtold, M.W., Heizmann, C. 1985 Parvalbumin in cross-reinnervated and denervated muscles. Muscle Nerve, 8:132-137.

Müntener, M., Rowlerson, A.M., Berchtold, M.W., Heizmann, C.W. 1986 Changes in the concentration of the calcium-binding parvalbumin in cross-reinnervated rat muscles. J. Biol. Chem., 262:465-469.

Nockolds, C.E., Kretsinger, R.H., Coffee, C.J., Bradshaw, R.A. 1972 Structure of a calcium-binding carp myogen. Proc. Natl. Acad. Sci. U.S.A., 69:581-584.

O'Farrell, P.H. 1975 High resolution two-dimensional electrophoresis of proteins. J. Biol. Chem., 250:4007-4021.

Obinata, T., Takano-Ohmuro, H., Matsuda, R. 1980 Changes in troponin-T and myosin isoenzymes during development of normal and dystrophic chicken muscles. FEBS Lett., 120:195-198.

Ogawa, Y., Tanokura, M. 1986 Steady-state properties of calcium binding to parvalbumins from bullfrog skeletal muscle: Effects of $Mg^{2+}$, pH, ionic strength and temperature. J. Biochem., 99:73-80.

Ontell, M., Feng, K.C., Klueber, K., Dunn, R.F., Taylor, F. 1984 Satellite cells, growth and regeneration in murine dystrophic muscle: A quantitative study. Am. J. Anat., 208:159-174.

Ovalle, W.K., Bressler, B.H., Jasch, L.G., Slonecker, C.E. 1983 Abnormal distribution of fiber types in the slow-twitch soleus muscle of the C57BL/$dy^{2J}$/$dy^{2J}$ dysyrophic mouse during postnatal development. Am. J. Anat., 168:291-304.

Ovalle, W.K., Dow, P.R. 1986 Alterations in muscle spindle morphology in advanced stages of murine muscular dystrophy. Anat. Rec., 216:111-126.

Ovalle, W.K., Smith, R.S. 1972 Histochemical identification of three types of intrafusal muscle fibers in the cat and monkey based on the myosin ATPase reactio. Can. J. Physiol. Pharm., 50:195-202.

Parry, D.J., Desypris, G. 1983 Slowing of twitch of dystrophic mouse muscle is partially due to altered activity pattern. Muscle Nerve, 6:397-407.

Parry, D.J., Parslow H.G. 1981 Fiber type susceptibility in dystrophic mouse. Exp. Neurol., 73:674-685.

Parslow, H.G., Parry, D.J.1981 Slowing of fast-twitch muscle in the dystrophic mouse. Exp. Neurol., 73:686-699.

Pearse, A.G.E. 1968 Histochemistry. Theoretical and Applied. Vol.I. Little Brown & Co., Boston, pp. 59-69.

Pearse, A.G.E. 1980 Histochemistry, Theoretical and Applied, Vol. I. Churchill Livingstone, New York, pp. 92-94.

Pechère, J.F. 1968 Muscular parvalbumins as homologous proteins. Comp. Biochem. Physiol., 24:289-295.

Pechère, J.F. 1974 Isolement d'une parvalbumine du muscle de lapin. C.R. Acad. Sci. Paris, 278:2577-2579.

Pechère, J.F., Capony, J.P. 1969 A comparison at the peptide level of muscular parvalbumins from several lower vertebrates. Comp. Biochem. Physiol., 28:1089- 1102.

Pechère, J.F., Capony, J.P., Demaille, J. 1973 Evolutionary aspects of the structure of muscular parvalbumins. System Zool., 22:533-548.

Pechère, J.F., Demaille, J., Capony, J.P. 1971 Muscular parvalbumins: Preparative and analytical methods of general applicability. Biochim. Biophys. Acta, 236:391-408.

Pechère, J.F., Derancourt, J., Haiech, J. 1977 The participation of parvalbumins in the activation-relaxation cycle of vertebrate fast skeletal muscle. FEBS Lett., 75:111-114.

Petell, J.K., Marshall, N.A., Lebherz, H.G. 1984 Content and synthesis of several abundant glycolytic enzymes in skeletal muscles of normal and dystrophic mice. Int. J. Biochem., 16:61-67.

Peter, J.B., Barnard, R.J., Edgerton, V.R., Gillespie, C.A., Stempel, K.E. 1972 Metabolic profiles of three fiber types of skeletal muscle in guinea pigs and rabbits. Biochem., 11:2627-2633.

Pette, D. 1980 Plasticity of Muscle. Walter de Gruyter, Berlin.

Pette, D., Klug, G., Reichmann, H. 1985 Parvalbumin reduction in relation to possible perturbations of $Ca^{2+}$-homeostasis in muscular dystrophy. Adv. Exp. Med. Biol., 182:265-267.

Pfyffer, G.E., Bologa, E., Herschowitz, N., Heizmann, C.W. 1984 Parvalbumin, a neuronal protein of brain cell cultures. J. Neurochem., 43:49-57.

Pierobon Bormioli, S., Sartore, S., Vitadello, M., Schiaffino, S. 1980 Slow myosins in vertebrate skeletal muscle. An immunofluorescence study. J. Cell Biol., 85:672-681.

Platzer, A. 1979 Embryology of two murine muscle diseases: Muscular dystrophy and muscular dysgenesis. Ann. N.Y. Acad. Sci., 317:94-113.

Platzer, A., Powell, J.A. 1975 Fine structure of prenatal and early postnatal dystrophic mouse muscle. J. Neurol. Sci., 24:109-126.

Potter, J.D., Johnson, D., Dedman, J.R., Schreiber, W.E., Mandel, F., Jackson, R.L., Means, A.R. 1977 Calcium-binding proteins: Relationship of binding, structure, conformation and biological function. In: Calcium-Binding Proteins and Calcium Function. R.H.Wasserman et al., eds. Elsevier North-Holland, New York, pp.239-250.

Reichmann, H., Pette, D. 1984 Enzyme activities and activity profiles in muscle fibers of dystrophic, immature-normal, and adult-normal BL6 mice. Muscle Nerve, 7:121-126.

Robertson, S.P., Johnson, J.D., Potter, J.D. 1981 The time-course of $Ca^{2+}$ exchange with calmodulin, troponin, parvalbumin and myosin in response to transient increases in $Ca^{2+}$. Biophys. J., 34:559-569.

Rogers, S.L. 1982 Muscle spindle formation and differentiation in regenerating muscle grafts. Dev. Biol., 94:265-283.

Rogers, S.L., Carlson, B.M. 1981 A quantitative assesment of muscle spindle formation in reinnervated and non-reinnervated grafts of the rat extensor digitorum longus muscle. Neuroscience, 6:87-94.

Saito, A., Law, P.K., Fleischer, S.1983 Study of neurotrophism in normal/dystrophic parabiotic mice. Muscle Nerve, 6:14-28.

Samaha, F.J. 1972 Tropomyosin and troponin in normal and dystrophic human muscle. Arch. Neurol., 26:547-550.

Samaha, F.J., Thies, W.H. 1979 Myosin light chains in Duchenne dystrophy and paraplegic muscle. Neurology (NY), 29:122-125.

Schiaffino, S., Gorza, L., Dones, I., Cornelio, F., Sartore, S. 1986 Fetal myosin immunoreactivity in human dystrophic muscle. Muscle Nerve, 9:51-58.

Schneeberger, P.R., Norman, A.W., Heizmann, C.W. 1985 Parvalbumin and vitamin D-dependent calcium-binding protein (Mr 28,000): Comparison of their localization in the cerebellum of normal and rachitic rats. Neurosci. Letters, 59: 97-103.

Silverman, H., Atwood, H.L. 1980 Increase in oxidative capacity in muscle fibers in dystrophic mice and correlation with overactivity in these fibers. Exp. Neurol., 68:97-113.

Smith, S.J., Woledge, R.C. 1985 Thermodynamic analysis of calcium binding to frog parvalbumin. J. Muscle Res. Cell Motil., 6:657-768.

Soukup, T., Vydra, J., Cerny M. 1979 Changes in ATPase and SDH reactions of the rat extrafusal and intrafusal muscle fibers after preincubations at different pH. Histochemistry, 60:71-84.

Soukup, T. 1976 Intrafusal fiber types in rat limb muscle spindles. Morphological and histochemical characteristics. Histochemistry, 47:43-57.

Sreter, F.A., Ikemoto, N., Gergely, J. 1966 Studies on the fragmented sarcoplasmic reticulum of normal and dystrophic mouse muscle. In: Exploratory Concepts in Muscular Dystrophy and Related Disorders. A.T. Milhorat, ed. Exerpta Medica Foundation, New York, pp.289-298.

Sreter, F.A., Salmons, S., Romanul, F.C.A., Gergely, J. 1973 Synthesis by fast muscle of myosin light chains characteristic of slow-twitch muscle in response to long-term stimulation. Nature New Biol., 241:17-19.

Staron, R.S., Pette, D. 1986 Correlation between myofibrillar ATPase activity and myosin heavy chain composition in rabbit muscle fibers. Histochemistry, 86:19-23.

Sternberger, L.A. 1979 Immunocytochemistry. L.A. Sternberger, ed. John Wiley, New York.

Stichel, C.C., Kagi, U., Heizmann, C.W. 1986 Parvalbumin in cat brain: Isolation, characterization, and localization. J. Neurochem., 47:46-53.

Strehler, E.E., Oppenberger, H.M., Heizmann, C.W. 1977 Isolation and characterization of parvalbumin from chicken leg muscle. FEBS Lett., 78:127-133.

Stuhlfauth, I., Reininghaus, J., Jockusch, H., Heizmann, C.W. 1984 Calcium-binding protein, parvalbumin, is reduced in mutant mammalian muscle with abnormal contractile properties. Proc. Natl. Acad Sci. USA, 81:4814-4818.

Sugita, H., Ishiura, S., Suzuki, K., Imahori, K. 1980 Ca-Activated neutral protease and its inhibitors: In vitro effect on intact myofibrils. Muscle Nerve, 3:335-339.

Sugita, H., Toyokura Y. 1976 Alteration of troponin subunits in progressive muscular dystrophy (DMP): I. Pattern of troponin subunits in DMP. Proc. Jpn. Acad., 52:256-259.

Summers, P.J., Parsons, R. 1981a An electron microscopic study of satellite cells and regeneration in dystrophic mouse muscle. Neruopath. Applied Neurobiol., 7:257-268.

Summers, P.J., Parsons, R. 1981b A quantitative assessment of dystrophic mouse (129 ReJdy/dy) myogenesis in vitro. Neuropath Applied Neurobiol., 7:269-277.

Swash, M. 1982 Pathology of the muscle spindle. In: Skeletal Muscle Pathology. F.L. Mastaglia J.N. Walton, eds. Churchill Livingstone, Edinburgh, pp. 508-537.

Swash, M., Fox, K.P. 1975 Abnormal intrafusal muscle fibers in myotonic dystrophy: a study using serial sections. J. Neurol. Neurosurg. Psych., 38:91-99.

Swash, M., Fox,K.P. 1976 The pathology of the muscle spindle in Duchenne muscular dystrophy. J. Neurol. Sci., 29:17-32.

Swett, J.E., Eldred, E. 1960 Distribution and number of stretch receptors in medial gastrocnemius and soleus muscles of the cat. Anat. Rec., 137:453-460.

Takagi, A., Ishiura, S., Nonaka, I., Sugita, H. 1982 Myosin light chain components in single muscle fibers of Duchenne muscular dystrophy. Muscle Nerve, 5:399-404.

Tanioka, Y., Tsukada, M., Esoki, K. 1973 A technique of ovarian transplantation in mice. Exp. Animals, 22:15-20.

Towbin, H., Staeklin, T., Gordon, J. 1979 Electrophoretic transfer of proteins from polyacrylamide gels to nitrocellulose sheets: Procedure and some applications. Proc. Natl. Acad. Sci. USA, 76:4350-4354.

Van Eldik, L.J., Zendegui, J.G., Marshak, D.R., Watterson, D.M. 1982 Calcium- binding proteins and the molecular basis of calcium action. Int. Rev. Cytol., 77:25-38.

Volpe, P., Mrak, R.E., Costello, B., Fleischer, S. 1984 Calcium release from sarcoplasmic reticulum of normal and dystrophic mice. Biochim. Biophys. Acta, 769:67-78.

Voss, H. 1937 Untersuchungen uber Zahl, Anordnung und Lange der Muskel-spindeln in den Lumbricalmuskeln des Menschen und einiger. Tiere. Z. mikr.-anat. Forsch., 42:509-524.

Vrbova, G. 1983 Neuromuscular diseases viewed as a distrubance of nerve-muscle interactions. In: Somatic and Autonomic Nerve-Muscle Interactions. Burnstock et al., eds. Elsevier Science Publishers, pp. 359-383.

Walsh, M.P., Vallet, B., Cavadore, J., Demaille, J.G. 1980 Homologous calcium-binding proteins in the activation of skeletal, cardiac and smooth muscle myosin light chain kinases. J. Biol. Chem., 255:335-337.

Wirtz, P., Loermans, H.M., Peer, P.G., Reintjes, A.G. 1983 Postnatal growth and differentiation of muscle fibers in the mouse: II. A histochemical and morphometrical investigation of dystrophic muscle. J. Anat., 137:127-142.

Wnuk, W., Cox, J.A., Stein, E.A. 1982 Parvalbumins and other soluble high-affinity calcium-binding proteins from muscle. In: Calcium and Cell Function. Vol.II, W.Y. Cheung, ed. Academic Press, New York, pp.243-297.

Wolfe, H.G., Southard, J.L. 1962 Production of all-dystrophic litters of mice by artificial insemination. Proc. oc. Exp. Biol. Med., 109:630-633.

Wood, D.S., Sorenson, M.M., Eastwood, A.B., Charash, W., Reuben, J.P. 1978 Duchenne dystrophy: Abnormal generation of tension and $Ca^{2+}$ regulation in single skinned fibers. Neurology (NY), 28:447-457.

Yellin, H. 1969 A histochemical study of muscle spindles and their relationship to extrafusal fiber types in the rat. Am. J. Anat., 125:31-46.

Yellin, H. 1974a Regional differences in the contractile apparatus of intrafusal muscle fibers. Am. J. Anat., 139:147-152.

Yellin, H. 1974b Spindle induction and differentiation in murine dystrophy. Experientia, 30:286-287.

Younger, L.E., Silverman, H. 1984 Breeding and offspring rearing ability of C57BL/6J dystrophic mice. Lab. Anim. Sci., 34:471-474.

Zelena, J. 1957 The morphogenetic influence of innervation on the ontogenetic development of muscle spindles. J. Embryol. Exp. Morphol., 5:283-292.

Zelena, J., Soukup, T. 1974 The differentiation of intrfusal fiber types in rat muscle spindles after motor denervation. Cell Tissue Res., 153:115-136.

Zuschratter, W., Scheich, H., Heizmann, C.W. 1985 Ultrastructural localization of the calcium-binding protein parvalbumin in neurons of the song system of the zebra finch, Poephila guttata. Cell Tissue Res., 241:77-83.